

OAK RIDGE NATIONAL LABORATORY

operated by

UNION CARBIDE CORPORATION

for the

U.S. ATOMIC ENERGY COMMISSION



ORNL - TM - 516

df

15

WASTE TREATMENT AND DISPOSAL PROGRESS REPORT FOR NOVEMBER-DECEMBER 1962, AND JANUARY 1963

This document has been approved for release
to the public by:

David R. Hamlin *7/28/95*
Technical Information Officer Date
ORNL Site

NOTICE

This document contains information of a preliminary nature and was prepared primarily for internal use at the Oak Ridge National Laboratory. It is subject to revision or correction and therefore does not represent a final report. The information is not to be abstracted, reprinted or otherwise given public dissemination without the approval of the ORNL patent branch, Legal and Information Control Department.

LEGAL NOTICE

This report was prepared as an account of Government sponsored work. Neither the United States, nor the Commission, nor any person acting on behalf of the Commission:

- A. Makes any warranty or representation, expressed or implied, with respect to the accuracy, completeness, or usefulness of the information contained in this report, or that the use of any information, apparatus, method, or process disclosed in this report may not infringe privately owned rights; or
- B. Assumes any liabilities with respect to the use of, or for damages resulting from the use of any information, apparatus, method, or process disclosed in this report.

As used in the above, "person acting on behalf of the Commission" includes any employee or contractor of the Commission, or employee of such contractor, to the extent that such employee or contractor of the Commission, or employee of such contractor prepares, disseminates, or provides access to, any information pursuant to his employment or contract with the Commission, or his employment with such contractor.

ORNL-TM-516

CHEMICAL TECHNOLOGY DIVISION

HEALTH PHYSICS DIVISION

WASTE TREATMENT AND DISPOSAL PROGRESS REPORT

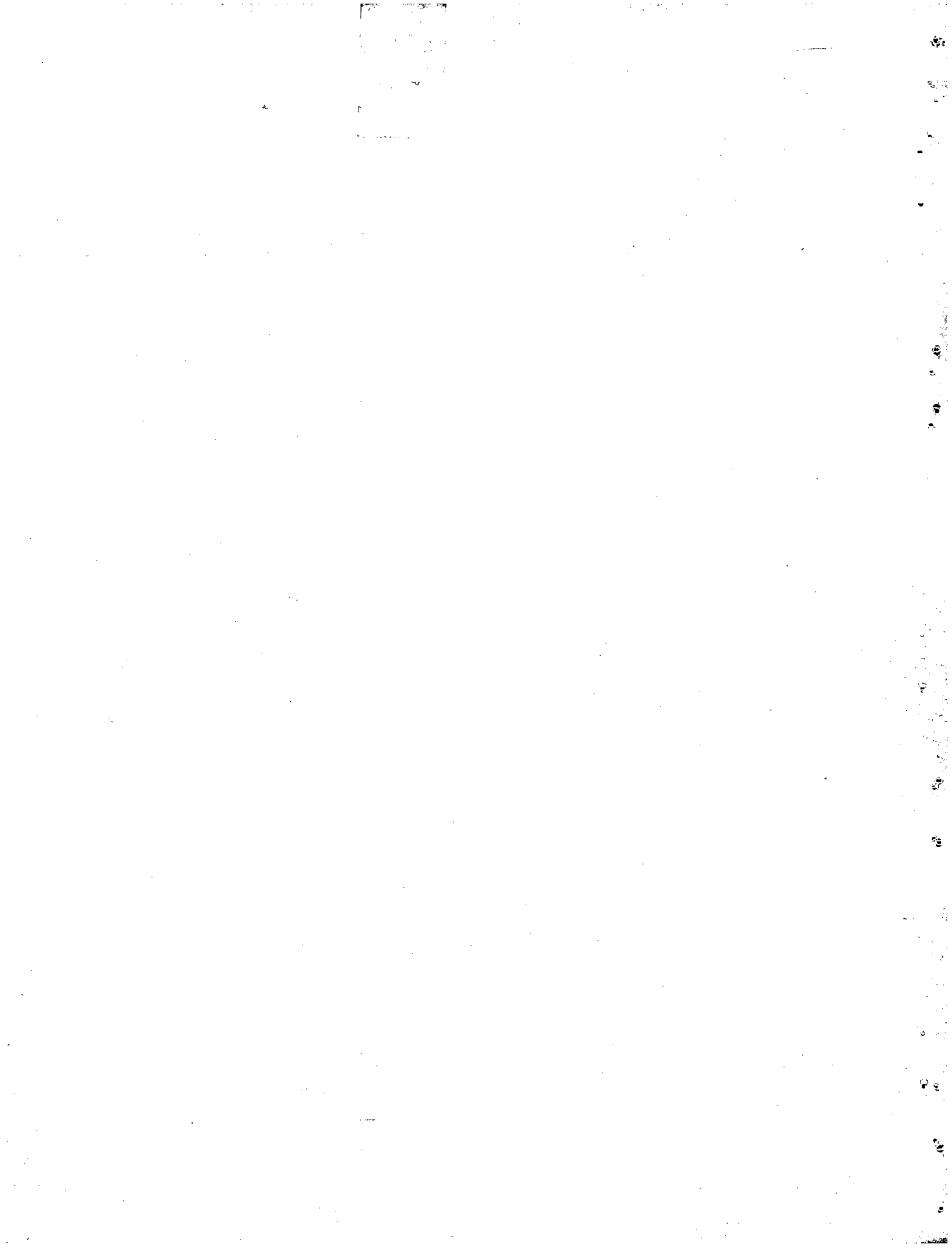
FOR NOVEMBER-DECEMBER 1962, AND JANUARY 1963

F. L. Parker and R. E. Blanco

DATE ISSUED

JUN 12 1963

OAK RIDGE NATIONAL LABORATORY
Oak Ridge, Tennessee
Operated by
UNION CARBIDE CORPORATION
for the
U. S. ATOMIC ENERGY COMMISSION



ABSTRACT

High-Level Waste Calcination. Two waste calcination tests were completed in the large-scale equipment: test-R-69, a TBP-25 gravity-feed calcination test, and test R-70, a formaldehyde-treated Purex-65 waste test, with continuous evaporation.

Test-R-69 was the last in a series of TBP-25 tests, and the purpose of this test was twofold: (1) rates and operating procedures were evaluated by using gravity feed as in run R-68; (2) the six-zone calcination furnace was rewired so that it would operate as a one-zone-controlled furnace. If any of the six thermocouples used for furnace control attained the set-point temperatures, all six of the furnace zones would turn off. The average feed rate was 14 liters/hr. In comparison, run R-68, a six-zone-control test, had an average feed rate of 26 liters/hr. The water-to-feed ratio for this test was 5.2. The resulting solid contained 1000 ppm of nitrate and had a bulk density of 0.64 g/cc. Control was good during this test; however, the one-zone furnace control made the over-all rate much lower.

Test R-70 was the first test of a waste composition formula that simulated 1965 formaldehyde-treated Purex waste. For this test, the furnace was split into three zones. The top and bottom zones were controlled independently, while the four middle zones were controlled as one zone. The average feed rate was 40 liters/hr, with a maximum rate of 200 liters/hr. No additional water was added to the evaporator to remove nitric acid because this waste was very dilute in total nitrate ion. The resulting solid had 200 ppm of nitrate and a bulk density of 1.25 g/cc; control was good. The calciner pot was removed and sand blasted after the test was completed, and there was seen a band of corrosion about 1 ft from the bottom, with pits as deep as 50 mils in the 100-mil-thick pot. Calcium nitrate had been added to the calcining pot to reduce the volatility of sulfate. The calcium nitrate added corresponded stoichiometrically to 10% of the sulfate plus 100% of the phosphate and fluoride in the feed.

Hard, microcrystalline solids, incorporating up to 45% Purex waste oxides, were prepared on a laboratory scale from simulated high sulfate and 1965 FTW waste solution by addition of phosphite or phosphate and sodium, calcium and/or magnesium. Simulated Darex waste was fixed on a semiengineering scale into a very hard, strong product that incorporated 25% waste oxides and represented a volume reduction of 5.17 from the waste solution. The feasibility of removing mercury from 1965 Hanford formaldehyde-treated (FTW) Purex waste by amalgamation with copper was demonstrated on a laboratory scale.

Type 304L stainless steel coupled to titanium 45A showed weight losses amounting to a maximum corrosion rate of 0.41 mil/month for 192 hr of exposure above refluxing Hanford 1965 FTW solution. Rates of solution and interface specimens were slightly lower. Titanium 45A showed slight weight gains for both coupled and uncoupled specimens.

Low-Level-Waste Treatment- The carboxylic resin, Amberlite IRC-50, effectively removed as much as 70 ppm of residual hardness from phosphate-contaminated waste prior to cesium loading on Duolite CS-100 resin. Under the worst conditions (70 ppm of hardness), the hardness broke through the IRC-50 pretreatment column after passage of about 1200 bed volumes of waste. This treatment is superior to the removal of hardness by the addition of Na_2CO_3 since the latter reduces the loading of cesium on the CS-100 resin because of competition of sodium with cesium. A residual hardness of 40 ppm, for example, caused 0.1% breakthrough of cesium on the CS-100 resin at about 570 bed volumes in the presence of the normal (0.01 M) sodium concentration vs about 900 bed volumes when the hardness was eliminated by the addition of 0.005 M Na_2CO_3 (0.02 M Na^+ total). However, removal of the residual hardness by the IRC-50 resin postponed the breakthrough to the value (about 2000 bed volumes) achieved in the absence of hardness and at the normal (0.01 M) sodium content. The IRC-50 resin, like CS-100, can be regenerated with 0.5 M HNO_3 .

Design was started on the equipment and piping changes to the ORNL Low-Level Pilot Plant for demonstrating the fixed bed and continuous contractor ion exchange processes proposed by I. R. Higgins, and for the installation of a new, agitated clarifier for the scavenging precipitation-ion exchange process.

Engineering, Economics, and Safety Evaluation. In a study based on optimistic expectations of future processes for fission product separations processes, estimated costs for the management of wastes from which 90 and 99% of all fission products had been removed were from 70 to 80% of those for the management of waste from which no fission products had been removed.

This saving of 20 to 30% is not believed to be sufficient to pay for the cost of fission product removal and final disposal of the concentrates; and hence does not represent an economic route for waste management unless a substantial market for separated fission products exists to provide a substantial income.

As a basis for this study, it was assumed that after fission product removal, the waste was identical to neutralized Purex waste in volume and in the composition of the major constituents. The sequential steps in the management of waste from processing 1500 metric tons per year of uranium converter fuel irradiated to 10,000 Mwd/ton were as follows: interim storage of liquid waste, conversion to solids by pot calcination, interim storage of calcined solid waste, shipment of 1000 miles, and final disposal in a salt mine. Minimum-cost schemes were worked out involving optimum choices of interim times of liquid and solid storage, diameter of the waste-calcination cylinder, and age at time of burial in the salt.

Costs for wastes from which fission products had been removed were the smallest for calcination in 24-in.-diam vessels, were not

strongly affected by age, and fell in the range of 0.017 to 0.019 mill/kwh_e. The lowest cost for acid Purex waste without fission product removal was about 0.024 mill/kwh_e, obtained by using either 12- or 24-in.-diam calcination vessels and burying them in salt after allowing 30 years for decay of the fission products in the calcined wastes.

Man may be exposed to radiation through a number of pathways due to the discharge of radioactive fluids to the Clinch River. Contaminated bottom sediments can contribute to the total dose. Based on sediment analyses and the assumption of a uniform, infinite source, the largest bottom sediment dose rate (at contact) of 12 millirads/day of exposure would have occurred in 1959 on the Clinch River and was derived from 0.4 beta and 0.6 gamma radiation. The beta dose rate is eliminated by about 1 cm of water shielding; the gamma dose rate is reduced by an average factor of 18 after attenuation through 3 ft of water.

Calculations of the activity of the fission products and transuranic elements contained in a single 400,000-gal storage tank were completed. Initial calculations were made of the dispersion into the atmosphere of this activity, using various assumed accidental situations.

Disposal in Deep Wells. Geothermal measurements in Joy No. 1 well and well 400 S, made by the U. S. Geological Survey, were compared with the thermal conductivity of core samples and a provisional rate of heat flow from the earth's interior ($0.73 \pm 0.04 \mu\text{cal}/\text{cm}^2$) was computed.

A surprising discovery of abnormally low fluid pressure in the lower Chickamauga and upper Knox, observed during the temperature survey in Joy No. 1 well after it had been cased, is discussed and its significance assessed.

Mineralogical analyses of 25 samples from the 3263-ft-deep Joy well are reported. They indicate a considerable difference in the samples from the several possible fracturing zones.

Unexplained anomalies in the pumping time of several mixes were reported by Westco, and their causes are being investigated. A program of mix evaluation was initiated by the Halliburton Company. The retention of radionuclides by the set grout was investigated, and it was shown that even under adverse conditions the bulk of the cesium and almost all the strontium will be retained.

The design of the injection well was completed, and contracts are being negotiated for drilling, logging, and cementing of the injection and observation wells. The current schedule calls for drilling and cementing the wells, completing the plant design, and installing the waste storage tanks, waste transfer line, and waste pumps this fiscal year.

Disposal in Natural Salt Formations. Additional observations were made of the condition of the heaters and of the 10-in.-diam holes used in the high-temperature heat tests. Failure of peripheral heaters in the array tests was due to localized high concentrations of nickel sulfide in grain boundaries, combined with the magnetostrictive effect. Heater sheaths made of type 304L stainless steel contained precipitated carbides at grain boundaries. Precipitated carbides were associated with intergranular corrosion. Type 304 stainless steel thermocouple sheaths also underwent heavy intergranular attack.

Removal from the structure of the wall heater hole as part of a large block made possible detailed examination and photography of the shattered zone around the heater. The maximum radius of the shattered zone from the center of the original hole was about 7 in. The limit of shattering could not be determined exactly because of the recompacting of shattered and expanded salt. Comparison of the shattered zone with temperature profiles confirms 290°C as the maximum temperature at which Hutchinson salt will shatter.

A possible explanation of the permanent increase in salt volume with increased temperature was found to be enlargement of negative crystals due to expansion of the liquid phase and creation of larger bubbles.

Clinch River Study. Gross gamma analyses of bottom-sediment cores from the Clinch River were begun. A specially designed "core scanner" is being used, and it consists of a 3- x 3-in. NaI scintillation crystal and matched phototube enclosed in a 4-in.-thick lead shield, with a 2- x 2-in. collimator slit. A hoist automatically moves the core vertically past the collimator in 2-in. increments. Results indicated that core drilling successfully samples the full depth of the radioactive sediments. Appreciable variations in radioactivity with depth have been noted in many of the cores.

Calcite deposited on a metal object suspended in the Clinch River contained concentrations of radioactive ruthenium and strontium that lie between concentrations in Clinch River bottom sediments and those in suspended sediments. Thus, if bottom sediments contain an appreciable amount of precipitated calcite, it would add materially to the radionuclide content of the sediment.

Fundamental Studies of Minerals. Strontium removals by four different sorbents were compared by using column methods. Tests were performed with a 0.5 M NaNO₃ solution adjusted to pH 10 and containing 10⁻⁵ M Sr (NO₃)₂; the flow rate was 3 ml min⁻¹cm⁻². Commercial-grade activated alumina was most efficient; the 50% breakthrough volume for 10 g of it was approximately 6500 cc for the first column and 27,000 for the second. The same weight of Dowex 50-X12 treated 2600 cc for the same breakthrough percentage. Both vermiculite and clinoptilolite were ineffective under these test conditions; in both cases breakthrough occurred when the throughput volume was less than 150 cc. Intermittent checks showed that the effluent pH from the

Dowex column had dropped to 9.7, whereas the pH from the alumina column showed readings generally between 8 and 9, with some readings as low as 7.5.

White Oak Creek Basin Study. A series of 250 core samples were taken in the bed of former White Oak Lake to determine the quantity, type, and distribution of radionuclides in the area. These cores show that the contaminated lacustrine sediment, which was deposited during the 1943-1955 impoundment, is as much as 20 in. thick in the lower part of the lake bed near the dam; however, there is a gradual thinning of the layer upstream and, in general, toward the shoreline.

Foam Separation. A 9-in.-diam sludge column was operated with low-activity process waste water at flow rates up to $60 \text{ gal ft}^{-2}\text{hr}^{-1}$. By making the water 0.005 M each in NaOH and Na_2CO_3 and 2 ppm in Fe^{3+} , the total dissolved hardness (as CaCO_3) was reduced to 2 to 5 ppm, and Sr^{90} decontamination factors of 10 to 15 were achieved. Average decontamination factors for Co^{60} , Cs^{137} , Ru^{106} , and Ce^{144} were 30, 1.1, 2.0, and 40, respectively. During these tests the average phosphate and alkylbenzene sulfonate concentrations in the process waste water were 1 to 2 and 0.75 ppm, respectively. Precipitation of calcium and magnesium by making tap water 0.004 M in NaOH and 60 ppm in PO_4^{3-} was found to be nearly complete in 3 min. The $\text{CaCO}_3\text{-Mg(OH)}_2$ sludge from caustic-carbonate precipitation can be incorporated in concrete.

As foam breakers, screen lined, perforated centrifuge bowls were tried. Foam was more efficiently condensed by 100- or 120-mesh-per-inch screen than by 40 or 200 mesh at low rates of dry foam than at high rates of wet foam and for lower centrifuge speeds if the capacity was not exceeded. The capacity increased as the speed increased. A 24-in.-diam column was installed for the study of scale-up problems without tracer. In a 6-in.-diam column, decontamination factors for the precipitation of calcium and magnesium (with $\text{NaOH-Na}_3\text{PO}_4\text{-FeCl}_3$), followed by foam separation using the slurry feed were 19 to 52, independent of whether "FAB" was present. Decontamination factors for this precipitation without foam separation was about 10. The strontium decontamination factors using effluent from operation of the laboratory clarifier on ORNL low-level waste (see above) was 27 for a run with flow rates selected for a strontium distribution factor of 1.7×10^{-3} cm. The strontium distribution factors of $(0.6 \text{ to } 2.4) \times 10^{-3}$ cm indicated by other column runs with clarifier effluent agree with values for about 5 ppm Ca^{2+} in laboratory studies.

CONTENTS

	Page
1. Introduction	8
2. High-Level Waste Calcination	9
2.1 Evaporation-Calcination	9
2.2 Mechanical Test Program	20
2.3 Fixation in Glass	23
2.4 Removal of Mercury from Waste Solutions	30
2.5 Corrosion	32
3. Low-Level Waste Treatment	34
3.1 Low-Level Waste Treatment	34
3.2 Design of Pilot Plant for Decontaminating Low-Level Waste	38
4. Engineering, Economics, and Hazards Evaluation	42
4.1 Engineering and Economics of Waste Management	42
4.2 Analysis of the Safety of Routine Operating Discharges From White Oak Creek to the Clinch River	49
4.3 Safety of Tank Storage of High-Level Liquid Wastes	55
5. Disposal in Deep Wells	57
5.1 Disposal by Hydraulic Fracturing	57
5.2 Design of the Fracturing Disposal Pilot Plant	72
6. Disposal in Natural Salt Formations	89
6.1 High Temperature Experiments	89
6.2 Thermal Stability of Salt	98
6.3 Permanent Expansion of Negative-Crystal Cavities	98
7. Clinch River Study	101
7.1 Bottom Sediments	101
8. Fundamental Studies of Minerals	106
8.1 Column Study of Several Sorbents for Strontium	106
9. White Oak Creek Basin Study	110
9.1 Distribution and Transport of Radionuclides in the Bed of Former White Oak Lake	110
9.2 Oak Ridge Area Hydrology	112

CONTENTS (contd.)

	Page
10. Foam Separation	114
10.1 Laboratory Development	114
10.2 Engineering Development	120
APPENDIX A, Results of Microscopic Examination	80
APPENDIX B, Clay Analyses	84

1. INTRODUCTION

This report is the tenth* in a series of bimonthly reports on progress in the ORNL development program, the objective of which is to develop and demonstrate, on a pilot-plant scale, integrated processes for the treatment and ultimate disposal of radioactive wastes resulting from reactor operations and reactor fuel processing in the forthcoming nuclear power industry. The wastes include those of high, intermediate, and low levels of radioactivity in liquid, solid, or gaseous states.

Principal current emphasis is on the high- and low-activity liquid wastes. Under the integrated plan, low-activity wastes, consisting of very dilute salt solutions such as cooling water and canal water, would be treated by scavenging and ion exchange processes to remove radioactive constituents, and the water would be discharged to the environment. The retained waste solids or slurries would be combined with the high-activity wastes. Alternatively, the retained solids or the untreated waste could be discharged to the environment in deep geologic formations. The high-activity wastes would be stored at their sites of origin for economic periods to allow for radioactive decay and artificial cooling.

Two methods are being investigated for the permanent disposal of high-activity wastes. One approach is conversion of the waste liquids to solids by high-temperature "pot" calcination or fixation in the final storage container (pot), itself, and storage in a permanently dry place, such as a salt mine. This is undoubtedly the safest method because complete control of radioactivity can be ensured within present technology during treatment, shipping, and storage. Another approach is the disposal of the liquid directly into sealed or vented salt cavities. Research and development work is planned to determine the relative feasibility, safety, and economics of these methods, although the major effort will be placed on conversion to and final storage as solids.

Tank storage or high-temperature calcination of intermediate-activity wastes may be unattractive because of their large volumes, and other disposal methods will be studied. One method, for example, the addition of solidifying agents prior to direct disposal into impermeable shale by hydrofracturing, is under investigation. Particular attention is being given to the engineering design and construction of an experimental fracturing plant to dispose of ORNL intermediate-activity wastes by this method if proved workable.

Environmental research on the Clinch River, motivated by the need for safe and realistic permissible limits of waste releases, is included in this program. The objective is to obtain a detailed characterization of fission product distribution, transport, and accumulation in the physical, chemical, and biological segments of the environment.

*ORNL-CF-61-7-3, ORNL-TM-15, ORNL-TM-49, ORNL-TM-133, ORNL-TM-169, ORNL-TM-252, ORNL-TM-376, ORNL-TM-396, and ORNL-TM-482.

2. HIGH-LEVEL WASTE CALCINATION

The pot calcination process for converting high-activity-level wastes to solids is being studied on both a laboratory and engineering scale to provide design information for the construction of a pilot plant. Development work has been with synthetic Purex, Darex, and TBP-25 wastes. The first phase of the program is concerned with direct calcination processes, where melting does not occur and little or no additives are combined with the wastes. A general flow-sheet was shown previously.¹ In the second phase, enough additives are used to induce melting and form a glass-like material in which the fission products are fixed.

2.1 Evaporation-Calcination

J. C. Suddath

C. W. Hancher

Process and equipment development for the ORNL Pot-calcination Process is continuing, with the objective of producing the experimental engineering data necessary for the design of a hot pilot plant to be built at Hanford. Experiments are conducted in a full-scale, integrated continuous evaporator--8-in.-diam by 96-in.-high pot system.

Two calcination tests were completed in the large-scale equipment: test R-69, a TBP-25 gravity-feed calcination test, and R-70, a formaldehyde-treated Purex-65 waste test with continuous evaporation.

Test R-69 was the last in a series of TBP-25 tests. The purpose of this test was twofold: (1) Rates and operating procedures were evaluated, using gravity feed as in run R-68.¹ (2) The six-zone calcination furnace was rewired so that it would operate as a one-zone-controlled furnace. If any of the six thermocouples used for furnace control attained the set-point temperatures, all six of the furnace zones would turn off. The average feed rate for this test was 14 liters/hr. In comparison, run R-68, a six-zone-control test, had an average feed rate of 26 liters/hr. The water-to-feed ratio for this test was 5.2. The resulting solid contained 1000 ppm of nitrate and had a bulk density of 0.64 g/cc. Control was good during this test; however, the one-zone furnace control made the overall rate much lower.

Test R-70 was the first test that used a waste composition formula simulating the 1965 formaldehyde-treated Purex waste (1965 FTW). For this test the furnace was split into three zones. The top and bottom zones were controlled independently, while the other four zones were controlled as one. The average feed rate for this test was 40 liters/hr, with a maximum rate of 200 liters/hr. No additional water was added to the evaporator to remove nitric acid because this waste was very dilute in nitrate ion. The

resulting solid had 200 ppm of nitrate and a bulk density of 1.25 g/cc; control was good. When the calciner pot was removed and sand blasted after the test had been completed, there was seen a band of corrosion approximately 1 ft from the bottom with pits as deep as 50 mils in the 100-mil-thick pot. Calcium nitrate had been added to the calcining pot to reduce the volatility of sulfate. The calcium nitrate corresponded stoichiometrically to 10% of the sulfate plus 100% of the phosphate and fluoride in the feed.

2.1.1 Operating Results and Conclusions for Test R-69

The operating conditions for test R-69 were identical to those used for test R-68, which was also a TBP-25 calcination test using gravity feed. The feed composition for R-69 was a standard TBP feed (Table 1). The material balance (Table 2) for test R-69 was satisfactory except for the iron and mercury. The nitrate and aluminum balances were 89 and 91%, respectively, while the iron balance was 499%. The iron in the solid was approximately five times normal. This must be due to stainless steel corrosion products from the calciner vessel. The mercury balance was 61%. However, when the evaporator and vapor lines were cleaned after the tests, a dark-brown sludge was washed out of the evaporator system.

The feed rate was held to a maximum of 44 liters/hr (necessary only in the first 3 or 4 hr) to limit the maximum rates of water addition necessary to steam strip nitric acid from the evaporator (Table 3, parts A and B). The water to feed ratio was 5.2, and the calcination period was 17 hr. In the last 6 hr of the calcination, the minimum temperature in the calciner was 850°C. The solid had a 1000 ppm of nitrate concentration and a 0.4 wt % mercury concentration. The bulk density of the solid was 0.64 g/cc (Table 1).

A total of 1890 g of mercury was fed to the system (4 g/liter of feed), and it was hoped that a large fraction of this would report to the mercury trap. The top of the calciner vessel and the off-gas lines were heated to about 500°C. This satisfactorily removed the mercury from this portion of the equipment. Only 4% of the total inventory remained in the top of the calciner top and in the off-gas lines (Table 4). Only 12% of the mercury stayed in the mercury trap and 34% was found in the evaporator bottoms at the end of the test.

2.1.2 Automatic Control for Test R-69

Since R-69 was a gravity feed test, the evaporator was filled with water at the start, and the nitric acid from the pot condenser was allowed to build up to about 1 M in the overhead of the evaporator and then was steam stripped by water addition. Density control of the evaporator was not used. The control settings for the four control variables (Table 5) were the same as were used for test R-68. The variables were controlled satisfactorily.

Table 1. Test R-69: Composition of the Feed and of the Solid

	NO ₃	Al	Fe	Hg
Feed, g/liter	423	45.5	0.24	4.03
Solid, wt %	0.1 (1000 ppm)	47.4	1.3	0.4
Bulk density	0.64 g/cc			

Table 2. Test R-69: Material Balance and Test Results

	NO ₃	Al	Fe	Hg
Feed-In, g	198,387	21,339	112	1,890
System-Out				
Evaporator, g	9,350	1,038	46	960 ^a
Solid, g	39	18,296	513	154
Condensate, g	166,592	--	--	57
Total-Out, g	175,981	19,334	559	1,161
Balance, %	88.7	90.6	499 ^b	61.4

Average feed rate = 15.6 liters/hr
Maximum feed rate = 44.0 liters/hr
Water to feed ratio = 5.2
Feed time = 30 hr
Calcining time = 17 hr (6 hr over 850°C in pot)

^aIncludes mercury trap.

^bIron in solid mainly corrosion products.

Table 3

TEST NO	HOURLY SYSTEM VARIABLES AND PARAMETERS - PART A								
	FEED TYPE - TRP-25				OPERATION MODE - CONTINUOUS				
RUN TIME HOURS	FEED LITERS	WATER LITERS	CALCINER ADDITIVE LITERS	EVAP. COND. LITERS	CALCINER FURNACE (HUNDRED-THOUSANDS OF BTUS)	CALCINER COND.	EVAP. COND.	SYSTEM OFF-GAS CU FT	EVAP. DENSITY GM/CC
1	44.	30.	0.	74.	0.	1.78	0.54	25.	1.01
2	80.	30.	0.	110.	1.50	3.43	1.33	47.	1.05
3	116.	56.	0.	172.	2.97	4.95	2.55	69.	1.16
4	160.	207.	0.	367.	4.34	6.38	7.82	96.	1.17
5	196.	411.	0.	607.	6.11	8.05	13.64	125.	1.14
6	234.	638.	0.	872.	7.44	9.29	19.16	151.	1.14
7	259.	808.	0.	1067.	8.88	10.41	23.12	177.	1.13
8	278.	974.	0.	1252.	10.28	11.29	27.15	205.	1.15
9	288.	1110.	0.	1398.	11.03	11.97	29.41	231.	1.14
10	302.	1193.	0.	1495.	12.05	12.70	30.77	258.	1.14
11	314.	1223.	0.	1536.	12.57	13.39	32.84	283.	1.11
12	325.	1306.	0.	1630.	13.15	14.70	35.58	309.	1.15
13	339.	1416.	0.	1754.	13.69	15.22	37.25	333.	1.14
14	353.	1446.	0.	1798.	14.45	15.71	37.44	359.	1.15
15	361.	1503.	0.	1863.	14.82	16.59	39.76	383.	1.15
16	379.	1582.	0.	1960.	15.44	17.29	41.01	408.	1.14
17	382.	1639.	0.	2020.	15.88	17.80	42.23	430.	1.16
18	389.	1722.	0.	2110.	16.39	18.30	44.43	456.	1.17
19	405.	1779.	0.	2183.	16.90	18.80	46.03	481.	1.18
20	405.	1836.	0.	2240.	17.38	19.39	47.64	505.	1.20
21	418.	1919.	0.	2336.	17.83	19.92	49.34	532.	1.23
22	427.	1972.	0.	2398.	18.20	20.46	51.01	556.	1.31
23	432.	2002.	0.	2433.	18.65	21.09	51.23	583.	1.36
24	441.	2028.	0.	2468.	19.09	21.68	53.42	609.	1.36
25	441.	2115.	0.	2555.	19.50	22.17	53.82	638.	1.38
26	455.	2141.	0.	2595.	19.84	22.75	54.01	670.	1.36
27	455.	2167.	0.	2621.	20.39	23.24	54.99	700.	1.37
28	455.	2193.	0.	2647.	20.73	23.67	56.24	729.	1.36
29	462.	2219.	0.	2680.	21.14	24.07	56.81	759.	1.37
30	469.	2245.	0.	2713.	21.55	24.40	57.61	789.	1.37
31		2298.	0.	2766.	21.96	24.81	58.19	819.	1.37
32		2324.	0.	2792.	22.37	25.06	58.40	850.	1.37
33		2324.	0.	2792.	22.71	25.14	58.59	881.	1.36
34		2350.	0.	2818.	22.85	25.41	59.02	911.	1.36
35		2376.	0.	2844.	23.19	25.73	59.21	942.	1.36
36		2376.	0.	2844.	23.43	25.99	59.21	974.	1.38
37		2402.	0.	2870.	23.77	26.32	59.21	1006.	1.36
38		2402.	0.	2870.	23.94	26.87	59.21	1049.	1.35
39		2428.	0.	2896.	24.14	27.12	59.21	1093.	1.55
40		2428.	0.	2896.	24.35	27.12	59.21	1139.	1.54
41		2428.	0.	2896.	24.62	27.52	59.21	1186.	1.54
42		2454.	0.	2922.	24.86	27.99	59.21	1233.	1.53
43		2454.	0.	2922.	25.00	27.99	59.21	1280.	1.53
44		2454.	0.	2922.	25.20	27.99	59.40	1328.	1.53
45		2480.	0.	2948.	25.41	28.43	59.61	1376.	1.53
46		2480.	0.	2948.	25.54	28.43	59.61	1424.	1.53
47		2514.	0.	2982.	25.71	28.69	59.61	1472.	1.31

Table 3 (continued)

TEST NO	HOURLY SYSTEM VARIABLES AND PARAMETERS - PART B									
	FEED TYPE - TBP-25					OPERATION MODE - CONTINUOUS				
RUN TIME HOURS	EVAP. LIQUID NITRATE MOLAR	EVAP. MAJOR CATION FE OR AL GM/LITER	CALCINER COND. NITRATE MOLAR	EVAP. COND. H+ MOLAR	EVAP. COND. MAJOR ICN FE OR AL GM/LITER	EVAP. COND. RU GM/LITER	EVAP. LIQUID TEMP. DEG.C	EVAP. VAPOR TEMP. DEG.C	CALCINER FEED TEMP. DEG.C	CALCINER OFF-GAS TEMP. DEG.C
1	0.76	0.0	1.57	0.05	0.	0.	100.	100.	109.	165.
2	3.48	0.1	2.89	0.17	0.	0.	101.	102.	111.	180.
3	7.38	0.0	4.79	1.21	0.	0.	109.	111.	121.	165.
4	7.11	0.1	5.98	1.22	0.	0.	108.	110.	131.	162.
5	6.44	0.1	6.19	0.90	0.	0.	105.	108.	134.	151.
6	6.25	0.1	5.94	0.81	0.	0.	106.	109.	132.	132.
7	6.41	0.1	5.68	0.78	0.	0.	106.	108.	124.	123.
8	6.46	0.1	6.56	0.84	0.	0.	106.	108.	124.	115.
9	6.14	0.1	5.71	0.78	0.	0.	106.	108.	120.	128.
10	6.11	0.1	6.10	0.76	0.	0.	106.	107.	118.	111.
11	7.13	0.1	5.83	1.24	0.	0.	106.	108.	119.	102.
12	6.46	0.1	5.87	0.95	0.	0.	107.	109.	122.	94.
13	6.38	0.1	6.00	0.89	0.	0.	106.	108.	118.	92.
14	6.94	0.1	5.63	0.94	0.	0.	107.	108.	115.	85.
15	6.43	0.1	6.10	0.97	0.	0.	107.	108.	120.	90.
16	6.37	0.1	5.60	0.89	0.	0.	106.	108.	118.	90.
17	6.83	1.0	6.37	0.97	0.	0.	106.	108.	117.	90.
18	6.51	9.0	6.67	0.94	0.	0.	106.	108.	118.	94.
19	6.70	12.0	6.10	0.95	0.	0.	107.	108.	119.	90.
20	6.67	18.0	5.11	0.95	0.	0.	107.	108.	118.	92.
21	6.87	31.0	8.30	0.94	0.	0.	108.	108.	118.	91.
22	7.62	58.0	4.52	0.83	0.	0.	110.	108.	124.	86.
23	8.40	63.0	4.71	0.72	0.	0.	112.	108.	122.	86.
24	8.48	65.0	6.35	1.08	0.	0.	113.	113.	127.	91.
25	8.65	72.0	7.48	0.97	0.	0.	113.	108.	122.	108.
26	8.19	66.0	3.13	1.06	0.	0.	112.	104.	119.	120.
27	8.52	85.0	4.32	1.10	0.	0.	113.	109.	122.	113.
28	8.32	61.0	4.11	1.11	0.	0.	113.	109.	123.	107.
29	8.43	46.0	4.43	1.06	0.	0.	113.	108.	120.	99.
30	8.22	63.0	3.94	1.11	0.	0.	112.	108.	123.	94.
31	8.44	67.0	6.16	1.06	0.	0.	113.	108.	121.	94.
32	8.30	63.0	5.84	0.98	0.	0.	112.	107.	120.	100.
33	8.43	62.0	5.67	1.08	0.	0.	112.	107.	121.	100.
34	8.33	62.0	5.03	1.06	0.	0.	112.	107.	120.	97.
35	8.32	57.0	4.21	0.97	0.	0.	111.	106.	119.	95.
36	7.75	58.0	2.19	0.90	0.	0.	110.	104.	118.	93.
37	7.71	58.0	1.75	0.62	0.	0.	110.	104.	117.	89.
38	7.41	54.0	0.87	0.57	0.	0.	99.	90.	115.	515.
39	7.14	42.0	0.89	0.40	0.	0.	100.	91.	116.	520.
40	7.02	54.0	1.27	0.16	0.	0.	98.	90.	114.	520.
41	6.89	42.0	1.37	0.13	0.	0.	100.	92.	115.	510.
42	6.81	42.0	1.21	0.11	0.	0.	98.	91.	114.	525.
43	6.76	44.0	0.95	0.10	0.	0.	98.	91.	114.	520.
44	6.44	47.0	0.	0.06	0.	0.	101.	94.	116.	530.
45	6.43	45.0	0.	0.49	0.	0.	100.	92.	114.	520.
46	6.44	48.0	0.	0.44	0.	0.	98.	91.	114.	530.
47	5.74	42.0	0.	0.21	0.	0.	93.	89.	111.	530.

Table 4. Mercury Balance for Test R-69

In:		
Feed, g	1890	
Out:		
Evaporator, g	648	34.3%
Solid, g	154	8.1%
Off-gas line, g	19	1.0%
Pot top, g	62	3.3%
Hg trap, g	221	11.7%
Condensate, g	57	3.0%
Total	<u>1161</u>	<u>61.4%</u>

Table 5. Control Settings for Test R-69

	Set Point (%)	Prop. Band (%)	Reset Rate (min)
Calciner liquid level	50	200	150
Evaporator liquid level	50	200	20
Evaporator conductivity	80	100	40
Evaporator vapor pressure	40	25	1

2.1.3 Operating Results and Conclusions for Test R-70

Test R-70 was a standard waste-calcination test using Purex-65 feed (Tables 6 and 7). Purex-65 waste has a composition expected in 1965 from formaldehyde-treated Purex waste that has been processed through a fission-product-recovery pilot plant. About 80 gal of Purex-65 waste represents one tonne of uranium, but it has a low salt concentration; it is about a fifth as concentrated as the standard IWW Purex waste which was previously tested.

Because the feed is so dilute in nitrate ion, very little water was added to the evaporator to strip out the nitric acid. The material balances for test R-70 were satisfactory (Table 8), except for mercury. The analyses for mercury in the solid product in the presence of a large amount of iron were erroneous, and, consequently, the material balance was 816%. The other analyses are accurate.

The average feed rate to the calciner system was approximately 40 liters/hr. The maximum feed rate to the system was 200 liters/hr during the first few hours of the test.

The calciner vessel was filled with solids to about 110% of the operating level. The solid level was at about 79 in. at the end of the test, and the controlling liquid-level point for 100% full was 72 in. The bulk density of the solid was 1.25 g/cc, which is about the standard density for Purex waste. The nitrate composition of the solid was 0.02%, which is high, considering that all of the solid was at a temperature with the calcined solids. Calcium nitrate was added to precipitate and hold the sulfate and corresponded stoichiometrically to 10% of the sulfate plus 100% of the phosphate and fluoride in the feed.

The mercury distribution in the system is shown in Table 9. The mercury analysis is uncertain because of the error in the analysis of the solid, but only 17% of the mercury fed to the system was caught in the mercury trap. It is apparent that the mercury trap is not working well because the temperature range for complete desublimation of the mercury is too wide.

When the solid was removed from the calciner, some corrosion was noted on the inside, about 3 or 4 in. from the bottom. A peripheral band about 3 in. wide was corroded, with some parts being as deep as 1/16 in.

2.1.4 Automatic Control for Test R-70

The control for test R-70 was good. The liquid level control for the calciner was exceptionally good. The calciner pot was filled on manual control at a rate of about 60 liters/hr. When the automatic calciner control instrument came on range, the control instrument's output was matched to the manual-control valve setting, and the

Table 6. Composition of the Feed and Calcined Solid from Test R-70

Feed total, 1818 liters
 $\text{Ca}(\text{NO}_3)_2$ total, 12 liters
 Weight of solid, 72 kg
 Additive, $\text{Ca}(\text{NO}_3)_2$, 2.5 M

	Ionic Composition					
	NO_3	Fe	Na	Hg	SO_4	Si
Feed, g/liter	78	11	6	0.7	16	0.2
Solid, wt %						
Top	0.01	25.4	15.0	16.53	30.2	0.4
Middle	0.04	24.6	14.6	14.64	30.8	1.3
Bottom	0.02	25.4	13.8	11.32	32.1	0.4
Average wt %	0.02	25.1	14.4	14.1	31.0	0.7

Table 7

TEST NO	HOURLY SYSTEM VARIABLES AND PARAMETERS - PART A								
	R-70	FEED TYPE -	PUREX	OPERATION MODE -	CONTINUOUS				
RUN TIME HOURS	FEED LITERS	WATER LITERS	CALCINER ADDITIVE LITERS	EVAP. COND. LITERS	CALCINER FURNACE (HUNDRED-THOUSANDS OF BTUS)	CALCINER COND. COND. OF BTUS)	EVAP. COND. COND. OF BTUS)	SYSTEM OFF-GAS CU FT	EVAP. DENSITY GM/CC
1	200.	0.	6.	206.	0.	1.08	5.24	28.	1.24
2	400.	26.	6.	432.	1.37	1.96	10.77	56.	1.29
3	591.	52.	6.	649.	2.87	3.39	15.95	84.	1.31
4	765.	52.	6.	823.	4.30	4.44	21.31	113.	1.33
5	876.	78.	6.	960.	5.60	5.28	26.52	142.	1.25
6	1084.	104.	6.	1194.	6.59	6.11	31.26	171.	1.35
7	1154.	104.	6.	1264.	7.72	6.72	35.88	200.	1.33
8	1223.	130.	6.	1359.	8.61	7.14	36.87	229.	1.30
9	1223.	187.	6.	1416.	9.43	7.58	38.30	259.	1.25
10	1284.	217.	6.	1507.	10.24	8.00	42.60	289.	1.23
11	1367.	274.	6.	1647.	10.83	8.37	43.24	319.	1.17
12	1367.	353.	6.	1726.	11.41	8.73	48.38	349.	1.14
13	1470.	410.	6.	1886.	11.99	8.99	49.59	379.	1.29
14	1496.	410.	6.	1912.	12.60	9.53	51.06	409.	1.27
15	1510.	436.	6.	1952.	12.87	9.70	52.07	439.	1.27
16	1536.	462.	6.	2004.	13.42	9.89	53.39	469.	1.27
17	1564.	481.	6.	2051.	13.93	10.25	54.81	499.	1.27
18	1592.	507.	6.	2105.	14.45	10.61	55.86	529.	1.28
19	1635.	507.	12.	2154.	14.82	10.78	56.66	559.	1.28
20	1666.	533.	12.	2211.	15.33	10.87	57.70	589.	1.28
21	1694.	559.	12.	2265.	15.78	10.96	58.59	619.	1.28
22	1707.	589.	12.	2308.	16.15	11.05	59.37	649.	1.28
23	1735.	589.	12.	2336.	16.43	11.05	60.59	679.	1.28
24	1763.	615.	12.	2390.	16.84	11.05	61.87	709.	1.26
25	1792.	641.	12.	2445.	17.25	11.05	62.89	739.	1.27
26	1804.	641.	12.	2457.	17.66	11.05	63.70	769.	1.30
27	1818.	675.	12.	2505.	17.93	11.05	64.67	799.	1.32
28	1818.	701.	12.	2531.	18.44	11.05	65.26	829.	1.31
29		727.	12.	2557.	18.71	11.05	65.86	859.	1.31
30		753.	12.	2583.	19.19	11.05	66.43	917.	1.30
31		779.	12.	2609.	19.57	11.05	67.26	947.	1.30
32		832.	12.	2662.	19.81	11.13	68.01	977.	1.31
33		858.	12.	2688.	20.05	11.13	68.78	1007.	1.32
34		884.	12.	2714.	20.35	11.13	69.56	1037.	1.32
35		910.	12.	2740.	20.56	11.13	70.36	1067.	1.32
36		963.	12.	2793.	20.83	11.13	71.15	1097.	1.32
37		989.	12.	2819.	21.21	11.13	71.97	1127.	1.31
38		1042.	12.	2872.	21.34	11.13	72.77	1156.	1.30
39		1068.	12.	2898.	21.62	11.13	73.59	1185.	1.30
40		1117.	12.	2947.	21.89	11.13	74.40	1214.	1.30
41		1143.	12.	2973.	22.10	11.13	75.03	1243.	1.29
42		1175.	12.	3005.	22.33	11.13	75.43	1272.	1.28
43		1182.	12.	3012.	22.68	11.13	75.83	1299.	1.28
44		1182.	12.	3012.	160.91	11.13	76.41	1328.	1.28
45		1208.	12.	3038.	23.09	11.13	76.64	1357.	1.25
46		1208.	12.	3038.	23.29	11.13	77.20	1386.	1.24
47		1234.	12.	3064.	23.50	11.13	77.60	1415.	1.26
48		1260.	12.	3090.	23.60	11.13	78.02	1444.	1.27
49		1286.	12.	3116.	23.87	11.13	78.42	1473.	1.27
50		1286.	12.	3116.	24.14	11.13	78.81	1502.	1.27
51		1312.	12.	3142.	24.25	11.22	79.22	1531.	1.27
52		1338.	12.	3168.	24.42	11.22	79.60	1560.	1.27
53		1364.	12.	3194.	24.69	11.22	79.97	1590.	1.27
54		1364.	12.	3194.	24.90	11.22	80.33	1620.	1.27

Table 7 (continued)

TEST NO	HOURLY SYSTEM VARIABLES AND PARAMETERS - PART B									
	NO R-70	FEED TYPE - PUREX		OPERATION MODE - CONTINUOUS						
RUN TIME	EVAP. LIQUID NITRATE	EVAP. MAJOR CATION FE OR AL	CALCINER COND. NITRATE	EVAP. COND. H+	EVAP. COND. MAJOR ION FE OR AL	EVAP. COND. CALCIUM	EVAP. LIQUID TEMP.	EVAP. VAPOR TEMP.	CALCINER FEED TEMP.	CALCINER OFF-GAS TEMP.
HOURS	MOLAR	GM/LITER	MOLAR	MOLAR	GM/LITER	GM/LITER	DEG.C	DEG.C	DEG.C	DEG.C
1	4.35	41.0	0.92	0.24	0.001	0.	101.	104.	95.	215.
2	5.81	55.0	2.40	0.57	0.001	0.	101.	104.	95.	210.
3	6.68	62.0	4.11	0.95	0.001	0.	104.	107.	96.	220.
4	5.92	50.0	4.67	0.94	0.001	0.	105.	108.	97.	215.
5	6.46	60.0	4.59	0.75	0.001	0.	104.	108.	94.	215.
6	6.17	64.0	5.17	1.03	0.001	0.	108.	109.	97.	193.
7	5.19	44.0	5.27	0.59	0.001	0.	106.	106.	93.	198.
8	6.29	42.0	7.87	1.19	0.001	0.	110.	109.	93.	145.
9	5.62	27.0	7.86	1.13	0.001	0.	108.	107.	91.	146.
10	5.29	41.0	5.95	0.75	0.001	0.	105.	107.	89.	143.
11	3.24	29.0	4.43	0.16	0.001	0.	103.	101.	82.	143.
12	6.86	51.0	4.71	0.52	0.001	0.	111.	111.	79.	131.
13	4.78	50.0	5.51	0.43	0.001	0.	106.	102.	92.	138.
14	5.17	46.0	4.49	0.44	0.001	0.	107.	106.	91.	135.
15	5.29	43.0	4.79	0.51	0.001	0.	107.	106.	93.	131.
16	5.43	40.0	5.11	0.75	0.001	0.	108.	107.	93.	130.
17	6.38	50.0	5.62	0.68	0.001	0.	108.	107.	92.	127.
18	5.35	43.0	5.57	0.83	0.001	0.	109.	108.	92.	126.
19	6.57	52.0	5.51	0.73	0.001	0.	108.	107.	93.	123.
20	5.33	43.0	5.44	0.71	0.002	0.	108.	107.	92.	123.
21	6.67	54.0	5.59	0.73	0.001	0.	108.	107.	93.	124.
22	5.54	43.0	6.02	0.71	0.001	0.	108.	107.	93.	121.
23	6.86	53.0	6.10	0.79	0.001	0.	108.	108.	95.	125.
24	5.49	41.0	5.68	0.71	0.001	0.	108.	107.	94.	120.
25	6.52	52.0	5.78	0.68	0.001	0.	108.	108.	93.	115.
26	6.43	52.0	9.51	1.35	0.002	0.	110.	109.	96.	115.
27	7.76	69.0	7.94	1.14	0.001	0.	111.	109.	100.	125.
28	5.52	52.0	5.49	0.75	0.002	0.	110.	107.	91.	500.
29	6.79	67.0	3.22	0.56	0.002	0.	108.	106.	91.	510.
30	6.48	65.0	3.03	0.43	0.002	0.	108.	105.	90.	510.
31	5.38	54.0	7.35	0.44	0.001	0.	108.	106.	91.	515.
32	5.48	54.0	10.43	0.49	0.001	0.	109.	106.	93.	515.
33	5.30	52.0	13.16	0.57	0.001	0.	108.	106.	93.	505.
34	5.37	53.0	13.78	0.52	0.001	0.	108.	106.	92.	510.
35	5.29	53.0	13.49	0.40	0.001	0.	108.	105.	92.	510.
36	5.08	51.0	12.30	0.29	0.001	0.	107.	104.	91.	515.
37	4.95	52.0	10.83	0.21	0.001	0.	105.	104.	92.	515.
38	4.70	52.0	9.25	0.16	0.001	0.	107.	104.	91.	510.
39	4.68	52.0	8.02	0.13	0.001	0.	105.	103.	91.	515.
40	5.35	60.0	6.92	0.10	0.001	0.	105.	102.	91.	515.
41	4.37	51.0	6.03	0.08	0.001	0.	105.	102.	90.	510.
42	5.05	58.0	5.51	0.05	0.001	0.	104.	101.	91.	515.
43	0.	-0.	0.	0.	-0.	0.	104.	101.	91.	500.
44	4.13	25.0	6.62	0.32	0.001	0.	104.	100.	90.	505.
45	4.40	22.0	3.40	0.25	0.001	0.	105.	100.	89.	510.
46	4.29	22.0	3.40	0.25	0.001	0.	103.	100.	88.	515.
47	4.29	21.0	3.40	0.25	0.001	0.	104.	100.	90.	500.
48	4.11	20.0	4.10	0.29	0.001	0.	104.	101.	89.	510.
49	5.81	31.0	4.10	0.49	0.001	0.	104.	101.	90.	510.
50	5.57	29.0	4.05	0.54	0.001	0.	104.	101.	90.	505.
51	4.49	23.0	1.56	0.27	0.001	0.	104.	101.	90.	510.
52	4.14	20.0	3.16	0.22	0.001	0.	104.	101.	90.	505.
53	4.08	20.0	2.87	0.24	0.001	0.	104.	100.	89.	500.
54	3.89	20.0	2.75	0.19	0.001	0.	104.	100.	90.	510.

Table 8. Material Balance for Test R-70

	Ions					
	NO ₃	Fe	Na	Hg	SO ₄	Si
In:						
Feed, g	142,000	20,000	10,900	1,272	29,200	364
Ca(NO ₃) ₂ g	3,600					
Out:						
Solid, g	14	18,000	10,500	10,050	22,300	490
Evap., g	7,930	1,440	540	87	1,420	13
Cond., g	117,500	6	2	90	20	--
Off-gas, g	--	--	--	216	--	--
Total, g	125,444	19,446	11,042	10,443	23,740	503
Balance, %	88.1	97.4	105	786	82.0	139

Table 9. Distribution of the Mercury in Test R-70

In:			
Feed	0.7 g/liter (1818 liters)		1,272 g
Out:			
Solid		10,050 g	792%
Evap.bottom		87 g	7%
Condensate		--	
System piping			
Off-gas line	18 g		
Hg trap	208 g	226 g	17%
Total	226 g	10,363 g	816% ^a

^aAnalysis of the solid for mercury involved a nitric acid leach, which allowed iron to contaminate the sample and give erroneously high results for mercury.

instrument was switched to automatic control of feed without any sign of upset. The other four control variables also controlled well. control settings are listed on Table 10. The evaporator conductivity

Table 10. Control Conditions for Test R-70

	Prop. Band (%)	Reset Rate (min)	Set Point (% of Scale)	Scale of System (%)		Acceptable Range of Operation (% of scale)	
				0	100	Upper	Lower
Calciner liq. level	200	150	50	58 (liters)	62	95	20
Evap. Density	100	5	26	1.0 (g/cc)	2.0	31	21
Evap. liq. level	100	10	50	22 (liters)	27	70	30
Evap. conductivity	100	10	50	1.2 (molar)	2.0	65	35
Evap. pressure	20	1	40	-5 (psig)	+5	42	38

instrument did not come on control range except for one or two short periods because of the great amount of water in this feed.

Toward the end of the test, the calciner feed-line purge was turned off through an oversight. Toward the end of the test the calciner feed valve closed. With no purge in the calciner feed line, the remaining feed in the calciner feed line calcined, causing a plug. Application of 300-psi pressure did not remove the plug, and the feed to the calciner was then terminated. Examination after the test showed that the plug was about an inch long and at the very tip of the calciner feed line. The plug was removed by driving a rod through it, but only with great difficulty.

2.2 Mechanical Test Program

J. M. Holmes E. J. Frederick J. O. Blomeke

Testing of the mechanical operations associated with the processing of high-level waste by pot calcination in the Hanford Hot Pilot Plant is being carried out by Georgia Nuclear Laboratories, Dawsonville, Georgia, for ORNL. Demonstration equipment installed

in a prototype hot cell at GNL (Fig. 2.1) includes a remotely operated filling station and a furnace dolly (containing a calciner pot) that automatically centers itself beneath the filling station and raises and lowers the pot to predetermined positions in which certain operations are conducted.

Positioning tests on the dolly were completed and previously reported results verified. Connect-disconnect tests with the gasketed head at ambient temperature and at 900°C were completed. Leak rates were too small to measure by the rotameter. Rate of pressure change was used to determine the extent and location of leakage, that is whether the leakage was past the gasket or inleakage through the pot clamp. Average maximum temperatures at various locations on the pot and filling station are reported in Table 11.

Table 11. Temperature Profile of Components of the Pot Calciner

Maximum pot temperature	- 953°C
Maximum pot temperature above support ring	- 532°C
Maximum temperature filling cap body	- 307°C
Maximum temperature filling cap base	- 172°C
Maximum temperature inside feed line (upper)	- 50°C at 13-liter/hr H ₂ O flow
Maximum temperature inside feed line (lower)	- 36°C at 13-liter/hr H ₂ O flow
Maximum temperature dust cap actuator	- 57°C
Maximum clamp temperature	- 105°C
Maximum slide mechanism temperature	- 72°C
Maximum bearing block temperature	- 61°C
Maximum screw ball temperature	- 52°C
Maximum limit switch temperature	- 77°C
Filling station base near center (top)	- 71°C
Filling station base near center (bottom)	- 331°C
Filling station base near outer edge (top)	- 55°C
Filling station base near outer edge (bottom)	- 127°C
Δ temperature filling station base cooling water	- 1°C
Δ temperature filling cap cooling water	- 23°C
Maximum time to cool pot wall from 950°C to 300°C	- 1:40 at 860 liters/min at 50 psi air

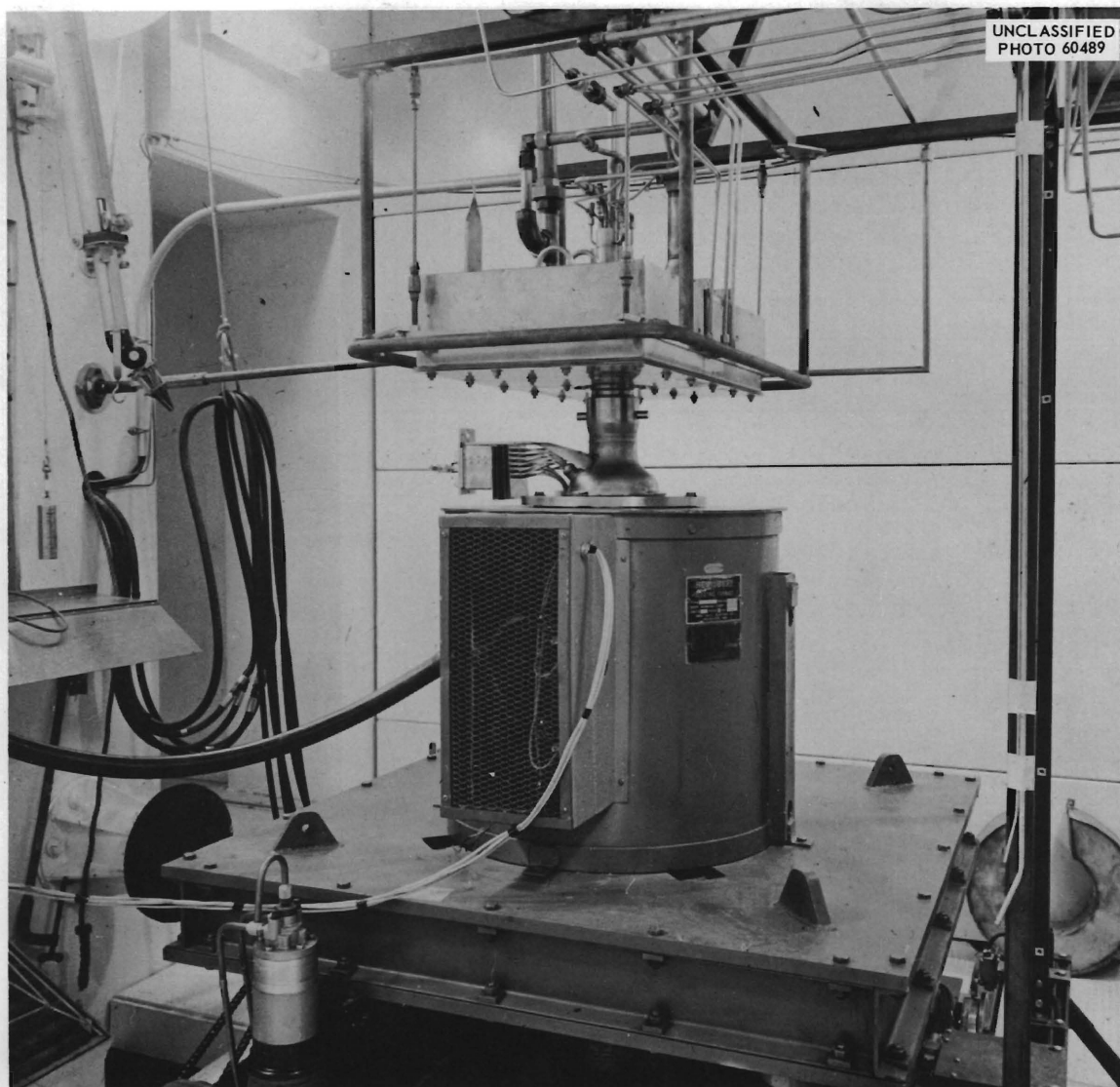


Fig. 2.1. Mockup of Mechanical Equipment Associated with the Processing of High-Level Waste (Georgia Nuclear Laboratories).

Remote maintenance concepts were developed and tested for the in-cell repair of the filling-station components. Table 12 lists the remote-handling operations completed and the time and tools required to perform them.

2.3 Fixation in Glass

W. E. Clark H. W. Godbee J. F. Easterly

2.3.1 Batch Studies

Continuing studies on fixation of high-sulfate Purex waste confirmed the general conclusion that a chemical excess of acid network formers (i.e., P_2O_5 , B_2O_3 , SiO_2) over alkali and alkaline earth oxides results in volatilization of a large fraction of the sulfate and that these conditions are necessary if the product is to have a glassy structure. On the other hand, very satisfactory products were prepared from melts that had a chemical excess of alkali and alkaline earth oxides and which retained nearly all the sulfate. These may contain as much as 43% waste oxides; a series of phosphate and borophosphate melts containing 35% waste oxides (Table 13) showed no improvement over earlier melts that contained 39 to 43% waste oxides. For example, none of the 35% products appeared to offer any improvement over the previously reported material (Quarterly Report, July-Sept. 1962, Melt No. 3, Table 1), which contained 42.6% waste oxides, 26.4% P_2O_5 , 9.0% MgO , 3.6% B_2O_3 and 18.5% added Na_2O . Weight loss of this specimen on heating to 980°C for 100 min was equivalent to 7.7% of the SO_3 theoretically present in the melt. A limited number of trials made with lead and barium additives rather than calcium produced no noticeable improvement of the product (Table 14). The few scouting melts made with silicate (Table 15) have not yet been analyzed thermogravimetrically.

2.3.2 Semicontinuous Fixation

One semi-engineering scale fixation was carried out on simulated Darex waste (composition, molarity): 0.7 H^+ , 1.21 Fe^{3+} , 0.36 Cr^{3+} , 0.18 Ni^{2+} , 0.04 Mn^{2+} , 0.002 Ru , and NO_3^- to balance) with the addition of sodium hypophosphite, phosphorous acid, aluminum nitrate and boric oxide to produce a melt. The product had a nominal composition of 25.0% waste oxides, 35.3% P_2O_5 , 13.2% Al_2O_3 , 13.2% Na_2O and 13.2% B_2O_3 . Previously reported small-scale studies² resulted in the formation of a very hard and mechanically strong solid product with a softening temperature of about 850°C and a bulk density of 2.65. The volume reduction expected from the waste solution was between 4.5 and 5.0.

Operation of the semi-engineering scale experiment (4- x 24-in. pot) was discontinued after about 14 liters of feed (representing about 9.4 liters of waste) had been fed in because calculation indicated that the pot should be about two-thirds full though the sensing

Table 12. Remote Handling of the Pot-Calciner Mockup

Operation	Time Required	Tools
Pot thermocouple connector - connect-disconnect	15 sec	GNL designed connector and two model 8 manipulators
Dust cap installation	2 sec	One model 8 for cap insertion More than 2 sec if cap cocks in well On Dec. 12, 75% of cap insertions were successful; on Dec. 13, after installation of filler beneath slider, 100% of cap insertions were successful in 100 tests.
Pot screw cap installation	1.3 min	Special wrench and two model 8 manipulators
Filling station disassembly Disconnected 1-in. vacuum line, two 1/2-in. fill lines, two 1/4-in. water lines, two 3/8-in. water lines, cap heater lines, and removed LS-8 limit switch	4.6 hr	Standard hot-cell tools
Disconnected 1-1/2-in. vent lines (2) and filling-station air supply "tee", and removed F.S. cap and cap deck	1.5 hr	Standard hot-cell tools
Removed clamp assembly, including screw, bearings, and springs; removed slide assembly and cap-loader actuator	1.7 hr	Standard hot-cell tools

Table 13. Fixation of High-Sulfate Purex Waste in Phosphate and Borophosphate Solids Containing 35% by Weight Waste Oxides

	Number													
	1A	2A	3A	4A	1B	2B	3B	4B	1C	2C	3C	1D	2D	3D
Additives (moles/liter)														
NaH ₂ PO ₂	2.10	2.21	2.20	2.18	1.33	1.50	1.75	2.00	2.00	2.00	2.00	--	--	--
NaH ₂ PO ₄	--	--	--	--	--	--	--	--	--	--	--	1.33	1.50	1.75
NaOH	--	--	0.40	0.80	0.68	0.55	0.36	0.16	0.08	0.55	0.94	1.46	1.33	1.14
Na ₂ B ₄ O ₇	--	--	--	--	0.34	0.275	0.18	0.08	0.04	0.075	0.07	0.33	0.265	0.17
Ca(NO ₃) ₂	1.00	0.80	0.60	0.40	0.80	0.80	0.80	0.80	1.00	0.60	0.40	0.40	0.40	0.40
Wt % Waste Oxides	35.0	35.0	35.0	35.1	35.0	35.0	35.0	35.0	35.1	35.1	35.1	35.0	35.0	35.0
Composition of Product (Wt % Oxides, theoretical)														
Na ₂ O	20.1	21.0	23.9	26.7	24.5	23.9	22.9	21.8	20.3	24.6	27.5	30.2	29.5	28.5
Al ₂ O ₃	1.2	1.2	1.2	1.2	1.2	1.2	1.2	1.2	1.2	1.2	1.2	1.2	1.2	1.2
CaO	13.5	10.8	8.1	5.4	10.8	10.8	10.8	10.8	13.5	8.1	5.4	5.4	5.4	5.4
Fe ₂ O ₃	9.6	9.6	9.6	9.6	9.6	9.6	9.6	9.6	9.6	9.6	9.6	9.6	9.6	9.6
Cr ₂ O ₃	0.2	0.2	0.2	0.2	0.2	0.2	0.2	0.2	0.2	0.2	0.2	0.2	0.2	0.2
NiO	0.2	0.2	0.2	0.2	0.2	0.2	0.2	0.2	0.2	0.2	0.2	0.2	0.2	0.2
RuO ₂	0.1	0.1	0.1	0.1	0.1	0.1	0.1	0.1	0.1	0.1	0.1	0.1	0.1	0.1
SO ₃	19.3	19.3	19.3	19.3	19.3	19.3	19.3	19.3	19.3	19.3	19.3	19.3	19.3	19.3
P ₂ O ₅	35.9	37.7	37.6	37.3	22.7	25.6	29.9	34.2	34.2	34.2	34.2	22.7	25.6	29.9
B ₂ O ₃	--	--	--	--	11.4	9.2	6.0	2.7	1.3	2.5	2.3	11.1	8.9	5.7
	100.1	100.1	100.2	100.0	100.0	100.1	100.1	100.1	99.9	100.0	100.0	100.0	100.0	100.0
Excess cation equivalents	0.6	0.19	0.20	0.20	0.20	0.20	0.20	0.20	0.60	0.20	0.20	0.20	0.20	0.20
Excess anion equivalents	--	--	--	--	--	--	--	--	--	--	--	--	--	--
Ratio: $\frac{(g \text{ eqs. Na}^+ + \text{Ca}^{+2})}{(g \text{ eqs. SO}_4^{2-} + \text{PO}_4^{3-} + \text{BO}_3^{3-})}$	1.15	1.05	1.05	1.05	1.04	1.04	1.05	1.05	1.14	1.05	1.05	1.04	1.04	1.05
Approx. Softening Temp., °C.	900	850	800	825	925	900	875	850	875	775	775	800	850	800
Approx. Melting Temp., °C.	925	900	850	875	975	950	925	900	875	825	825	825	875	850
Maximum TGA Temp., °C.	--	--	--	--	1100	1100	1100	1100	1100	1100	1100	--	--	--
% SO ₂ Loss for 100 min at Maximum Temp.	--	--	--	--	48.5	70.4	99%	100%	~84%	~88%	72.2%	--	--	--
Description	Gray-green crystal-line; brown material segregated.	Gray, hard crystal-line.	Gray, hard crystal-line. Some fuming noted.	Gray, crystal-line, hard. Some fuming.	Brown crystal-line rock.	Porous green crystal-line rock.	Brown-green, crystal-line. Gassing at ~900°. Many voids.	Green, near glassy, some voids. Gassing at ~900°.	Greenish, crystal-line rock. Some voids. Gassing at ~900°.	Green, crystal-line rock. Some voids. Gassing at ~800°.	Green, crystal-line, hard rock. Some voids. Gassing at ~800°.	Light green crystal-line.	Light brown crystal-line.	Gray, crumbly crystal-line.

25

Table 14. Scouting Experiments in the Fixation of High-Sulfate Purex Waste

	Number							
	1	2	3	4	5	6	7	8
Additives, moles/liter								
NaH ₂ PO ₂	2.0							3.0
NaH ₂ PO ₄						5.0	2.0	
H ₃ PO ₃		2.0	3.48	2.42	2.22			
Na ₂ B ₄ O ₇ ·10H ₂ O						0.325		0.5
H ₃ BO ₃		0.12	0.18	0.12	0.12	--	0.13	--
B ₂ O ₃								--
Al(NO ₃) ₃ ·9H ₂ O			0.46	0.06	0.06	4.05	1.62	3.0
Ba(NO ₃) ₂		1.06	0.80	0.80	0.80			0.5
Ca(NO ₃) ₂						0.8	0.8	
Pb(NO ₃) ₂	1.0							
NaOH						0.65	0.26	
Weight % Waste Oxides	25.4	32.0	26.7	32.5	33.6	14.7	29.7	19.8
Composition of Product (Wt % oxides, theoretical)								
Na ₂ O	14.1	4.1	3.4	4.2	4.3	21.6	18.1	19.4
Al ₂ O ₃	0.9	1.1	5.2	1.8	1.9	21.3	17.9	21.5
BaO	--	35.8	22.5	27.4	28.3			4.2
CaO	--	--	--	--	--	4.5	9.2	
PbO	39.0	--	--	--	--			
Fe ₂ O ₃	7.0	8.8	7.3	8.9	9.2	4.0	8.2	5.4
Cr ₂ O ₃	0.1	0.2	0.1	0.2	0.2	0.1	0.2	0.1
NiO	0.1	0.2	0.1	0.2	0.2	0.1	0.2	0.1
RuO ₂	0.1	0.1	0.1	0.1	0.1	0.1	0.1	0.1
SO ₃	14.0	17.6	14.7	17.9	18.5	8.1	16.4	10.9
P ₂ O ₅	24.8	31.3	45.3	38.4	36.4	35.8	29.0	28.9
B ₂ O ₃	--	0.9	1.2	0.9	1.0	4.6	0.9	9.5
	100.0	100.1	99.9	100.0	100.1	100.1	100.2	100.0
Excess Cation equiv. (incl. Pb)	0.60	--	--	--	--	0.20	0.33	--
Excess Anion equiv.	--	1.40	3.46	2.34	2.14	--	--	1.40
Ratio: $\frac{(g \text{ eq. Na}^+ + \text{Ca}^{++} + \text{Ba}^{++} + \text{Pb}^{++})}{(g \text{ eq. SO}_4^{--} + \text{PO}_3^{--} + \text{BO}_3^{--})}$	1.15	0.66	0.33	0.49	0.51	1.02	1.03	0.80
Approx. Softening temp. (°C).	800	900	900	not carried to melting	not carried to melting	900	950	800
Approx. Melting temp. (°C).	850	1000	1000	not carried to melting	not carried to melting	--	incomplete 1050	950
Description	Light gray, crystal-line.	Dark gray, partly glassy. Gassing at ~600°.	Green, partly glassy. Gassing at ~600°.	Gassed profusely at ~600°.	Gassed profusely at ~600°.	Highly segregated.	Partly glassy, segregated, very fluid.	Glassy segregated, brown, very fluid. Lost 90% SO ₃ at 1100°.

Table 15. Phosphosilicate Melts Containing 40% Oxides from Simulated High-Sulfate Purex Waste

	Si-1	Si-2	Si-3	Si-4
Additives, moles/liter				
H ₃ PO ₃	2.31	2.05	1.79	1.54
NaOH	1.66	2.24	2.83	4.16
SiO ₂	0.363	0.363	0.363	0.363
Weight % waste oxides	40.0	40.0	40.0	40.0
Nominal Composition of Product, wt % theoretical				
Al ₂ O ₃	1.4	1.4	1.4	1.4
Na ₂ O	14.1	19.1	24.1	29.1
Fe ₂ O ₃	11.0	11.0	11.0	11.0
Cr ₂ O ₃	0.2	0.2	0.2	0.2
NiO	0.2	0.2	0.2	0.2
RuO ₂	0.1	0.1	0.1	0.1
SO ₃	22.0	22.0	22.0	22.0
P ₂ O ₅	45.0	40.0	35.0	30.0
SiO ₂	6.0	6.0	6.0	6.0
Totals	100.0	100.0	100.0	100.0
Ratio: $\frac{(g \text{ eqs } Na^+)}{(g \text{ eqs } PO_3^- + SiO_3^- + SO_4^{2-})}$	0.449	0.598	0.761	1.12
Approx. softening temp., °C	950	900	825	825
Approx. melting temp., °C	1050	1000	900	900
Description of the Melts				
	Light-brown rock; internal voids	Very glassy but segregated; dark green	Smooth textured, almost white; rock like	---

thermocouples failed to confirm this. Upon cooling, the fixation pot was found to have expanded, so that it was necessary to remove the stainless steel liner from the furnace along with the pot. Removal of the pot from the liner was difficult. Upon examination it was found that the level of solid in the pot was not nearly so high as had been calculated. The pot was, therefore, returned to the unlined furnace, and operation was continued until a total of 21.7 liters of feed had been fed in. At this time, the pot was slightly more than half full. The volume of solid product corresponding to the filling was 2.83 liters, which indicates a volume reduction of 5.17 and a density of 2.64 g/cc. Ruthenium volatility was 15.4% of the total added.

Upon examination the pot was found to have corroded through at a point corresponding closely to the level reached by the solid when operation was first suspended. The 1-in.-diam internal tube had also corroded through at about this same point. (A detailed investigation of the failure will be made when the pot is sectioned.) It is postulated that corrosion at about the initial solid level was accelerated by the stress caused by expansion of the solid product on cooling. This appears likely since there was no particular indication of corrosion prior to the first shutdown. The use of an unusually high temperature, 1060°C maximum, for fixation may also have played a part in accelerating the corrosion. There was no loss of solution nor any apparent loss of gas at the point of failure, though the diameter of the perforation was about 1.5 in. This indicates that the solid was almost completely dry when penetration occurred.

2.3.3 X-Ray Examination of Solid Products (Work done by the Ferro Corp. of Cleveland Ohio under the direction of R. W. Pelz.)

Seven solid products of previously reported compositions (Table 16) were submitted to the Ferro Corporation for x-ray analysis. While the phase relationships cannot be accurately deduced from this data, it appears that the amount of crystalline sodium sulfate was generally increased by the addition of magnesium and was decreased or eliminated by the addition of calcium. Relatively large percentages of borate and magnesium appear to have caused the separation of crystalline Fe_2O_3 .

The probable existence of hydrates in this material may explain the accelerated corrosion that has occasionally been observed in small-scale batch studies, particularly in the presence of magnesium. There is, unfortunately, a possibility that the hydrate observed was formed by absorption of atmospheric moisture during preparation of the specimens for shipment.

2.3.4 Hanford 1965 Formaldehyde-Treated Purex Waste (FTW)

Studies were initiated on the fixation properties of the waste type expected to be generated at Hanford by 1965. The principal

Table 16. Nominal Compositions and Results of X-Ray Investigations of Solids Prepared from Simulated High-Sulfate Purex Waste

	Melt Number						
	1	2	3	4	5	6	7
	Waste Oxides (W.O.), wt %						
Fe ₂ O ₃	11.4	10.7	10.7	11.9	10.4	11.8	11.7
NiO	0.2	0.2	0.2	0.2	0.2	0.2	0.2
Cr ₂ O ₃	0.2	0.2	0.2	0.2	0.2	0.2	0.2
Al ₂ O ₃	1.5	1.4	1.4	1.5	1.3	1.5	1.5
NO ₂ O	5.3	5.0	5.0	5.5	4.8	5.5	5.4
SO ₃	22.9	21.5	21.6	23.9	20.9	23.7	23.5
RuO ₂	0.1	0.1	0.1	0.1	0.1	0.1	0.1
% W.O.	41.6	39.1	39.2	43.3	37.9	43.0	42.6
	Theoretical Additive Oxides, wt %						
NO ₂ O	14.8	16.8	10.3	19.6	29.6	15.6	19.3
CaO	--	--	16.6	--	--	--	6.6
MgO	9.2	8.7	--	4.8	4.2	9.5	--
P ₂ O ₅	30.9	29.0	28.9	32.2	28.2	31.9	31.6
B ₂ O ₃	3.4	6.4	5.2	--	--	--	--
Total	99.9	100.0	100.2	99.9	99.9	100.0	100.1
	Species Indicated by X-Ray						
Na ₂ SO ₄	minor	minor (>No.1)	--	sig.	sig. (=No.4)	minor	trace?
Fe ₂ O ₃	sig.	major	--	trace	trace (<No.4)	sig. (=No.1)	minor
Acid sodium orthophosphate	--	--	--	--	major	trace?	sig.
α-calcium orthophosphate	--	--	sig.	--	--	--	trace
β-calcium orthophosphate	--	--	minor	--	--	--	--
Unknown "d" ^a							
3.44	sig.	sig.	--	--	--	minor	--
5.37	sig.	sig.	--	trace	--	sig.	--
6.18	major	major	--	minor	trace	major	--
Approx. softening Temp.(°C)	850	840	900	830	875	850	900
Pouring temp.	900	900	950	900	900	1000	1000
% SO ₃ lost at 950°C (100 min)	63.0	51.2	42.1	53.2	9.54	45.4	44.8

^aPattern was similar to Mg₃(PO₄)₂·3H₂O but was shifted enough to cause suspicion of a solid solution with Fe₂O₃ or some other iron compound.

differences between this waste and the high-sulfate Purex wastes heretofore studied are that the FTW waste is more dilute (about 82 gal per ton of uranium processed) and that it consists of 0.15 M Na_2SO_4 , in 0.5 M HNO_3 , with 0.1 M $\text{Fe}(\text{NO}_3)_3$, smaller amounts of Al^{3+} , Cr^{3+} , Ni^{2+} and Hg^{2+} nitrates, plus small amounts of phosphate, fluoride, and silicate (Table 17).

Preliminary boildown studies indicated that the waste solution can be volume-reduced by a factor of 4 without visible precipitation of solids from the solution, even on cooling. Reduction of volume by a factor of 8 resulted in the precipitation of solids. Vapor-liquid equilibria for the original waste solution and for the solutions that had been volume-reduced by factors of 2 and 4 were determined by distillation in a Gillespie equilibrium still. The results (Table 18) indicated that there was appreciable entrainment in the nonequilibrium boildown experiments. Apparent ruthenium volatility was much greater for the boildown experiments than anticipated for equilibrium distillation, but the ruthenium found in the one Gillespie still distillate which contained a measureable concentration corresponded almost exactly to that predicted from previous Gillespie-still studies with nitric acid solutions.³ Volatilization of sulfate was negligible in all cases of equilibrium distillation. The reported volatilization of 0.014 g of mercury per liter in the equilibrium distillation of the waste, volume reduced by a factor of 4 (pot temperature, 105°C; still head temperature, 106°C), appears to be questionable in view of previous difficulties with mercury analysis.

Three scouting calcinations were made on the waste with and without added calcium oxide and magnesium oxide. Calcinations were carried to 650°C, the condensates were collected and analyzed for ruthenium, and the solid was analyzed thermogravimetrically to 1100°C. The results (Table 19) indicate that with this particular waste composition, additives are of value only if they improve the density, insolubility and/or other physical properties of the product.

Two series of experimental fixation experiments were run to determine meltdown characteristics and thermal stabilities. Both series incorporated 45% by weight of waste oxides and 30% by weight of P_2O_5 . One series contained a total of 27.2% Na_2O , the other 22.2%. Calcium, magnesium and aluminum oxides were the variables (Table 20). The results confirm the supposition that in general a high sodium content lowers the softening temperature and improves retention of sulfate. The greatest sulfate loss from the high-sodium series was 12.4%, while the smallest from the low-sodium series was 19.7%.

2.4 Removal of Mercury from Waste Solutions

Since mercury forms no compounds that are stable at high temperatures, any mercury in the waste solution can be expected to collect in the evaporator or in the off-gas line from the fixation pot. Experiments performed on both laboratory- and unit-operations

Table 17. Compositions of Simulated High-Sulfate Purex and 1965 FTW Purex Waste Solutions

Constituent	Molarity of Constituents	
	High-Sulfate Purex Waste ^a	1965 FTW Purex Waste ^b
H ⁺	5.6	0.5
Na ⁺	0.6	0.3
Al ³⁺	0.1	0.05
Fe ³⁺	0.5	0.10
Cr ³⁺	0.01	0.02
Ni ²⁺	0.01	0.01
Hg ²⁺	Not specified	0-0.0035
SO ₄ ²⁻	1.0	0.15
PO ₄ ³⁻	Not specified	0.005
SiO ₃ ²⁻	Not specified	0.01
F ^{-c}	Not specified	0.02
NO ₃ ⁻	To balance	To balance

^aForty gallons represents 1 ton of uranium.

^bEighty-two gallons represents 1 ton of uranium.

^cThese are the compositions of the solutions employed in the tests reported here.

Table 18. Boildown Data for Hanford 1965 FTW Purex Waste Solution Initial Volume 250 ml

Volume of Condensate (ml)	Final Boiling Temp. (°C)	Ru in Condensate (mg/ml)	% of Total Ru Volatilized	SO ₄ ²⁻ Condensate (ppm)	F ⁻ in Condensate (ppm)
140	165	2 x 10 ⁻⁵	--	0.01	50
160	175	2 x 10 ⁻⁵	--	0.01	50
180	175	3 x 10 ⁻⁵	--	0.01	50
200	180	1.8 x 10 ⁻⁴	0.007	0.01	50
220	180	6.2 x 10 ⁻⁴	0.024	0.01	50
240	200	7.3 x 10 ⁻³	0.28	0.01	50
250	200	0.46	8.8	0.01	50
260	240	1.80	34.3	0.01	75

Table 19. Volatilization of Sulfur Trioxide and Ruthenium from Scouting Calcinations of 1965 FTW Waste

Material Calcined	% SO ₃ Lost (1100°C)	% Ru Lost (650°)
Waste, no additive	3.5	5.4
Ca additive ^a	3.3	12.3
Mg additive ^a	8.9	8.6

^aTo the waste solution sufficient CaO or MgO was added to fulfill the expression:

$$\frac{\text{equivalents Ca}^{2+} \text{ (or Mg}^{2+}) + \text{Na}^+}{\text{equivalents SO}_4^{2-} + (6\text{x}\text{F}^-) + \text{PO}_3^- + \text{SiO}_3^{2-}} = 1.1.$$

scales indicated that it will probably be impractical to trap more than about 50% of the mercury in the off-gas line when operating a semicontinuous fixation process.

A series of scouting experiments indicated the feasibility of removing more than 99% of the mercury by passing 1965 FTW waste through a column packed with copper turnings and copper shot. Copper in the effluent analyzed 0.054 M, 4 times more than the stoichiometric amount required for displacement of mercury. In a test on "acid-killed" Purex solution, the column soon plugged, apparently because of local supersaturation with copper sulfate. Modification of the method to allow extension of its use to the more concentrated waste will be investigated.

2.5 Corrosion

Work Done by P. D. Neumann, Reactor Chemistry Division

A type 304L stainless-steel calcination pot was subjected to an evaporation-calcination cycle with synthetic Hanford 1965 FTW Purex waste while loaded to 315 lb/in.². After heating to 1050°C for 96 hr, one side of the pot showed an elongation of 1.49 x 10⁻³ in./in., while the other side showed no measurable change. This indicates that the total elongation in an 8-ft pot over a normal evaporation-calcination cycle (estimated as ≤ 48 hr) should be less than 0.1 in.

Welded specimens of type 304L stainless steel, titanium 45A, and Hastelloy F exposed in solution, at the interface, and in the vapor of simulated 1965 FTW waste showed weight gains that varied from 0.2 mg/cm² for Hastelloy F exposed for 552 hr in the vapor to 5 mg/cm² for titanium-45A exposed for 840 hr in the solution. Coupled specimens

Table 20. Fixation Experiments on Simulated Hanford PW 1965 Purex Waste Solution Product to Contain 45% Waste Oxides by Weight

Waste Composition, M: 0.5 H⁺, 0.3 Na⁺, 0.05 Al³⁺, 0.10 Fe³⁺, 0.02 Cr³⁺, 0.01 Ni²⁺, 0.0035 Hg²⁺, 0.15 SO₄²⁻, 0.005 PO₄³⁻, 0.01 SiO₃²⁻, 0.02 F⁻, NO₃⁻ to balance.

	Number										
	A-1	A-2	A-3	A-4	A-5	B-1	B-2	B-3	B-4	B-5	B-6
Additives, moles/liter											
H ₃ PO ₃	0.34	0.34	0.34	0.34	0.34	0.34	0.34	0.34	0.34	0.34	0.34
NaOH	0.38	0.38	0.38	0.38	0.38	0.26	0.26	0.26	0.26	0.26	0.26
Ca(OH) ₂	0.07	0.14	0.07	--	--	0.21	0.14	0.07	--	0.14	--
MgO	--	--	0.10	0.20	0.10	--	0.10	0.20	0.30	--	0.20
Al(NO ₃) ₃ ·9 H ₂ O	0.08	--	--	--	0.08	--	--	--	--	0.08	0.08
Weight % Waste Oxides	45.0	45.0	45.0	45.0	45.0	45.0	45.0	45.0	45.0	45.0	45.0
Oxides, Weight % Theoretical ^a											
Al ₂ O ₃	7.9	2.9	2.9	2.9	7.9	2.9	2.9	2.9	2.9	7.9	7.9
CaO	5.0	10.0	5.0	--	--	15.0	10.0	5.0	--	10.0	--
MgO	--	--	5.0	10.0	5.0	--	5.0	10.0	15.0	--	10.0
Na ₂ O	27.2	27.2	27.2	27.2	27.2	22.2	22.2	22.2	22.2	22.2	22.2
Fe ₂ O ₃	10.0	10.0	10.0	10.0	10.0	10.0	10.0	10.0	10.0	10.0	10.0
Cr ₂ O ₃	1.9	1.9	1.9	1.9	1.9	1.9	1.9	1.9	1.9	1.9	1.9
NiO	0.5	0.5	0.5	0.5	0.5	0.5	0.5	0.5	0.5	0.5	0.5
RuO ₂	0.4	0.4	0.4	0.4	0.4	0.4	0.4	0.4	0.4	0.4	0.4
SO ₂	15.7	15.7	15.7	15.7	15.7	15.7	15.7	15.7	15.7	15.7	15.7
P ₂ O ₅	30.9	30.9	30.9	30.9	30.9	30.9	30.9	30.9	30.9	30.9	30.9
SiO ₂	0.1	0.1	0.1	0.1	0.1	0.1	0.1	0.1	0.1	0.1	0.1
F ⁻	0.5	0.5	0.5	0.5	0.5	0.5	0.5	0.5	0.5	0.5	0.5
Ratio: $\frac{(g \text{ equiv. Na}^+ + \text{Ca}^{+2} + \text{Mg}^{+2})}{(g \text{ equiv. PO}_4^{3-} + \text{SO}_4^{2-} + \text{F}^- + \text{SiO}_3^{2-})}$	1.24	1.45	1.53	1.61	1.32	1.46	1.55	1.63	1.71	1.26	1.42
Approx. softening temp. (°C)	850	900	900	875	850	950	950	925	925	925	900
Approx. melting temp. (°C)	900	950	950	925	900	1050	1050	1000	1000	1000	950
Max. TGA temp. (°C)	950	980	980	960	950	1100	1100	1100	1100	1100	980
% SO ₃ loss for 100 min at max. temp.	9.2%	9.0%	9.6%	9.6%	12.4%	33.2%	29.9%	38.8%	28.7%	44.3%	19.7%
Description	Hard micro-crystal-line rock, dark brown.	Hard micro-crystal-line rock, dark brown.	Hard micro-crystal-line rock, Black.	Hard, micro-crystal-line rock, Gray.	Crystal-line rock, Brown.	Very hard micro-crystal-line rock, Gray.	Very hard micro-crystal-line rock, Black.	Very hard, micro-crystal-line rock, Brown-black.	Segregated, yellow-brown, micro-crystal-line.	Brown, micro-crystal-line rock.	Mottled, rock-like. Corrosion of crucible evident.

^a Assumes all Hg to be volatilized.

of titanium 45A and type 304L stainless steel likewise gained weight. Upon defilming, the type 304L stainless steel specimens were found to have corroded at rates of 0.41, 0.34, and 0.14 mil/month for specimens exposed for 192 hr in the vapor, at the interface, and in the solution, respectively.

3. LOW-LEVEL WASTE TREATMENT

A scavenging-ion exchange process^{4,5} is being developed for decontaminating the large volumes of slightly contaminated water produced in nuclear installations, with ORNL low-activity-waste as a medium for study. The process uses phenolic resins, as opposed to polystyrene resins, since the phenolic resins are much more selective for cesium in the presence of sodium; the Cs/Na separation factor is 160 for phenolic groups and 1.5 for sulfonic groups. Other cations, for example, strontium and rare earths, are also sorbed efficiently. Inorganic ion exchangers, such as vermiculite and clinoptilolite, are being studied as alternatives. The waste solution must be clarified prior to ion exchange, since these media do not remove colloidal materials efficiently. Water clarification techniques are being developed for both the ion exchange processes and for the ORNL lime-soda process waste water treatment plant, in both development and pilot plant programs. Two topical reports describing the laboratory development⁶ and pilot plant demonstration⁷ of the ORNL Scavenging-Precipitation Ion-Exchange process for decontamination of low-level waste are now in press. The pilot plant is being modified to test various process improvements.

3.1 Low-Level Waste Treatment

R. R. Holcomb

W. E. Clark

The scavenging-precipitation ion-exchange process developed for decontaminating the large volumes of slightly radioactive process waste produced in nuclear installations employs a sodium hydroxide precipitation as the head-end treatment. This treatment, like the lime-soda process, is not very effective in the cold with waters containing less than 100 to 150 ppm of hardness. Unless special precautions are taken, the softening obtained is poor, and the softened water will be supersaturated with hardness salts. Phosphates in the waste stream also hinder complete precipitation and thus tend to stabilize the supersaturation. The laboratory studies have been aimed at describing and counteracting the natural tendency to supersaturation and the added detrimental effect of phosphates.

The stabilized supersaturation encountered in the treatment of ORNL low-level waste was initially attributed to hexametaphosphate.⁹ The effect is the same as the "threshold" treatment¹⁰ of water with very low

concentrations of "Calgon." This treatment depends upon surface phenomena rather than stoichiometric chemical reactions. The concentration of hexametaphosphate is accordingly a great deal less (1 to 5 ppm) than would be required if sequestration of metal ions were accomplished (more than 100 ppm). This remarkable property of hexametaphosphate depends on its ability to isolate any nuclei from which crystals of calcium carbonate might grow. The precipitation or crystallization which normally starts upon the surfaces of these nuclei is stopped, so that conditions of marked supersaturation are stabilized. This effect was studied in more detail than previously¹¹ in the laboratory-model clarification system, and ORNL tap water with its normal phosphate concentration of 0.02 ppm was used.

In these studies, from 72 to 120 hr of continuous operation was allowed in order to establish equilibrium for the various concentrations with different phosphate additives. The standard caustic-copperas flow-sheet treatment⁶ of the water (0.01 M NaOH and 5 ppm Fe) produced a residual hardness of 1 to 3 ppm. The residual hardness or degree of supersaturation increased as the concentration of hexametaphosphate was increased, showing steady-state values of 8 to 9, 30 to 40, and 60 to 70 ppm at hexametaphosphate concentrations of 1, 2, and 3 ppm, respectively. However, exactly the same residual hardness results were obtained when ortho-, pyro-, or polyphosphate was used in place of hexametaphosphate at the same concentration with respect to PO_4^{3-} . Thus, it apparently does not matter which of these phosphates is present in the waste.

As reported previously,¹¹ the "threshold" effect of up to 3 ppm of phosphate can be counteracted by making the water 0.005 M in Na_2CO_3 , thereby causing near complete precipitation of hardness (see also³ Sec 10.1, this report). Another approach to the supersaturation problem would be to accept the high residual hardness when phosphates are present, to allow premature breakthrough of the ion-exchange resin, and to regenerate the resin oftener. A residual hardness of about 20 ppm reduced the breakthrough capacity of the carboxylic-phenolic resin for cesium by 50% (Fig. 3.1). Thus, two regenerations were required. Economically, this did not compare favorably with making the water 0.005 M in Na_2CO_3 ,⁷ but the cost of removing the hardness with the ion-exchange resin² was based on the carboxylic-phenolic resin, which has a capacity of 0.4 to 0.5 meq of calcium per cubic centimeter of wet sodium-form resin. Another carboxylic resin, Amberlite IRC-50, achieved a loading of 1.45 meq of calcium per cubic centimeter of wet sodium-form resin. While this resin had little capacity for cesium (Fig. 3.2) and thus could not be used as the principal resin, when used as a pretreatment column, it protected the capacity of the phenolic resin from saturation with hardness. Since this pretreatment column could also be eluted with 0.5 M HNO_3 , the cost of removing hardness by ion exchange would compare favorably⁷ with the cost if the sodium carbonate method were used. It should be emphasized that the sodium carbonate treatment involved the addition of excess Na^+ , which competed with cesium for ion-exchange sites (Fig. 3.1), while the ion exchange method introduced only

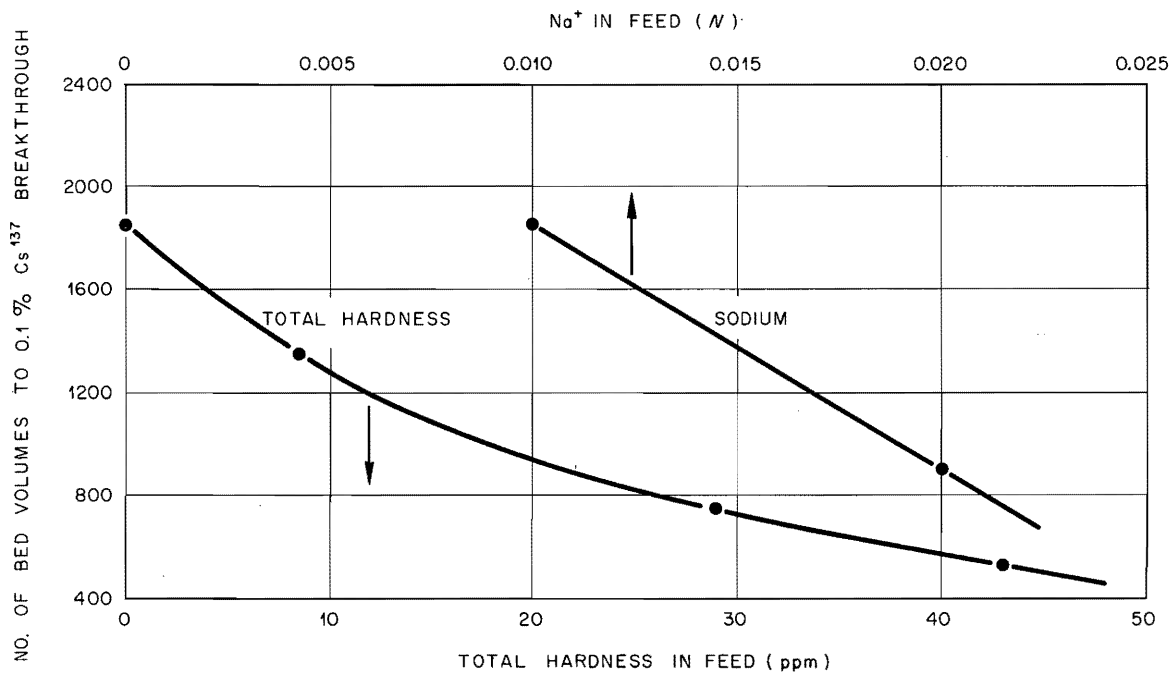
UNCLASSIFIED
ORNL-LR-DWG 78653

Fig. 3.1. The Effect of (1) Total Hardness on Cs¹³⁷ Breakthrough Capacity in the Presence of 0.01 \underline{N} Na⁺, and (2) Sodium on Cs¹³⁷ Breakthrough Capacity in the Absence of Total Hardness, with Duolite CS-100 Resin.

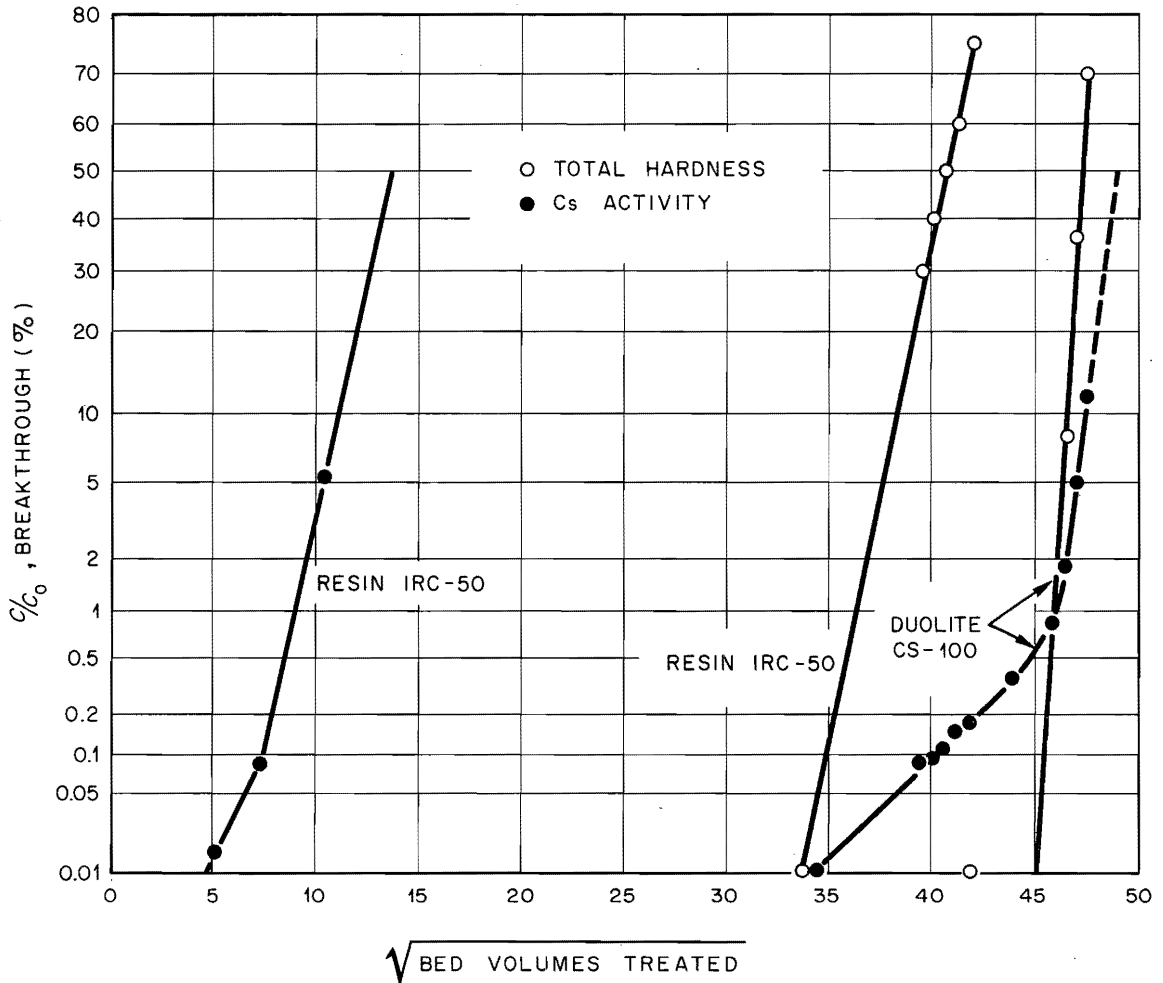
UNCLASSIFIED
ORNL-LR-DWG 78654

Fig. 3.2. Cs^{137} Loading of Duolite CS-100 Resin When 60 to 70 ppm of Total Hardness Had Been Removed on Amberlite IRC-50 Pretreatment Column.

stoichiometric amounts of sodium and thus protected the loading capacity of the phenolic resin for cesium (Fig. 3.2).

The life of the pretreatment column depended on the concentration of residual hardness in the clarifier effluent, which was a function of the phosphate concentration in the waste stream (Table 21). Since the residual hardness reached a maximum at about 70 ppm (the fraction of hardness due to calcium), the ion-exchange method of removing hardness was independent of phosphate concentrations over 4 ppm. Conversely, the sodium carbonate requirement depended on the phosphate concentration, doubling to 0.01 M at 4 to 5 ppm of phosphate and trebling to 0.015 M at 5 to 6 ppm of phosphate. This tended to make the ion-exchange method more attractive than the other, in which sodium carbonate was added to the water.

Table 21. Hardness Removal with Amberlite IRC-50

Phosphate in Waste (ppm)	Residual Hardness in Clarifier Effluent (ppm)	No. Bed Volumes to Hardness Breakthrough on IRC-50 Resin Column
0	0-2	> 10,000
1	8-9	> 10,000
2	30-40	8,400
3	60	2,400
4-5	70	1,200
> 5	70	1,200

3.2 Design of Pilot Plant for Decontaminating Low-Level Waste

J. M. Holmes

J. O. Blomeke

Design changes for the equipment and piping to the ORNL Low-Level Pilot Plant were studied. This pilot plant is for the demonstration of the fixed bed and continuous contactor ion exchange processes proposed by I. R. Higgins.¹² Design was also studied for installation of a new agitated clarifier for the scavenging precipitation-ion-exchange process. The fixed bed ion exchange process has a potential advantage over the scavenging-ion exchange process in that it may require less chemicals for wastes that have less than 400 ppm of hardness. The agitated clarifier has produced satisfactory precipitation and separation of hardness from low-level waste in laboratory-scale tests. Throughput rates per

unit area were up to 4 times higher than those used in the present clarifier. The pilot plant will demonstrate this equipment at a 10-gpm rate.

3.2.1 Fixed-Bed Ion Exchange Process

The Fixed-Bed Ion Exchange Process involves the use of two beds in series: a weak-acid resin followed by a strong-acid resin. The weak-acid resin does most of the separation and permits efficient regeneration by a dilute acid in almost stoichiometric proportion to the calcium and sodium concentrations in the feed. The strong-acid bed is regenerated with 5 M HNO_3 that can then be used to regenerate the weak-acid bed at more frequent intervals. Decontamination factors of 1000 and 100 for strontium and cesium, respectively, are expected for this process.

A flowsheet proposed for the Low-Level Pilot Plant equipment is shown in Fig. 3.3. It will utilize the present 34.3-gal beds, with the first bed filled with Amberlite IRC 50 resin followed by Dowex 50 in the second. An anthracite filter will be used upstream of the beds to remove algae and suspended matter from the feed. At a feed rate of 10 gpm, it is estimated that the IRC 50 will require regeneration daily, while the Dowex 50 might operate for three days before breakthrough. The calculations were based on a feed hardness of 115 ppm (as calcium carbonate). Regeneration of the Dowex 50 resin will involve upflow feeding of 0.58 bed volume of 5 M HNO_3 . The residual acid in the bed after regeneration will be removed by draining in order to prevent the diluting effect during upflow flush through the bed. Two acid cuts will be used to regenerate the IRC-50 bed. The first will be the final 0.30-volume cut from the prior IRC-50 regeneration, and the second will comprise 0.24 bed volume of the acid collected from the Dowex 50 regeneration. This second cut will then be collected for use as the first cut in the next IRC-50 regeneration, according to this method. Stoichiometric regeneration of the beds can be accomplished, producing about 2 N calcium plus sodium nitrate salt solutions. The rinses from both regenerations will be collected and recycled to the beds during normal operation.

3.2.2 Agitated Clarifier

The present nonagitated clarifier in the Low-Level Pilot Plant has a velocity of $15.6 \text{ gal hr}^{-1} \text{ ft}^{-2}$ in the main blanket section. This is considerably lower than the velocities used in the usual industrial practice (25 to $100 \text{ gal hr}^{-1} \text{ ft}^{-2}$). Laboratory studies (see Sec 10.1) with agitated clarifiers up to 9 in. in diameter showed that the outlet turbidities were not significantly higher for rates up to $60 \text{ gal hr}^{-1} \text{ ft}^{-2}$. These studies were performed on Oak Ridge tap water and ORNL low-level waste treated with 0.01 M caustic and 5 ppm iron (same treatment as used in the Low-Level Pilot Plant). Therefore, the design basis of a new 4-ft-diam agitated clarifier (see Fig. 3.4) for the Pilot Plant used a maximum velocity of $60 \text{ gal hr}^{-1} \text{ ft}^{-2}$ for the maximum throughput rate of 12.6 gpm and a normal velocity of $47.5 \text{ gal hr}^{-1} \text{ ft}^{-2}$ for the 10-gpm rate.

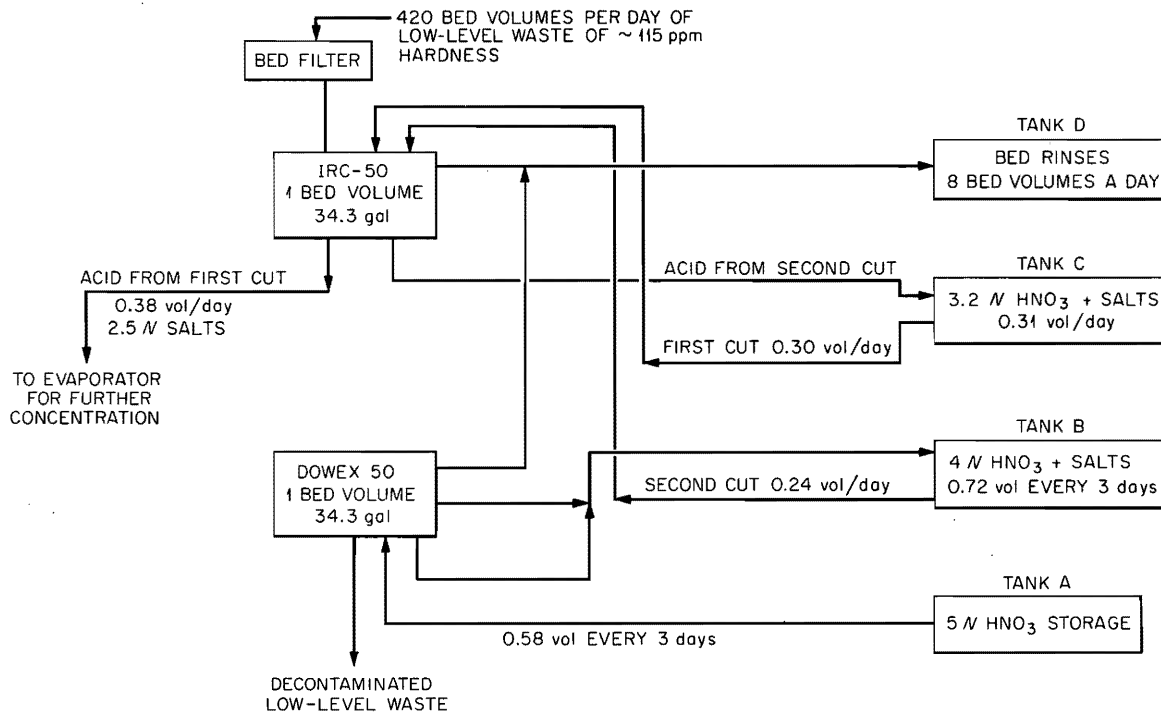
UNCLASSIFIED
ORNL-LR-DWG 78655

Fig. 3.3. Low-Level Pilot Plant: Proposed Fix-Bed Ion Exchange Process.

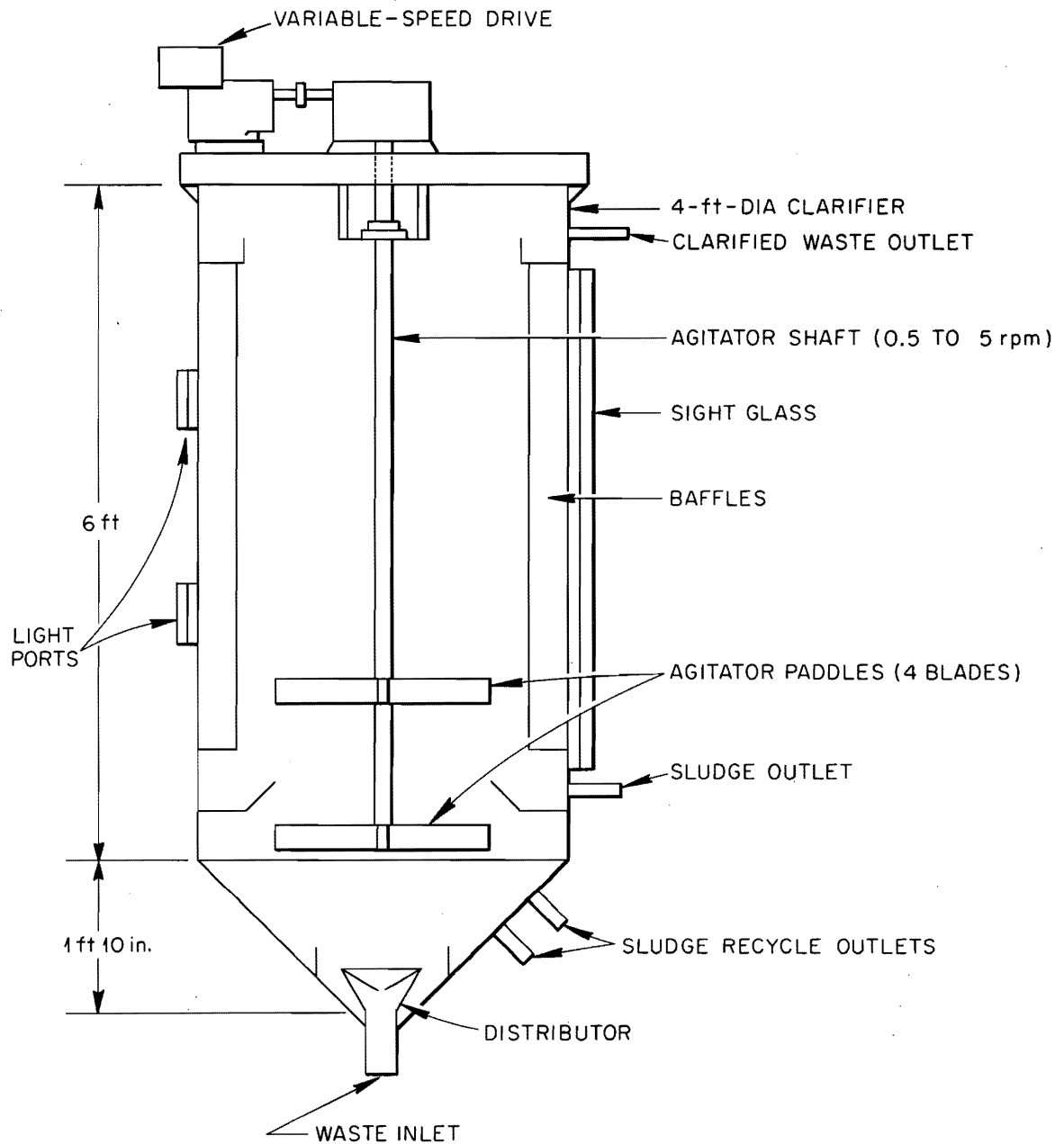


Fig. 3.4. Low-Level Pilot Plant: Agitated Clarifier.

The clarifier design includes a bottom conical inlet section for forming the floc and the sludge blanket. A distributor is positioned just above the inlet to prevent channeling of the inlet waste through the center of the bed. The two 4-bladed agitator paddles can be positioned at any point along the shaft. Either can be removed during the tests, if needed. The purpose of the agitator is to promote precipitation of the hardness in the sludge blanket and to provide a better distribution of the solids in the blanket, thereby preventing channeling. The required speed range for the agitator (0.5 to 5 rpm) was scaled up from the laboratory data by using a constant volumetric power input according to the following equation.

$$N_P = N_L \left(\frac{d_L}{d_P} \right)^{2/3},$$

where

- N_P = speed of pilot-plant agitator,
- N_L = speed of agitator used in laboratory,
- d_P = diameter of agitator in pilot plant,
- d_L = diameter of agitator used in laboratory.

4. ENGINEERING, ECONOMICS, AND HAZARDS EVALUATION

4.1 Engineering and Economics of Waste Management

J. J. Perona

J. O. Blomeke

R. L. Bradshaw

A study of the effects of fission product removal on the costs of waste management was completed and will be published as ORNL-3357. In this study, the management costs for wastes from which large fractions of fission products have been removed by improved processes representative of the best future technology are compared with the costs for managing the original wastes with all fission products present. Three cases were studied, each representing a different degree of uniform removal of all fission products: 0, 90, and 99%. The waste was assumed to be acid Purex produced by a plant processing 1500 metric tonnes/year of uranium converter fuel irradiated to 10,000 Mwd/ton. It was assumed also that the wastes after fission product removal were identical in volume and chemical composition to neutralized Purex waste. No attempt was made to estimate the costs of fission product removal or subsequent disposal of used fission product sources, because there is not yet sufficient information about the separation processes or source configuration to permit accurate cost estimates.

Costs estimated in each case for interim storage of the liquid waste, pot calcination, and the shipment of calcined solids were given in a previous report of this series.¹³ Results can now be presented for the

interim storage of calcined solids and their final disposal in salt mines, as well as for the effects of fission product removal on the total costs of waste management.

4.1.1 Costs of Interim Storage of Calcined Solids

The same conceptual designs and methods of cost estimation were used as in a previous study of this series.¹⁴ The cylinders were assumed to be stored in concrete-walled canals filled with water as a shielding material. The water also serves as a coolant and is continuously withdrawn and circulated through heat exchangers in which heat is transferred to a loop connected to a cooling tower. A portion of the water is withdrawn from the primary cooling loop and sent through a demineralizer system.

The canal walls are coated with an epoxy paint for water tightness and to facilitate decontamination. The canals were designed with 25% excess capacity and compartmentalized so that canal segments could be emptied and maintained. Aluminum partitions were used to subdivide the water flow through the canals to expedite detection and location of any leaky cylinders.

Fission product removal permits the water depth to be lowered 1 to 2 ft, but the total canal depth, with 12 ft of water required to cover the tops of the cylinders and 12 to 16 ft required for shielding, is 24 to 28 ft. A lighter crane for shipping cask handling can be used with the depleted wastes, but total capital costs were not appreciably affected by shielding considerations.

The cost of the cooling system did decrease significantly with fission product removal and became a small enough part of the total cost that the difference between the total costs for the interim storage for 90%-depleted waste and 99%-depleted waste was not appreciable.

The only important operating expense was for labor. As in the case of interim liquid storage, four watchmen and a supervisor were assumed to be required for round-the-clock surveillance. In addition, one health physicist and one maintenance man were assumed to be required, resulting in a total labor cost per year of \$87,500, including overhead. Most of the maintenance labor would be used on the cooling system; hence, the maintenance labor was reduced for the storage of fission-product-depleted wastes from the 3 man-years assumed for other wastes.

Costs of interim storage of calcined wastes depleted in fission products ranged from 0.0015 to 0.0046 mill/kwh for storage periods of 1 to 30 years (Fig. 4.1). For short storage periods, where the incremental cooling system costs were important, storage of fission-product-depleted wastes was cheaper than storage of acid Purex containing all the fission products. For long storage periods, the cooling requirements for the Purex wastes decrease, and the larger number of cylinders required to store depleted wastes becomes controlling. Hence, the cost of Purex waste storage becomes less than depleted-waste storage.

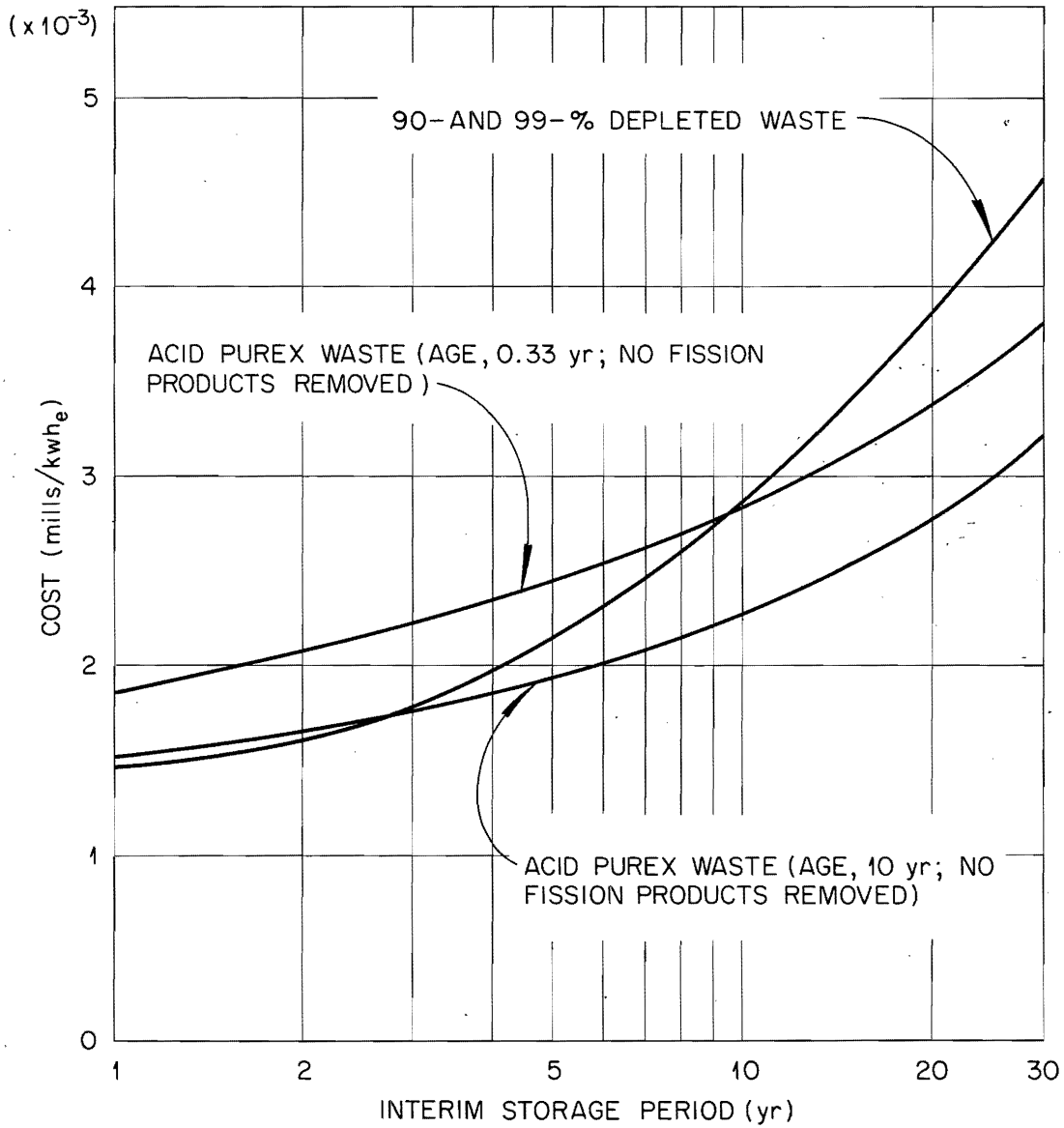
UNCLASSIFIED
ORNL-LR-DWG 76068A

Fig. 4.1. Costs for the Interim Storage of Calcined Solid Wastes, as Functions of Storage Period and Age at Start of Storage.

4.1.2 Cost of Final Storage of Calcined Wastes in Salt Mines

In the conceptual design, a shipping cask containing cylinders of calcined waste is unloaded from a rail car and moved into a hot cell, which contains cask-decontamination and cylinder-recanning facilities, cylinder-storage space, and encloses a shaft down which the bare cylinders can be lowered one at a time to the working level. Offices and a change house would also be located at the hot cell. A second, larger shaft would be located nearby for use in the salt mining operations. It was assumed that the hot cell and pair of shafts would serve a one-square-mile disposal area.

Upon reaching the storage level, a cylinder of waste would be loaded remotely into a motorized, shielded carrier that would be driven through the mine corridors until a mined room, ready for final storage use, was reached. The amount of undisturbed salt left between these rooms would be determined by the heat generation rate of the waste and the desired degree of closure of the room due to plastic flow of the salt. Waste cylinders would be placed in holes drilled in the floor of the room. The distance between the holes is governed by heat transfer principles, the criteria being that temperatures reached during calcination must not be exceeded during final storage or that the temperatures of the salt not exceed 400° F. After lowering the cylinder into place, the hole is backfilled with several feet of crushed salt to permit access to the room.

The removal of fission products would decrease the heat generation rate of the waste and thus allow closer spacing of the cylinders in the floor of the room. For depleted wastes, the limiting salt temperature of 400° F was controlling rather than the limiting calcination temperature of 1650° F at the axis of the waste cylinder. Mine space requirements range from 2 to 6 acres/yr for acid Purex waste, 0.2 to 1.3 acres/yr for 90%-depleted waste, and 0.04 to 0.17 acres/yr for 99%-depleted waste. The minimum age at which acid Purex waste in 24-in.-diam cylinders can be placed in the salt formation is about 30 yr, so only a single point is plotted for this case. Minimum center-to-center spacings were assumed to be 2, 5.3, and 8 ft for 6-, 12-, and 24-in.-diam cylinders. Six- and 12-in. cylinders filled with 99%-depleted waste would be stored at the minimum spacing for all ages.

Disposal costs were calculated according to the assumption that total closure of the salt rooms by creep or flow of the salt would be permissible, provided that the time required would be on the order of decades. Accordingly, 60% of the salt could be extracted for a facility 1000 ft below the surface. About 25 to 30% of the mined space would be required for corridors and ventilation tunnels, and the remainder would be available for cylinder-storage space.

All mining costs, including amortization of the mining lift but not the shaft, were included in the mining charge of \$2 per ton. Amortization factors were computed at 4% interest.

Total costs for disposal in salt formations of wastes up to 30 yr in age ranged from 6.7 to 13.2×10^{-3} mills/kwh for acid Purex waste (no fission products removed) and from 3.7 to 5.6×10^{-3} mills/kwh_e for depleted wastes (Fig. 4.2).

4.1.3 Total Waste-Management Costs

The term, "total waste-management costs," is used here to mean the cost of disposal in a salt formation plus the costs of all necessary preliminary steps. The disposal cost is a function of the age at burial, diameter of the cylindrical container, and degree of fission product removal. Thus, total waste-management costs reflects these functions.

Minimum ages for burial in salt are 2.3, 5.5, and 30 yr for untreated acid Purex waste in 6-, 12-, and 24-in.-diam vessels; and 1.2 yr for 90%-depleted waste in 24-in.-diam vessels. For all other cases for depleted wastes, the minimum age is 0.33 yr, the assumed age at the time of discharge from the fuel-processing plant. In addition to minimum burial ages, there are minimum pot-calcination ages for acid Purex waste, which are 0.6, 2.2, and 6.5 yr for 6-, 12-, and 24-in.-diam vessels.

In computing the costs of interim storage, it should be recognized that storage as calcined solid is cheaper than storage as liquid for acid Purex, but for the depleted wastes, liquid storage is cheaper. Even so, some liquid storage must be used for untreated acid Purex waste due to the minimum pot-calcination ages. In obtaining the total waste management costs, the minimum cost of interim storage was used subject to the various minimum-age requirements.

The results are shown in Fig. 4.3. For the case of untreated acid Purex in 6-in.-diam cylinders, the largest shipping cask, which results in lowest costs, cannot be used prior to a waste age of 2.8 yr; hence the break in the curve in Fig. 3.

Total waste-management cost for acid Purex decreased as age at burial increased, and at 30 yr, the upper limit used in the study, was about 0.025 mill/kwh_e with both 12- and 24-in.-diam cylinders. Costs for depleted wastes were cheaper with 24-in.-diam vessels and not so strongly affected by age, falling in the range of 0.017 to 0.019 mill/kwh_e for both 90- and 99%-depleted wastes for ages from 0.33 to 30 yr. Relatively little cost reduction (~ 7%) is achieved by increasing the fraction of fission products removed from 90% to 99%.

4.1.4 Conclusions

A rather optimistic estimate of the amount to be gained in waste-management costs with removal of 90 to 99% of the fission products is about 0.006 mill/kwh_e, which is equivalent to about \$400 per tonne of uranium processed. Thus, the cost of managing wastes that contain only 1% of the fission products is 70% as much as the cost for wastes containing all the fission products, representing a savings of 30%. Because

UNCLASSIFIED
ORNL-LR-DWG 78657

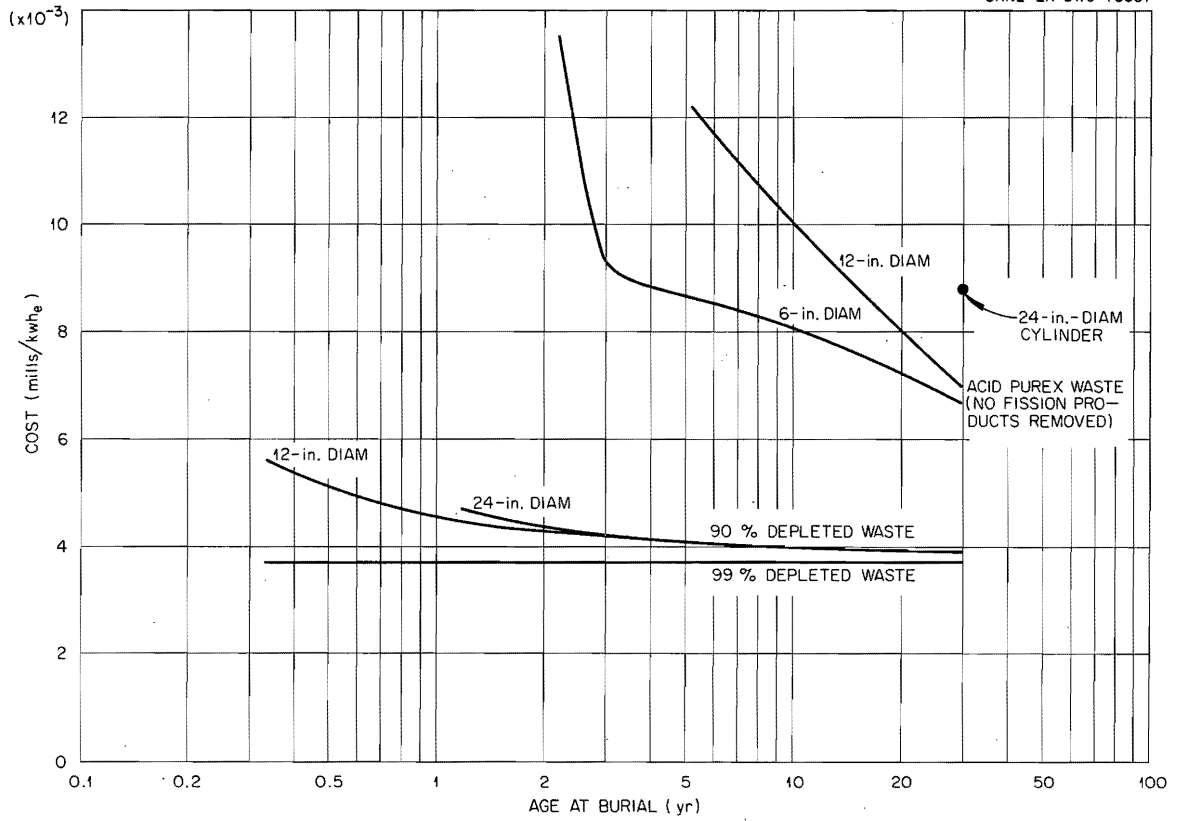


Fig. 4.2. Costs for Waste Burial in a Salt Mine.

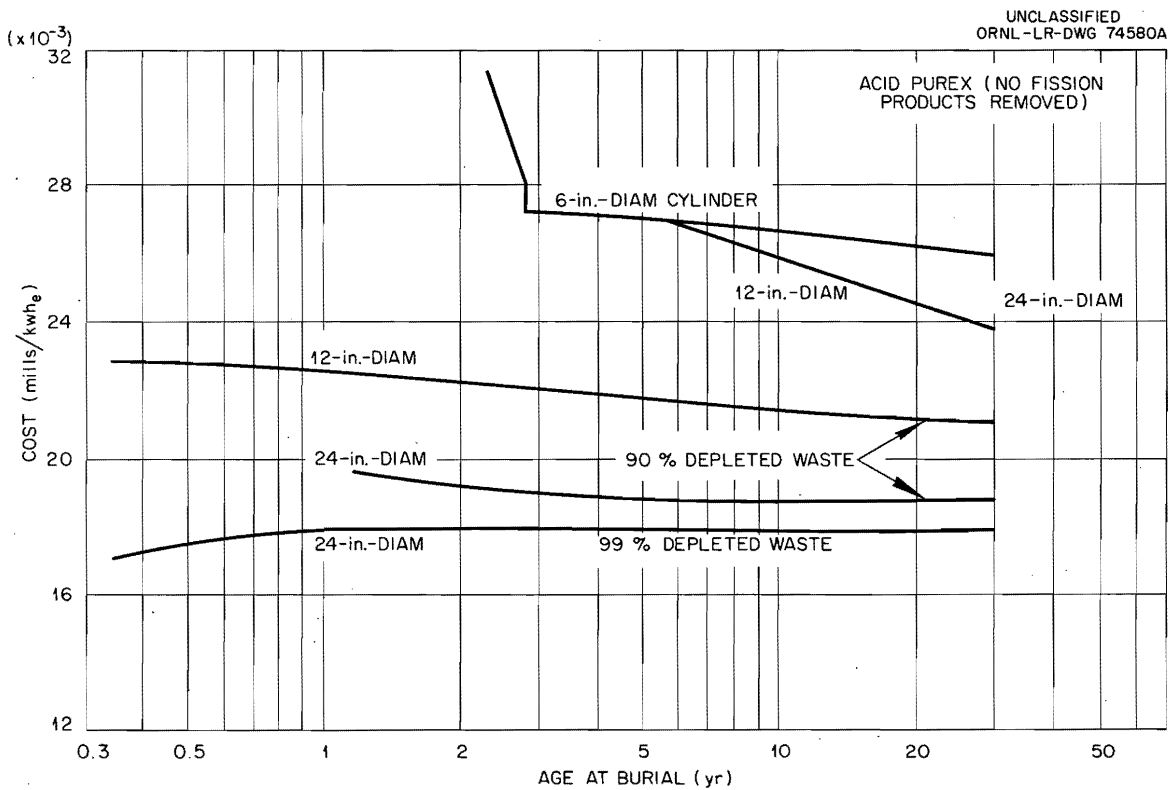


Fig. 4.3. Total Cost for Interim Storage, Pot Calcination, Shipment, and Final Disposal of Wastes in a Salt Mine.

this saving is not nearly enough to pay for fission product separation, packaging, and disposal, such practices would not be carried out as part of a waste management scheme but would necessarily depend on a large and diverse market for fission products to pay the major portion of these costs.

4.2 Analysis of the Safety of Routine Operating Discharges From White Oak Creek to the Clinch River

K. E. Cowser

Man may be exposed to radiation through a number of pathways due to the discharge of radioactive fluids to the Clinch River. Estimates of exposure by drinking contaminated water and by immersion in contaminated water have been reported.¹⁵ Calculations of the likely dose received by other pathways of exposure are in progress.

Radionuclides associated with solids that have settled to the bottom of the river can be expected to contribute to the total dose received. Although earlier calculations assumed complete dilution of fission products in the river, annual surveys made by the ORNL Applied Health Physics Section show that some of the radionuclides are retained by the bottom sediments.¹⁶

Measurements were made at 50-ft intervals at cross sections 2 miles apart in the Clinch River. In the Tennessee River and TVA Reservoirs, measurements were made at tenth points approximately 10 miles apart. Measurements consisted of gamma counts obtained with a multiple G-M detector ("Flounder"), lowered to the surface of the bottom sediments, and analyses were made of the mud samples taken at each measurement point. Average concentrations of specific radionuclides in bottom sediments were calculated by averaging all values for the entire study reach of the Clinch and Tennessee rivers. The principal radionuclides associated with these sediments were Cs¹³⁷, Ce¹⁴⁴, Co⁶⁰ and, more recently, Ru¹⁰⁶. Reasons for such selectivity are enumerated elsewhere.¹⁷

The "Flounder" is used principally to furnish qualitative information on the build-up of gamma-emitting radionuclides in the sediments. Its construction makes it insensitive to beta radiation. Although the "Flounder" is calibrated routinely with a sealed radium source (as a stability or sensitivity check), the complex spectrum of gamma rays from both the contaminated sediments, as well as from the radium source, prevents the exact determination of exposure dose. Estimates of exposure dose can be made, but it is necessary to recognize the limitations of such data (Tables 22 and 23). Figure 4.4 shows the average gamma-counting rate in the Clinch and Tennessee rivers, as determined by the "Flounder" and averaged for the entire study reach of each, and the curies per year of Cs¹³⁷ and Co⁶⁰ released. In a general way, the measurements in the Clinch River reflect the quantity of Cs¹³⁷ and Co⁶⁰ released each year. Of the measurements that were made, the maximum

Table 22. Estimated Dose from Contaminated Sediments in Clinch River

Year	Measured ^a		Calculated ^b			
	Average	Maximum	Beta	1/2 Gamma	Total	Attenuated ^c 1/2 Gamma
1951	39			90 ^d		
1952	88			320 ^d		
1953	53			160 ^d		
1954	57	110	60	160	220	9.5
1955	60	110	130	180	310	11
1956	130	260	300	630	930	35
1957	96	180	180	460	640	24
1958	100	200	210	360	570	19
1959	160	280	450	710	1160	39
1960	150	280	510	460	970	25
1961	95	170	530	290	820	15

^aIn 10^{-2} mr per 24-hr exposure as measured by the "Flounder" (data from Applied Health Physics Section).

^bIn 10^{-2} millirad per 24-hr exposure.

^cAttenuation through 3 ft of water.

^dEstimated from correlation relationship.

Table 23. Estimated Dose from Contaminated Sediments in Tennessee River

Year	Measured ^a		Calculated ^b			Attenuated ^c 1/2 Gamma
	Average	Maximum	Beta	1/2 Gamma	Total	
1951	13					
1952	22					
1953	23					
1954	19	30	22	50	72	3.0
1955	26	43	60	68	128	4.2
1956	36	69	65	110	175	6.1
1957	33	58	37	80	117	4.2
1958	35	63	55	62	117	3.5
1959	30	63	48	56	104	3.1
1960	33	49	75	61	136	3.3
1961	26	48	95	54	149	2.8

^aIn 10^{-2} mr per 24-hr exposure (data from Applied Health Physics Section).

^bIn 10^{-2} millirad per 24-hr exposure.

^cAttenuation through 3 ft of water.

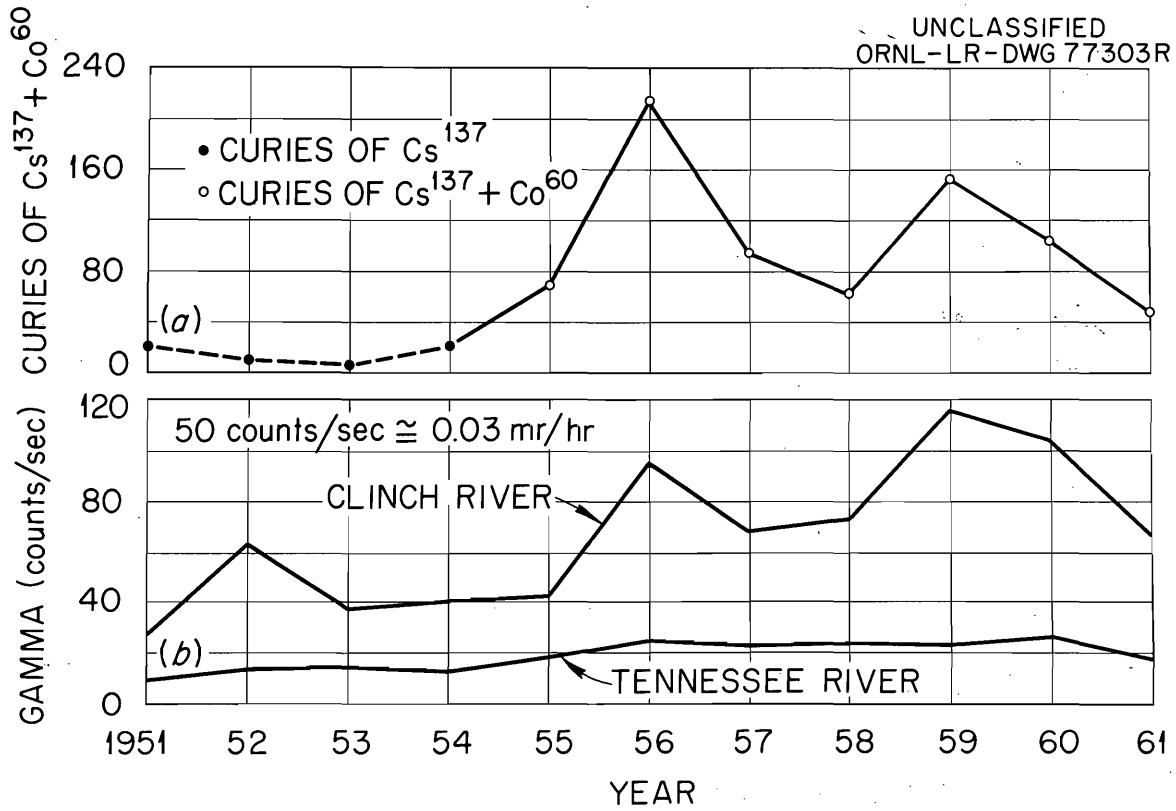


Fig. 4.4. Curies of Cs^{137} and Co^{60} Released to Clinch River (a), and Average Gamma Count at Surface of Bottom (b).

readings in the Clinch River [generally at Clinch River Mile (CRM) 8.3] were larger than the average readings by a factor of 1.9 ± 0.09 ; similarly, the ratio in the Tennessee River was 1.8 ± 0.2 . For estimating the radiation dose to man, calculations of dose were made by using the average radionuclide composition of the sediments. It was assumed that this average composition was distributed uniformly in an infinite source. To assume an infinite source containing the maximum concentration of radionuclides observed seems overly conservative. Further, it was assumed that the individual would be exposed to half the submersion dose of gamma emissions (that is, from half a sphere). Such an assumption is reasonable, since the individual receiving the dose is likely to be standing on or floating above the contaminated sediments. Normally, only the feet would be subjected to the beta dose rate and to some fraction greater than half of the gamma dose rate.

Calculated dose rates from bottom sediments in the Clinch and Tennessee rivers are listed in Tables 22 and 23. Since the source is not infinite in extent, the calculated values give a larger estimated dose rate than that actually available. Accordingly, the largest calculated bottom sediment dose rate of 12 millirads per day of exposure would have occurred in 1959, and it was derived from 0.4 beta and 0.6 gamma radiation. The contribution of the various radionuclides to the beta and gamma dose rates is listed in Table 24. The total rare earths, Cs^{137} , and, more recently, Ru^{106} are the principal contributors to beta dose rates, and Co^{60} and Cs^{137} account for the largest fraction of gamma dose rate.

An estimate can be made of the bottom sediment gamma dose rate in the Clinch River for periods when only "Flounder" measurements were made. This is made possible by the apparent relationship between such measurements and calculated gamma dose rates and is expressed as a coefficient of correlation of 0.90. With "Flounder" measurements X as abscissa and gamma dose rates Y as ordinates, the relationship is given by the equation: $Y = -0.84 + 4.64 X$. The 95% confidence limits of the regression curve slope ± 2.31 . The correlation coefficient for similar data from the Tennessee River is 0.58, and the slope of the regression curve and its 95% confidence limits is 0.19 ± 3.45 . Thus, estimates of bottom sediment gamma dose rates in the Tennessee River are not justified with the data available.

Since bottom sediments are in general covered by water, the gamma dose rate to the gonads of an individual standing on the river bottom would be reduced by attenuation. An average attenuation coefficient for water was calculated by weighing both the fraction of time a photon of a given energy was emitted by a particular radionuclide and the fraction each radionuclide contributed to the total loading of the bottom sediments. The gamma dose rates after attenuation through 3 ft of water are listed in Tables 22 and 23.

Table 24. Percentage Contribution to Estimated Bottom Sediment Dose Rate
by Radionuclides

Type of Radiation	Nuclide	Clinch River		Tennessee River	
		1954-1959	1960-1961	1954-1959	1960-1961
Beta	TRE ^a	50	23	52	15
	Ru ¹⁰⁶	14	64	22	75
	Cs ¹³⁷	31	13	21	10
Gamma	Co ⁶⁰	44	25	50	31
	Cs ¹³⁷	53	55	45	47
	Ru ¹⁰⁶	1	14	3	22

^aTotal rare earths.

4.3 Safety of Tank Storage of High-Level Liquid Wastes

L. C. Emerson

Previously reported modifications¹⁸ in the design specifications of hypothetical fuel reprocessing plant made it necessary to recalculate the fission product and transuranic radioisotope concentrations in the feed stream to the waste storage tanks. The method for determining these concentrations has already been described.¹⁹ Although the size of the tanks cannot be determined until the correlative engineering and economic evaluation is complete, it nevertheless was necessary to select a specific tank size in order that a definite filling time (5.33 yr) could be established. For this purpose the previously used tank capacity of 400,000 gal was chosen.¹⁹ Actually, this capacity is in the range of tank capacities being considered in the engineering and economic evaluation of the interim storage of liquid waste.

Figure 4.5 shows the initial activity levels (at the time of filling) of fission products and transuranics and how the levels change with time. These calculations show the following: Of the 4×10^9 curies in the tank at the time of filling, about 14% is due to strontium and its daughter products, and 13% is due to the Cs¹³⁷ chain. It is expected that these fission products will largely determine the extent of hazard for the first several hundred years. Fifty percent of the activity is found to be due to the Ce¹⁴⁴-Pr¹⁴⁴ combination, while the only other major contributor, Pm¹⁴⁷, accounts for 14%. The initial transuranic content is 1.2×10^6 curies, with the isotopes of americium contributing 52% of the transuranic activity. As found earlier,¹⁹ the combined activity of the transuranics is less than that due to the fission products, except for the interval between 400 and 20,000 yr in the storage period. For the purpose of this study it was assumed that 99% of the plutonium is recovered from the spent fuel elements and therefore does not contribute materially to the waste tank activity.

4.3.1 Atmospheric Diffusion

A study of atmospheric contamination patterns that could be expected under typical release condition was begun. The results of a comprehensive investigation of the meteorological phenomena²¹ within the Oak Ridge environs is being used to establish parameters for the study. A particular phase of this hazard evaluation is that of developing estimates of the type and extent of possible tank failure. These possible releases will then be analyzed in terms of their temporal and spatial behavior by use of the generalized Gaussian plume model described by Gifford.²²

Until estimates of the type and magnitude of activity releases become available, the analysis of atmospheric diffusion and dispersion will be based on an assumed unit release from the specified location of the tank-farm site. The reduction factors resulting from diffusion and convection will then be determined at various locations downwind and crosswind from the release point. The initial calculations were carried out

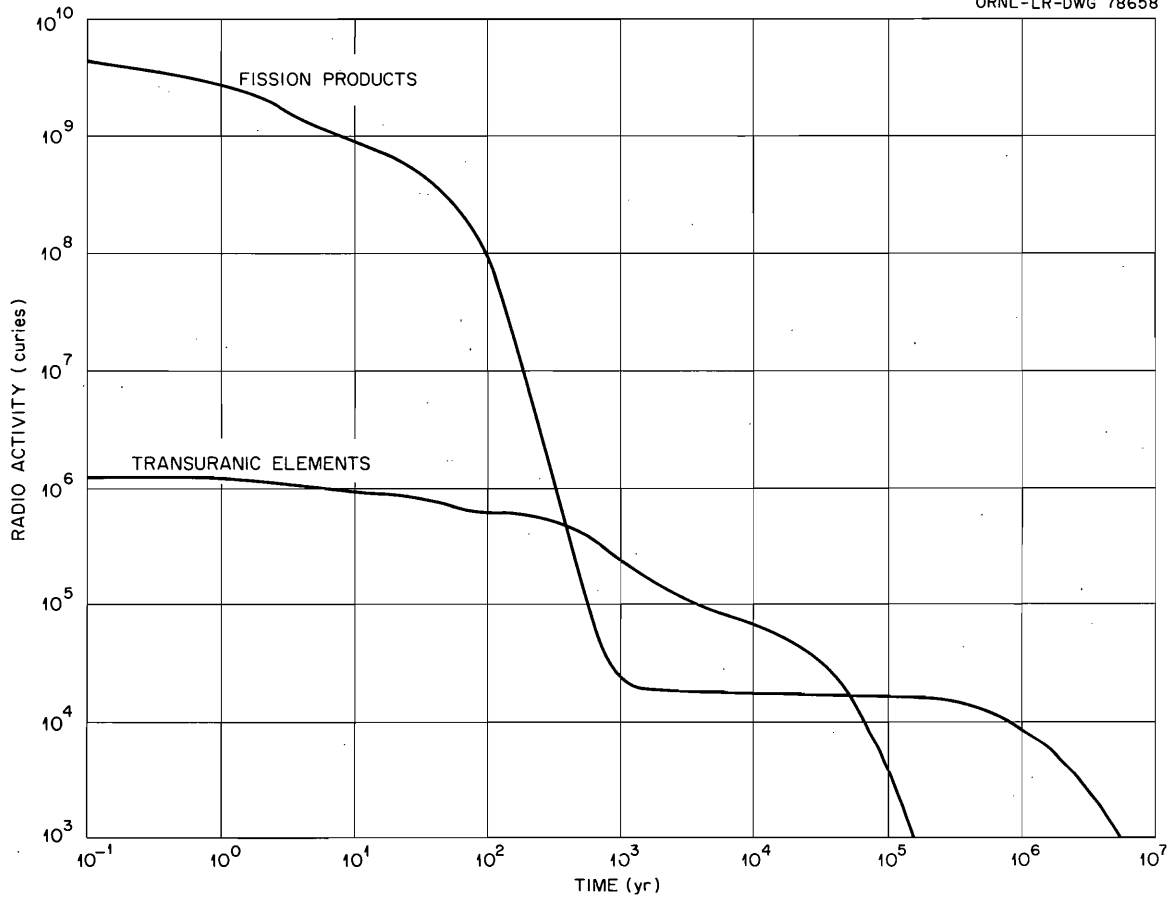
UNCLASSIFIED
ORNL-LR-DWG 78658

Fig. 4.5. Amounts of Radioactivity in Storage Tank as a Function of Time.

for various downwind distances out to a maximum of 18 miles, although this distance is probably beyond the range at which the theory is valid.

Calculations of contamination patterns were completed for the case of a localized and continuous release at any specified height. Such a condition might result from a slow release to the atmosphere of activity that had previously been leaked to the ground through some type of tank failure. Loss of cooling would result in a temperature rise that could cause vaporization of certain of the fission products, with subsequent escape to the atmosphere. The effective height of the initial injection into the atmosphere would relate, in some fashion, to the temperature. Dilution downwind from the release point for the cases completed range to minimum values of 10^{-7} and 10^{-8} , depending on the assumed degree of atmospheric turbulence. Later studies will relate these values to population exposures.

5. DISPOSAL IN DEEP WELLS

5.1 Disposal by Hydraulic Fracturing

5.1.1 Geological Studies (W. de Laguna, T. Tamura)

The problem of defining quantitatively the various properties of the geologic formations into which it is proposed to dispose of waste-cement mixtures by hydraulic fracturing will be long and complex. To date, from the 3263-ft-deep Joy No. 1 test well, gamma-ray, resistivity and self-potential logs, and a complete core of all of the formations of direct interest to the fracturing program were obtained (the middle and lower Conasauga shale, the Rome sandstone, the Chickamauga limestone, and a short section of the upper part of the Knox dolomite). Representative sections of the core were tested for permeability, porosity, and crushing strength, and their mineralogical and ion exchange properties were measured and described. The U. S. Geological Survey (U.S.G.S.) has made measurements of the thermal conductivity of certain selected samples and correlated them, at least provisionally, with a temperature log of the test well. The U.S.G.S. also made detailed measurements of the specific gravity of selected samples of the core to help them in the interpretation of a detailed regional survey of magnetic and gravity anomalies made in 1962. The previously reported fracturing experiments²³ provided some empirical data as to how certain of these rocks behave when hydraulically fractured in the field.

Study of the regional geology of the Valley and Ridge province, in which Oak Ridge is located, was begun by J. M. Stafford in 1856 and has since been carried forward by a number of geologists, including Bailey Willis in the closing years of the nineteenth century and John Rodgers in 1953. Thus, a general background into which these detailed studies must be fitted already exists.

The correlation of all these data into a single inclusive picture is underway; meanwhile, certain basic data, such as Grim's study of the mineralogical and ion exchange properties of selected rock samples from the core of Joy No. 1 test well and U.S.G.S. temperature measurements, are presented as an aid to understanding the scope and experimental procedures of the fracturing program.

Mineralogical Analysis.-- A thorough study of the mineralogy, particularly the clay mineralogy of the shale zones of the Chickamauga Formation, was recommended by the Health Physics Division Advisory Committee in their October 1961 report to A. M. Weinberg, Director of the Oak Ridge National Laboratory. The committee reported that the injection of significant quantities of actual waste into the shales within the Chickamauga Formation above the Knox Dolomite would be more suitable (pending the mineralogical study) than injection into the shales above the Rome Formation orthoquartzite and that a mineralogical study would provide an indication of the exchange capacity of these potential injection zones. The clays in these shale zones, with relatively high exchange capacities, would serve as natural barriers to the movement of radionuclides and therefore would provide an additional safety factor.

Twenty-five selected samples of the core from the Joy No. 1 test well were submitted to R. E. Grim (University of Illinois) for detailed analysis of the mineralogy, exchange capacity, and acid-soluble components. He completed his study, and the results are summarized here.

Figure 5.1 is a general description of the core from Joy No. 1 test well, showing which samples were selected for Grim's analyses. Table 25 contains a list of the samples analyzed and their identity as to depth (in feet) and rock type.

Mineralogy of the core samples is reported in two ways. The "microscopic examination" section describes the mineralogy of the entire sample, including the general features of the clay minerals (Appendix A). The "clay analysis" section covers the results of the analysis by x-ray diffraction of particles 2 μ or less in diameter (Appendix B).

Returning to Table 25, samples 719 to 942, 1648 to 1867, and 2648 to 2852, inclusive, represent samples from zones considered suitable for fracturing.²⁴ In the 719- to 942-ft zone, clay minerals make up the bulk of the samples. Quartz is present in moderate quantities, but calcite is conspicuous by its absence. In the 1648- to 1867-ft zone, the material is principally limestone, with calcite the dominant mineral. The sample taken at 1648 ft represents the more shaly area in this zone; this sample contains about 40% calcite. This mineral distribution is in contrast to the very low calcite content of the shale in the 719- to 942-ft zone. In the 2648- to 2852-ft zone, the calcite and clay minerals occur in moderate amounts. The sample from 2705 ft represents a coarser textured limestone, and this is reflected by the higher calcite content; the more typical samples of this zone are represented by samples 2701 and 2826. In three zones, the clay mineral illite is most abundant in

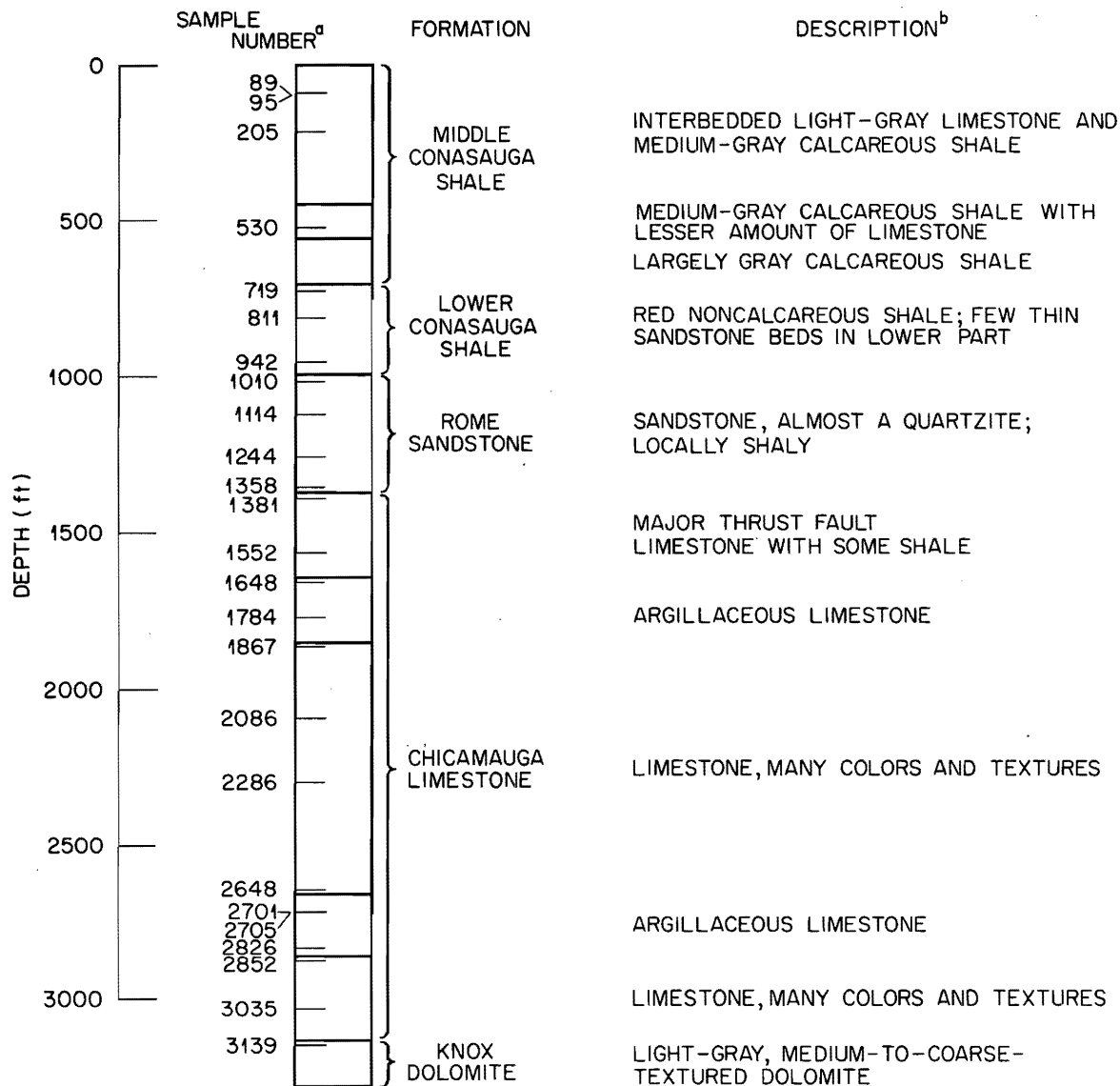
UNCLASSIFIED
ORNL-LR-DWG 78659^a SAMPLE NUMBER ALSO CORRESPONDS TO DEPTH IN FEET.^b DESCRIPTION FROM DATA OF W. deLAGUNA.

Fig. 5.1. General Description of Core from Joy No. 1 Test Well, Showing Samples Selected for Detailed Mineralogical Analysis.

Table 25. Identification of Representative Core Samples Subjected to
Detailed Mineralogical Analysis

Sample Number (depth in feet)	Description
89	Representative limestone
95	Representative shale
205	Sandy-textured limestone
530	Dark-gray shale
719	Pumpkin Valley member of Conasauga shale
811	Red shale with glauconite
942	Lower red shale
1010	Typical white quartzite from upper part of Rome formation
1114	Pinkish quartzite
1244	Shaly sandstone
1358	Main fault in lower Rome formation
1381	Calcareous red shale representing upper Chickamauga
1552	Light-gray limestone typical of "lithographic" limestone
1648	Massive calcareous shale
1748	Typical, light-medium-red limestone
1867	Fossiliferous light-gray limestone
2086	Dark-red shaly limestone
2286	Typical interbedded limestone and shale
2658	Dark-gray argillaceous limestone
2701	Dark-red shaly limestone
2705	Banded pink and white, fine, sandy limestone
2826	Dark-red argillaceous limestone
2852	Medium-dark-gray limestone
3035	Greenish limestone specimen with red limestone
3139	Sandy, light-gray dolomite

the deepest and in the shallowest zones. Kaolinite and chlorite make up a substantial portion of the minerals in the shallow zone (719 to 924 ft).

Two formations considered unsuitable for fracturing include the Rome Sandstone and the Knox Dolomite. The Rome Sandstone is represented by samples from 1010 through 1360 ft. The very hard sandstone samples (1010 and 1114 ft) differ from the more argillaceous sandstone samples (1244 and 1358 ft) by their higher quartz content. Associated with the higher quartz content is feldspar, present up to 10% in this formation. In the Knox Dolomite formation, represented by sample 3139, the calcareous mineral is the only one identified positively.

Data are also reported on the exchange capacities and acid-soluble fractions of the core samples. These values are shown in Table 26. Exchange capacities range from 5.4 to 29.4 meq/100 g. The lowest value represents the core with extremely high calcite and dolomite content (3139 ft); the highest value comes from the core at 1358 ft, which is in the thrust-fault zone.

In general, the lower exchange capacities correspond to lower clay mineral content. Of the minerals identified, quartz, calcite, dolomite and feldspars have little or no exchange capacity; kaolinites have low capacities (1 to 10 meq/100 g); illites and chlorites have moderate capacities (15 to 25 meq/100 g); and montmorillonites have high capacities (100 meq/100 g). Studies of several illites here showed that their exchange capacities can range from 12 to 30 meq/100 g, and, since illite is the dominant clay mineral in the core, it is suspected that the exchange capacity variations observed in samples mineralogically similar may be due to differences in the nature of the illite in the core.

The percentage of acid-soluble components is a measure of the calcite content in geologic formations. These analyses show that samples from the shallow zone (719 to 942 ft) contain very little calcite, whereas considerable calcite is found in the two deeper zones considered favorable for fracturing. Two samples, with about 90% acid-soluble components, are from a fossiliferous zone (1867 ft) and a dolomite zone (3139 ft). It is somewhat surprising that the dolomite sample should show such high acid-soluble content, since dolomites are known to be less soluble than calcite. Generally, however, the concentrations of acid-soluble components agree well with estimates of the calcite content based on optical and x-ray diffraction techniques.

On the basis of clay mineralogy, both the shallow (719 to 942 ft) and the deepest (2648 to 2852 ft) zones appear to be favorable for fracturing because of their high illite content. Illite is highly selective for cesium sorption and will serve as a barrier to the movement of radiocesium if grout sheets are subject to leaching.

Geothermal Measurements.-- Detailed temperature surveys of the Joy No. 1 test well and well 400S of the second fracturing experiment were made by W. H. Diment and E. C. Robertson of the U.S.G.S. in December 1961, and March 1962. Temperature measurements were also made in the

Table 26. Exchange Capacity and Acid-Soluble Components

Sample Number (ft)	Exchange Capacity (meq/100 g)	Acid-Soluble Component (%)
89	13.1	54.1
95	22.99	27.3
205	7.3	26.4
530	21.05	1.2
719	8.12	5.3
811	9.94	9.6
942	15.44	7.8
1010	5.76	6.4
1114	7.50	4.3
1244	10.35	5.7
1358	29.4	0.01
1381	5.9	44.9
1552	10.80	77.5
1648	7.32	34.6
1784	9.84	78.8
1867	13.17	90.7
2086	11.87	30.7
2286	9.43	70.7
2648	7.17	48.6
2701	16.0	33.0
2705	18.15	64.7
2826	7.48	23.5
2852	15.85	25.4
3035	13.35	28.9
3139	5.44	89.2

Joy No. 1 well in October 1962, after it had been cased down to 2900 ft. There were only minor changes in the temperatures in the Joy No. 1 well between these dates. The temperature gradients were compared with the thermal conductivity of rock samples from the core of the test well, and a computation was made of the rate of heat flow from the earth's interior. Diment and Robertson obtained a provisional value of $0.73 \pm 0.04 \mu\text{cal}/\text{cm}^2$, a relatively low rate, but this value may be revised as the result of subsequent observations.

Figure 5.2 is a plot of the temperatures in Joy No. 1 well to a depth of 2900 ft. The measurements are probably correct to within less than 0.1°F , but they may not represent the normal thermal gradient. Subsequent to the last temperature measurements (October 1962), the water level in the casing in the Joy No. 1 well was found to be dropping slowly, whereas it had been assumed that the water was stagnant. This downward flow of cooler surface water into the warmer, deeper horizons has to some unknown degree locally reduced the normal temperature gradient so that some minor adjustment of the computed rate of heat flow will be required.

The temperature gradient in well 400S, from about 400 ft to the bottom of the well at 1025 ft, is very similar to that measured in the same interval in the Joy No. 1 well, although the temperatures in well 400S averaged about 0.3°F higher. This suggests that the departure from the normal thermal gradient in the Joy No. 1 well are less than 1°F and that the reported temperatures can be used to determine the pumping and setting times of the waste-cement mixes under development.

The marked differences in the thermal gradients in the two wells down to a depth of 200 ft were explained by Diment and Robertson as probably due to the slow circulation of ground water down to this depth. The disturbances in the gradient caused by this circulation down to 200 ft slowly disappear in the interval between 200 and 400 ft. There is no reason to believe that there is any ground water movement below 200 ft, although the data do not entirely rule out this possibility.

At some future date the bottom of the casing in the Joy well will be plugged, and the temperature gradient will again be measured after true equilibrium has been established.

Abnormally Low Pressures in Depth in Joy No. 1 Well.-- For the first year after Joy No. 1 well was drilled there was no way to determine that water was flowing out bottom of the well into the deeper formations; the water level in the then uncased well was maintained by its interconnection at the surface with the main water table. However, in June 1962, a 1-1/4-in. casing was cemented into the well down to a depth of 2900 ft, leaving open the interval below 2900 ft and the bottom of the well at 3263 ft. This open-hole section is in the lower part of the Chickamauga limestone and the upper part of the Knox Dolomite, all rock that appears to have no significant permeability or porosity. These rocks, however, may contain minute fractures, most of which would be expected to be parallel to the bedding planes.

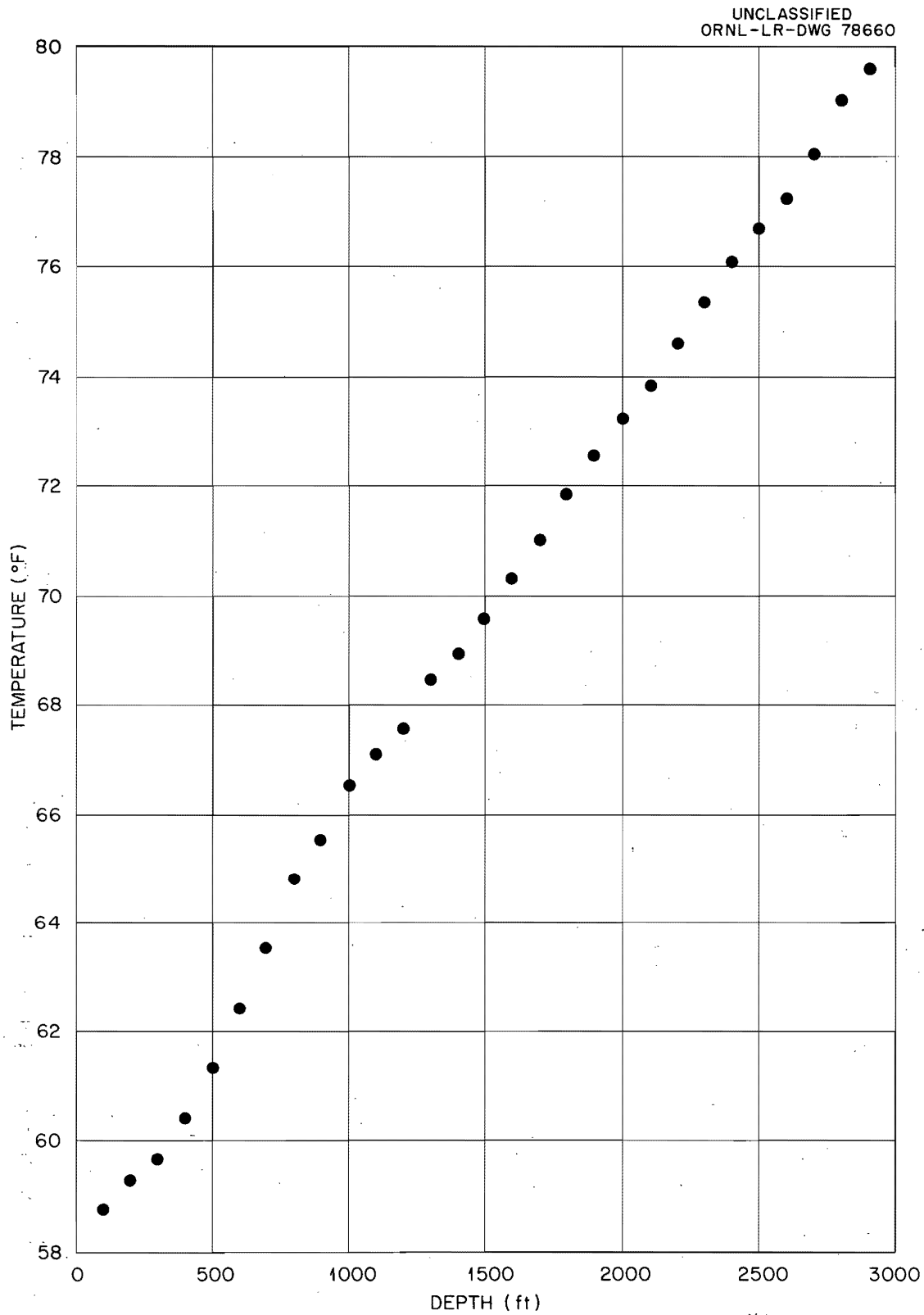


Fig. 5.2. Joy Well No. 1, October 1962: Temperature Measurements by U.S.G.S. Provisional data, subject to revision.

The temperature measurements made in October 1962 were surprising, because they showed that the water level in the casing was 100 to 150 ft below land surface. Following some preliminary tests, the casing was filled to the surface on October 16. Figure 5.3 shows the subsequent water level in the well. Soon this level was below that of Watts Bar Dam, which determines the lowest possible level of the water table for a wide surrounding area, and it became evident that the water was being taken into the lower Chickamauga and upper Knox as the result of an abnormally low liquid pressure in these formations.

This low pressure might conceivably be attributed to the elastic expansion of these rocks due to removal of overburden during the last few million years. However, this process appears to be far too slow, compared with the possible rate of movement of water down through the overlying cover rocks, impermeable as this cover appears to be. Differences in chemical concentration, in temperature, and in electric potential can cause very slow fluid flow through rocks of low permeability by a process which is or closely resembles osmosis. Representatives of the Petroleum Research Corporation (Denver) pointed out that areas of such abnormally low fluid pressure, where they occur as reservoir rocks of considerable extent, thickness and porosity, offer marked advantages for the direct disposal of low-level liquid wastes. The very low porosity and permeability of the rocks penetrated by the bottom open-hole section of Joy No. 1 well suggest, however, that the pressure gradients would be quickly reversed if an attempt were made to pump fluid waste directly into these deeper horizons, with or without the use of hydraulic fracturing to get the fluid out into the rock. The significance of this abnormally low fluid pressure in these deep horizons is that there can be no possible pathways of appreciable permeability between them and the water table.

5.1.2 Waste Mix Studies (T. Tamura)

Mix Development at Westco Research.-- One of the more promising mixes developed for the ORNL intermediate-level waste uses carboxymethylhydroxyethylcellulose (CMHEC) as a fluid-loss additive. In this mix, calcium lignosulfonate (CLS) also acts to reduce fluid loss, though its primary function is to act as a dispersant and retarder. Since CLS costs only 10 cents a pound, and CMHEC costs \$1.00 a pound, it is desirable to substitute CLS for CMHEC as much as possible. To obtain some information about the limits of this substitution, the fluid loss of mixes containing different amounts of CLS and CMHEC was measured. The results are shown in Fig. 5.4 for mixes with simulated ORNL intermediate-level waste and in Fig. 5.5 for mixes with simulated ORNL waste concentrated tenfold. Concentrations of CLS greater than 1.2% were not considered because of the long setting times of such mixes. These figures indicate that if a low fluid loss is desired, CMHEC must be used; if a fairly high fluid loss is acceptable, CLS is an effective substitute for CMHEC; and, whatever the desired fluid loss, some substitution of CLS for CMHEC is probably justified. More specific conclusions are not yet justified, because variation of other components of the mix also affects the fluid loss to

UNCLASSIFIED
ORNL-LR-DWG 78661

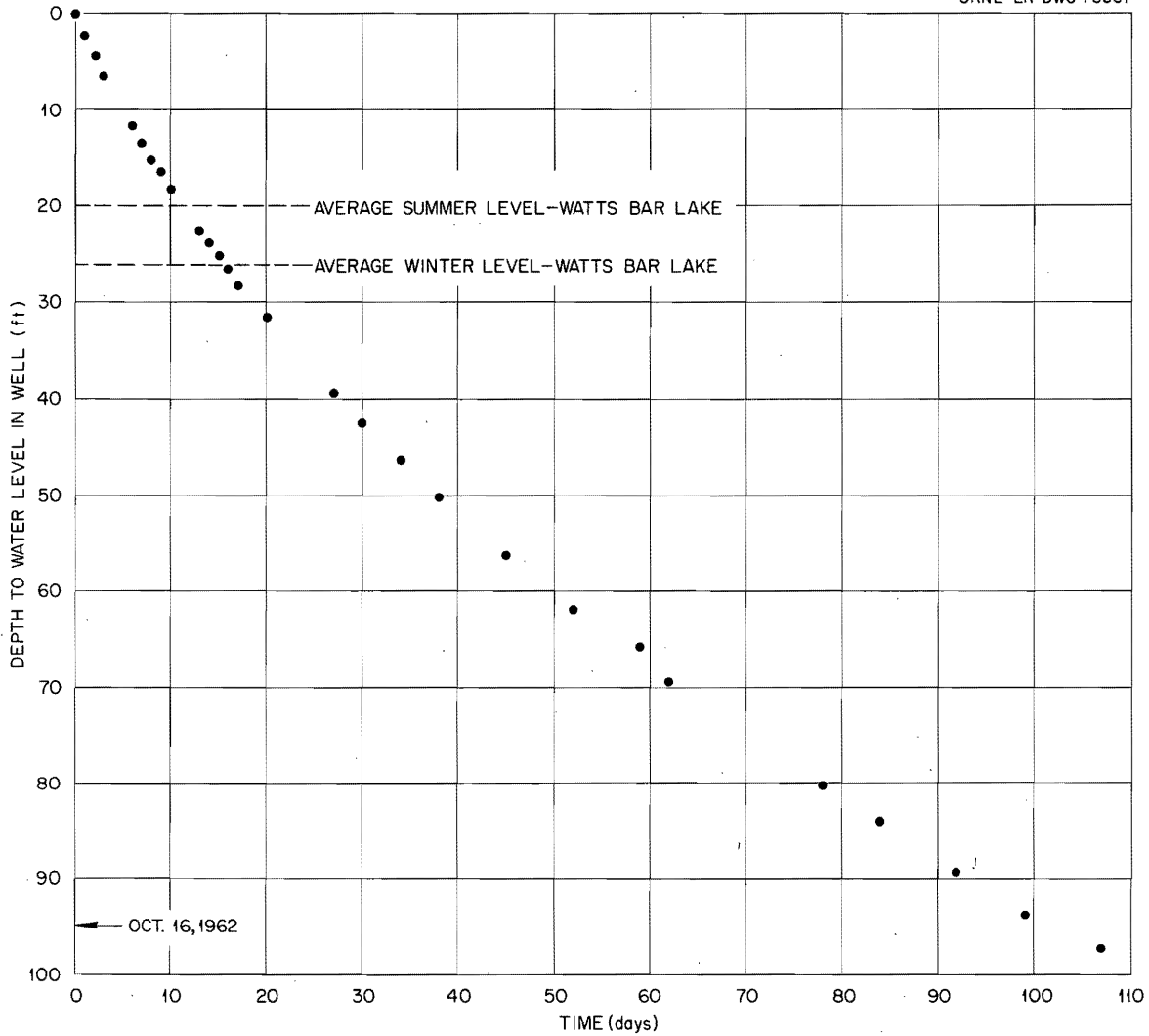


Fig. 5.3. Drop in Water Level in Cased Joy No. 1 Well.

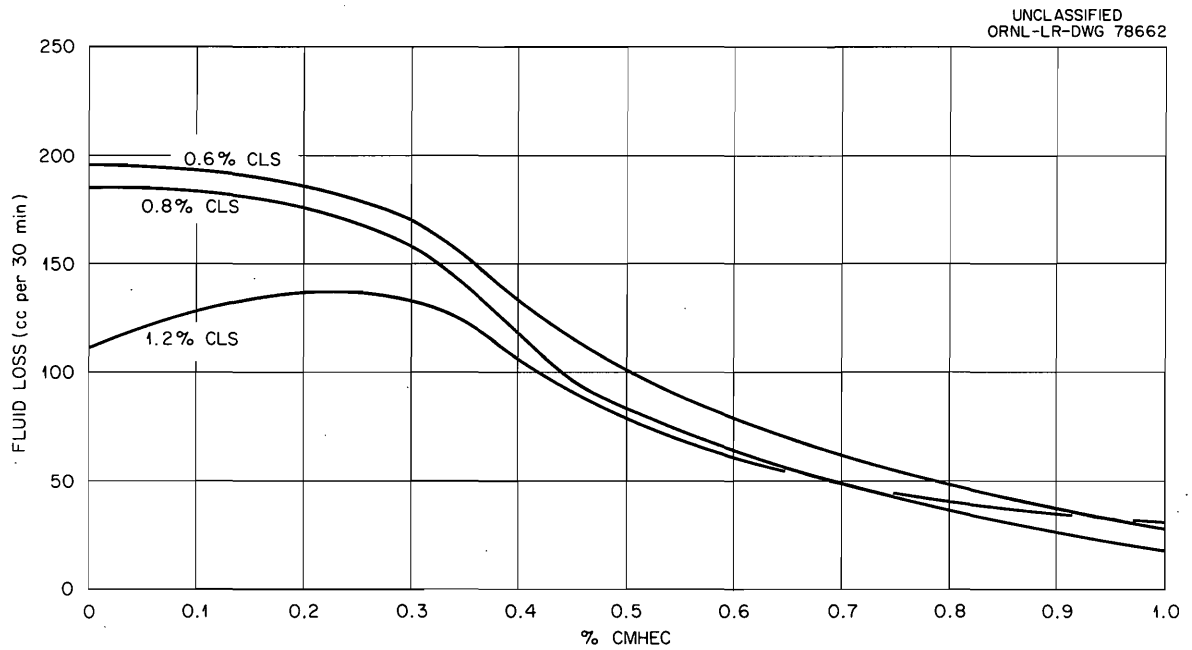


Fig. 5.4. Fluid Loss of Slurries Containing Different Amounts of Carboxymethylhydroxycellulose (CMHEC) and Calcium Lignosulfonate (CLS). Simulated ORNL waste (265 cc), plus portland cement (1 lb).

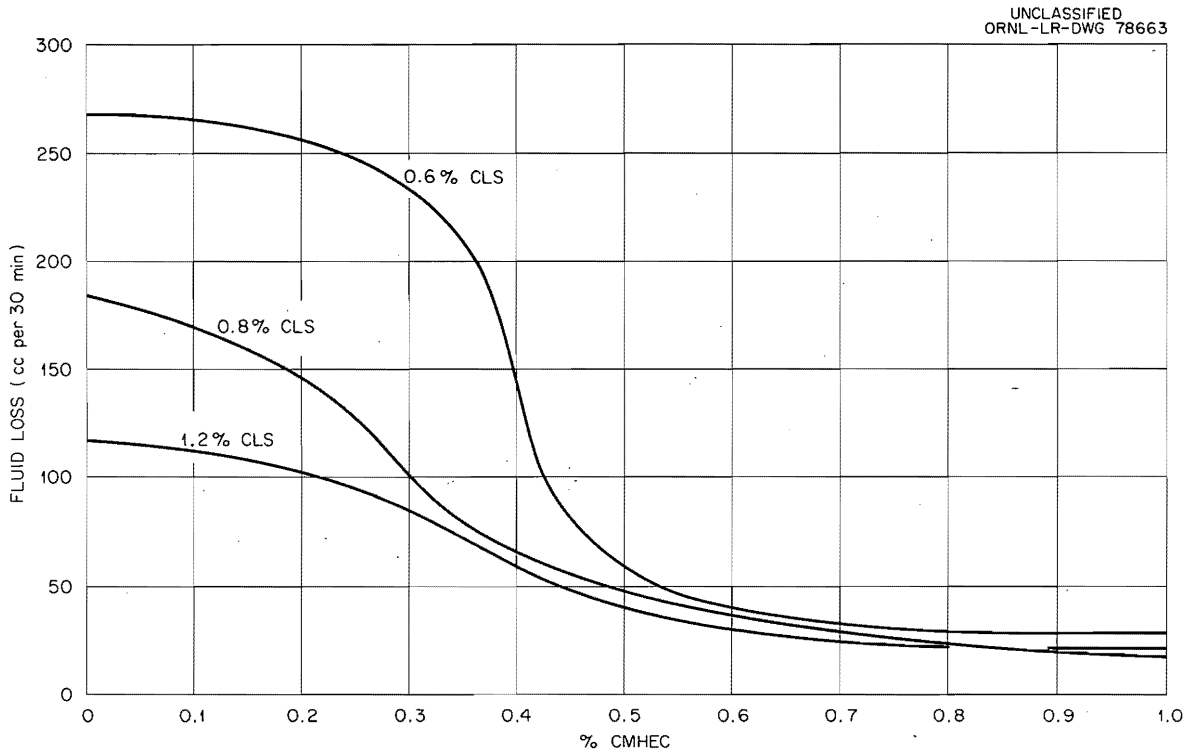


Fig. 5.5. Fluid Loss of Slurries Containing Different Amounts of Carboxymethylhydroxycellulose (CMHEC) and Calcium Lignosulfonate (CLS). Simulated ORNL waste, concentrated tenfold (265 cc), plus cement (1 lb) and bentonite (6%).

an undetermined extent. The above tests were run with a bentonite concentration of 6%. Tests made with a 12% concentration gave similar results with unconcentrated waste; with concentrated waste a low fluid loss (100 cc per 30 min) was noted in the tests with no CMHEC, and the effect of different CLS concentrations was slight. Obviously, bentonite concentration is also a significant variable.

In recent reports from Westco, mix-pumping times that were significantly lower than previous values were reported; the cause for this discrepancy has not been determined. Even with this reduction, the pumping time for mixes with normal ORNL waste is adequate; for mixes with concentrated waste adequate pumping times can be obtained by slightly altering the composition of the mix. The contract with Westco Research was terminated and will not be extended at this time, although there is much work to be done in mix development.

Mix Evaluation at Halliburton Company.-- A contract to provide assistance in the hydrofracturing experiment was signed with the Halliburton Company by ORNL. As part of the contract, mixes developed by Westco are to be evaluated by Halliburton to provide confirmatory data. Discussions were held with members of the Chemical Research and Development Department of Halliburton to consider a program of mix evaluation. The following program was agreed upon, and authorization to proceed was given:

1. Check the Westco mix formulation by using simulated ORNL Intermediate-level waste, with CMHEC as the fluid-loss additive. The following characteristics are to be measured:
 - a. Pumping time under 1000-ft test schedule.
 - b. Fluid loss under 100 psi and 1000 psi.
 - c. Compressive strength of the set grout after three days of curing; the grout is to be prepared from both fresh slurry and pumped slurry.
 - d. Density of slurry.
 - e. Free liquid of the set grout.
2. If the fluid loss under the 1000-psi test (item 1-b) is greater than that for 100 psi, a mix with a higher CMHEC concentration is to be formulated which will maintain a fluid loss of less than 60 cc at 1000 psi. Pumping time and compressive strength will also be determined for the revised mix.
3. Using the usual sodium hydroxide concentration of ORNL waste (0.2 M) as the reference, the pumping time of formulations with 0.1, 0.3, and 0.5 M NaOH will be measured.
4. The properties of a mix containing 0.4% Na₂CO₃ (the reported concentration in ORNL waste) will be measured. The formulation of the mix will depend on the results of tests 1 and 2 above.

5. A bentonite-cornstarch-water mix with maximum fluid-retention properties will be developed for a fluid-loss test in the injection well at ORNL.

6. Simulated wastes prepared with technical-grade chemicals will be tested to establish pumping time.

7. Pumping times will be established with "new" batches of cement obtained from Volunteer Cement Company of Knoxville to provide determinations of the uniformity of the cement.

These tests are being performed at Halliburton and will be reported at a later date.

Mix Evaluation at ORNL.-- The studies at ORNL on waste mixes have been concerned with the retention of radionuclides in mixes developed by Westco Research. In the proposed hydrofracturing experiment, low fluid loss is necessary to prevent dehydration of the slurry when it is in contact with a permeable formation and to keep the radionuclides within the slurry where they will eventually be incorporated in the set grout. The amount of cesium and strontium that might be lost from the grout by fluid loss is determined by tests made with slurries prepared from concentrated waste solutions. Test slurries were tagged with Cs¹³⁷ (0.001 mc/ml) and Sr⁸⁵ (0.0002 mc/ml).

The cesium activity lost by the slurry is shown in Table 27. The slurry was prepared with the following materials:

265 cc of concentrated waste solution
 1 lb of Volunteer Portland cement
 6% bentonite, except as noted
 0.8% calcium lignosulfonate, except as noted
 1.0% fluid-loss additive, except as noted

The slurry was mixed in a Waring Blendor for 35 to 45 sec and poured into a cup lined on the bottom with a 325-mesh screen. A pressure of 100 psi was applied and the filtrate collected for 30 min. One milliliter of the filtrate was counted. The activity reduction reported in the table is the ratio of the activity of the cesium in the filtrate and in the original waste, multiplied by 100. The amount of activity lost is calculated from the specific activity in the filtrate and the total quantity of fluid lost in 30 min.

The results in Table 27 show that cesium activity in the filtrate was reduced by 65% to 75% except in the case of runs 14 and 15, where the reduction was about 10%. The mix formulation used in runs 14 and 15 contained no fluid-loss additive, calcium lignosulfonate, or bentonite. The formulation used in runs 21 and 13 had no fluid-loss additive, and the mix used in runs 6 and 7 had no calcium lignosulfonate. The cesium retention in all four cases was 65% or better. A comparison of these results with the results of runs 14 and 15 forces the conclusion that

Table 27. Cesium Activity in Filtrate from Fluid-Loss Tests with Concentrated Simulated Waste

Number	ORNL Test Number	Fluid-Loss Additive	Fluid-Loss (cc/30 min)	Activity (counts min ⁻¹ ml ⁻¹) in:		Activity Reduction (%)	Activity Lost in Filtrate (%)
				Waste	Filtrate		
1	62-11-5	CMHEC 1.0%	9.3	27,400	7,625	72	0.98
2	62-11-14	CMHEC 1.0%	7.8	27,200	7,270	73	0.79
3	62-11-19	CMHEC 1.0%	8.6	27,400	7,100	74	0.84
4	62-11-11	CMHEC 0.5%	29.6	27,190	8,460	69	3.48
5	62-11-21	CMHEC 0.5%	27.5	27,000	7,945	70	3.05
6	62-11-12	CMHEC 0.5%	43 ^a	26,990	9,175	66	5.52
7	62-11-22	CMHEC 0.5%	44 ^a	26,890	9,417	65	5.82
8	62-11-8	Cemad 1.0%	23.8	27,300	8,615	68	2.83
9	62-11-16	Cemad 1.0%	23.6	27,000	8,640	68	2.85
10	62-11-10	ET-181-6 1%	107 ^b	27,130	8,575	68	--
11	62-11-20	ET-181-6 1%	85 ^b	27,220	8,810	68	--
12	62-11-7	--	73	27,290	8,805	68	8.89
13	62-11-15	--	72	26,780	8,290	69	8.41
14	62-11-13	--	53 ^c	27,130	24,240	11	--
15	62-11-23	--	64 ^c	27,110	25,050	8	--

^aNo calcium lignosulfonate in these mixes.

^bThese mixes flash set. Mix was scooped out for test; no reported fluid-loss value at time of blowout.

^cNo fluid-loss additive, calcium lignosulfonate and bentonite; fluid loss not measured at time of blowout.

bentonite is the additive responsible for cesium retention in the slurry. This conclusion is strengthened by the fact that other work here has shown that bentonites can sorb cesium even in the presence of competing cations such as sodium. Bentonite, then, serves to retain cesium, in addition to acting as a dispersant and as a fluid-loss additive.

The data in Table 28 show that very little strontium is lost with the fluid. Variation of the additives in the mix had no appreciable effect on strontium retention. The primary variable seemed to be the presence or absence of small particles that sometimes passed through the screen in the first few seconds. This strong association of strontium with the solid particles is about what would be expected from the structure of cements. Since cements are primarily solid calcium silicates which react with water to form hydrated calcium silicate, any small amount of predissolved strontium would quickly enter into reactions common with calcium.

It may be noted in passing that the fluid-loss values reported in Tables 27 and 28 are similar to the values reported by Westco.

Studies are now in progress to determine the leachability of ions from grouts that have been allowed to cure for several days.

5.2 Design of the Fracturing Disposal Pilot Plant

5.2.1 Final Design of Injection Well (Halliburton Company)

Surface Fittings.-- A sketch of the wellhead for the injection well is shown in Fig. 5.6. Not shown in this sketch are the fittings that will be attached to the 2-7/8-in.-OD tubing; these fittings will be varied, depending on the operation being performed in the well.

5.2.2 Well Construction (R. C. Sexton, W. de Laguna)

Plans for the drilling, logging, casing, and cementing of the injection and observation wells are virtually complete. A contract is being negotiated with the Jack Terry Well Drilling Company for the drilling of the two wells, and the casing, tubing, and fittings are being procured. Contracts for logging and cementing the wells are being negotiated.

Current plans call for various steps in drilling, logging, and cementing the two wells to take place in the following sequence:

Injection Well

1. Drill a 12-in.-diam hole to a depth of 150 ft and set the 9-5/8-in. casing string.
2. Cement in, under pressure, the 9-5/8-in. casing string.

Table 28. Strontium Activity in Filtrate from Fluid-Loss Tests with Concentrated Simulated Wastes

Number	ORNL Test Number	Fluid-Loss Additive	Fluid-Loss (cc/30 min)	Activity (counts min ⁻¹ ml ⁻¹) in:		Activity Reduction (%)	Activity Lost in Filtrate (%)
				Waste	Filtrate		
16	62-10-14	CMHEC 1.0%	10.5	26,370	1,625	93.8	0.24
17	62-10-19	CMHEC 1.0%	8.0	25,350	770	98.0	0.09
18	62-10-18	CMHEC 0.5%	22.0	25,070	285	98.9	0.09
19	62-11-2	CMHEC 0.5%	25.8	23,500	200	99.1	0.08
20	62-11-4	CMHEC 0.5%	29.8 ^a	23,260	145	99.9	--
21	62-10-16	Cemad 1.0%	22.4	25,150	2,890	88.5	0.97
22	62-10-21	Cemad 1.0%	25.0	24,570	1,476	94.0	1.10
23	62-10-17	ET-181-6 1.0%	51.5	25,450	535	97.9	0.41
24	62-10-22	ET-181-6 1.0%	51.5 ^a	23,500	200	99.1	0.08
25	62-10-15	--	83.0 ^b	26,510	1,155	95.6	1.36
26	62-10-20	--	78.0 ^b	24,720	740	97.0	0.88
27	62-11-3	--	74.0 ^c	23,260	165	99.3	--

^aNo calcium lignosulfonate in this mix.

^bNo fluid-loss additive in this mix.

^cNo fluid-loss additive, calcium lignosulfonate, or bentonite.

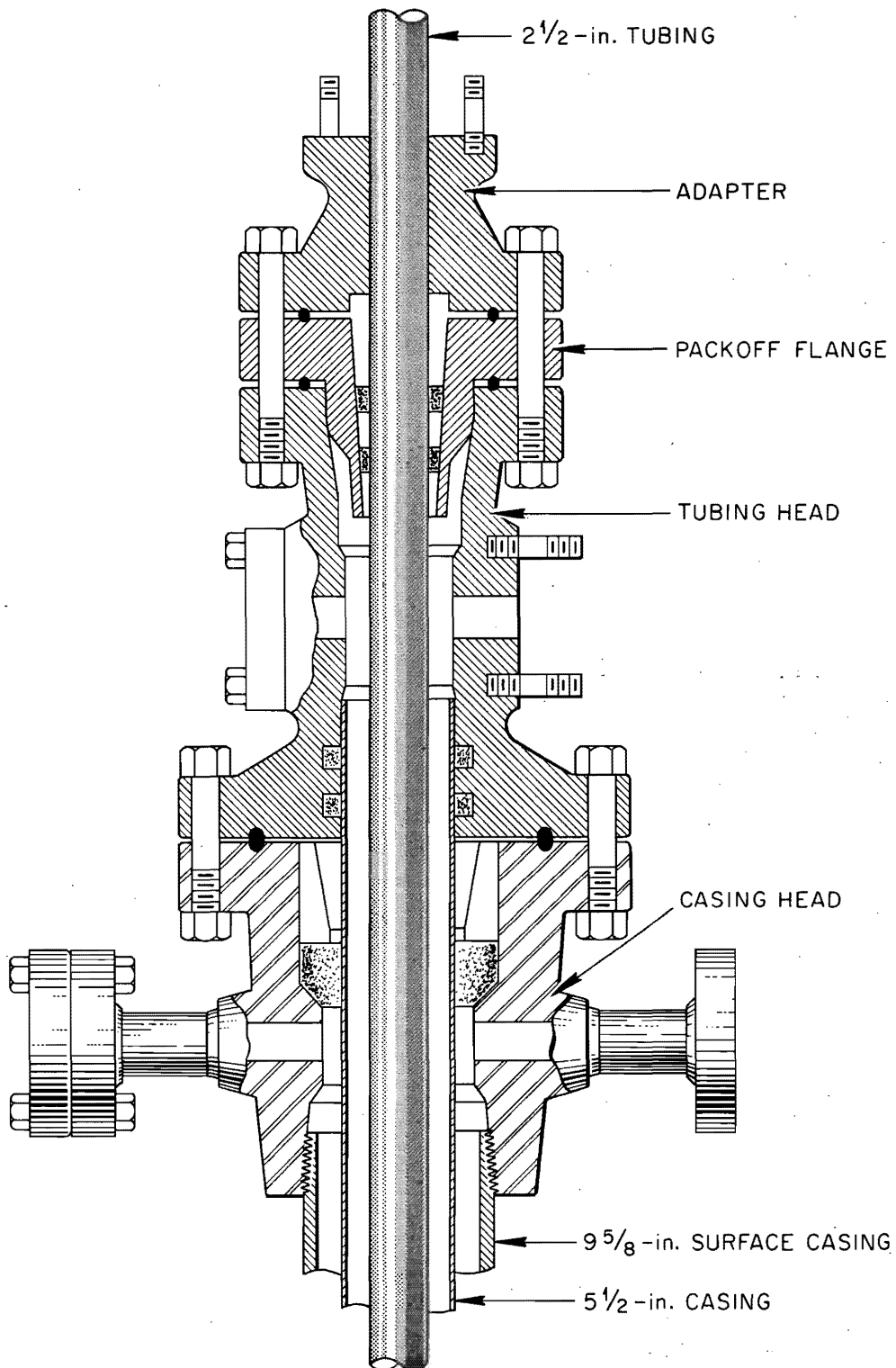


Fig. 5.6. Wellhead for Injection Well.

3. Drill a 8-3/4-in.-diam hole from the bottom of the 9-5/8-in. casing string to a depth of 1050 ft.
4. Perform a directional and inclination survey on the above well.
5. Run an electric (resistivity and self-potential log) and a gamma-ray log on the above well.
6. Set about 1050 ft of 3-1/2-in. casing (type N-80 extreme line) in the well, being particularly careful to get all joints tight.
7. Cement in, under pressure, the 5-1/2-in. casing string.

Observation Well

1. About 150 ft north of the injection well, drill a 10-in-diam hole 100 ft deep and set the 7-in. casing string.
2. Cement in, under pressure, the 7-in. casing string.
3. Drill a 6-in.-diam hole from the bottom of the 7-in. casing string to a depth of 1050 ft.
4. Perform a directional and inclination survey on the above well.
5. Run an electric and a gamma-ray log on the above well.
6. Set about 1050 ft of 2-7/8-in.-OD tubing in the well. The joints on the lower 350 ft of this tubing are to be welded; the lower 350 ft is to be coated with tar.
7. Cement in, under pressure, the tubing string.

5.2.3 Design of Pilot Plant (H. Weeren)

Schedule of Design and Construction.-- Under the present schedule the following phases of the hydrofracture experiment will be completed this fiscal year:

1. Detail design of the injection facility.
2. Drilling, logging, casing, and cementing of the injection and observation wells.
3. Installation of a waste transfer line from near waste trench 7 to the site of the hydrofracture experiment, and expansion of existing electrical facilities. These items will be done with GPP funds.
4. Modification of the existing waste storage tanks and installation at the site.

5. Modification of the existing waste transfer pumps and installation at the site.

6. Installation of the bulk of the waste transfer and service piping.

In addition, work will continue under the contract with the Halliburton Company on design assistance and mix development.

Site Layout.-- A sketch of the proposed site layout is shown in Fig. 5.7. Not shown on this sketch is the site of the observation well (which is 150 ft north of the injection well) and the location of the existing water tank (which is about 80 ft east of the injection well). A graveled all-weather road is slightly to the south of the area shown on the sketch.

Waste Transfer Line.-- A 2-in. plastic line is to be run from a connection on the existing plastic waste line feeding waste trench 7 to the site of the hydrofracture experiment. The connection will be made at a valve box at station 11 + 22.2. The valving will be so arranged that, if necessary, waste can be pumped from the hydrofracture site to the waste trench.

The waste transfer line is a capital item; design and construction will be paid for with GPP funds.

Waste Storage Tanks and Waste Pumps.-- Surplus mild-steel tanks were found in storage at Oak Ridge, and they will serve as waste storage tanks after slight modification. Three tanks will be used: Two are 8 ft in diameter and 44 ft long; one is 10 ft in diameter and 22 ft long. The total capacity of the three tanks is 45,000 gal; hence, the volume of waste injected in any single experiment will be somewhat less than the 50,000 gal originally proposed.

Modification of these tanks will include the installation of a float-type level indicator, air spargers, and an off-gas connection on each tank. A single sampler for the three tanks will be provided at the pump pit, and the valving at the pump will be so arranged that solution from any one of the tanks can be pumped through the sampler.

Two surplus Moyno pumps were obtained for use as a waste transfer pump and spare. These pumps are type 2L14H, capable of delivering 240 gpm at a 205-psi head. A third Moyno pump (type 2L10H) was obtained for use as a water pump. All three pumps are equipped with Vari-Drives.

Layout of Mixing Cell.-- A tentative layout of the mixing cell is shown in Figs. 5.8 and 5.9. During an injection, one operator will observe the solids level in the mixer hopper through windows in the cell wall and mixer assembly and will control this level by adjustment of a butterfly valve located in the bottom of the hopper tank. The second operator will observe the level of grout in the sump tub and adjust the flow of waste into and the flow of grout out of the sump tub to keep this level approximately constant.

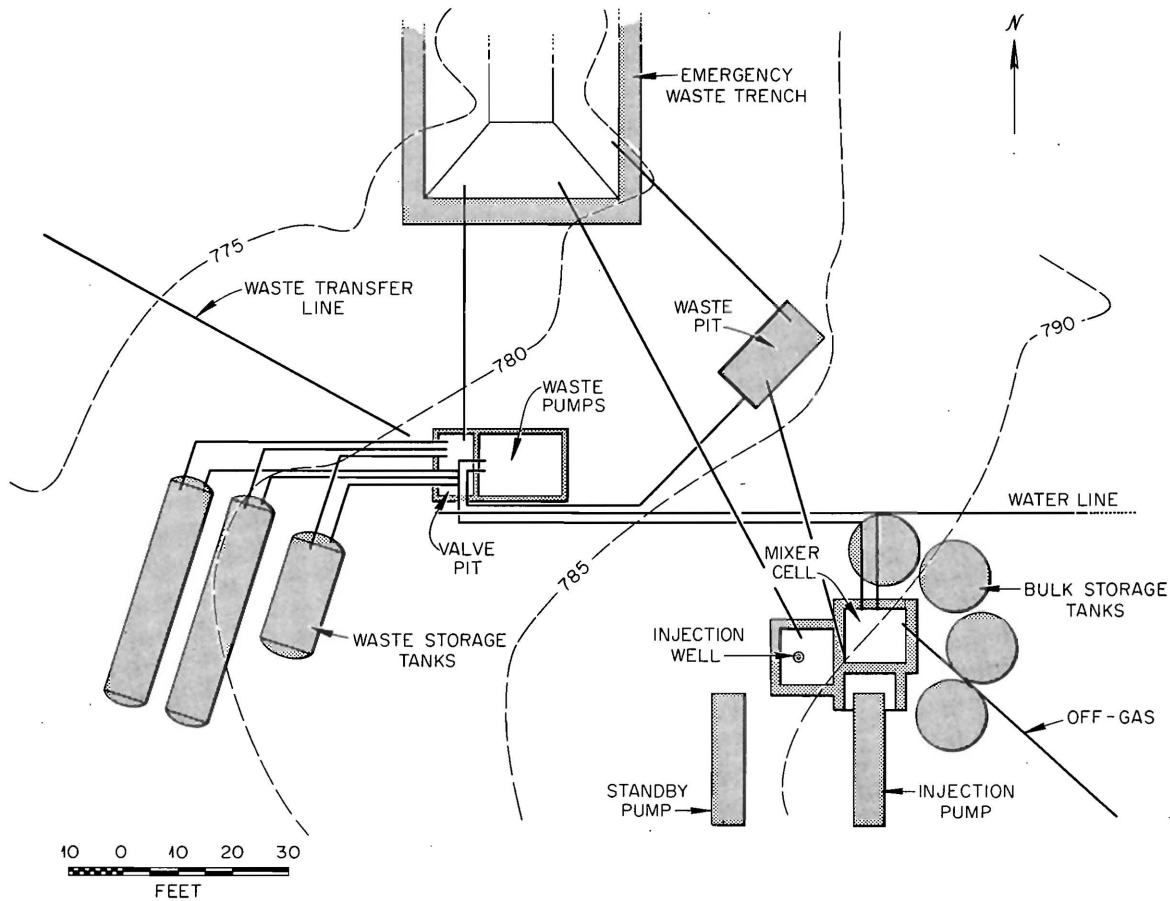


Fig. 5.7. Layout of the Fracturing-Disposal Pilot Plant.

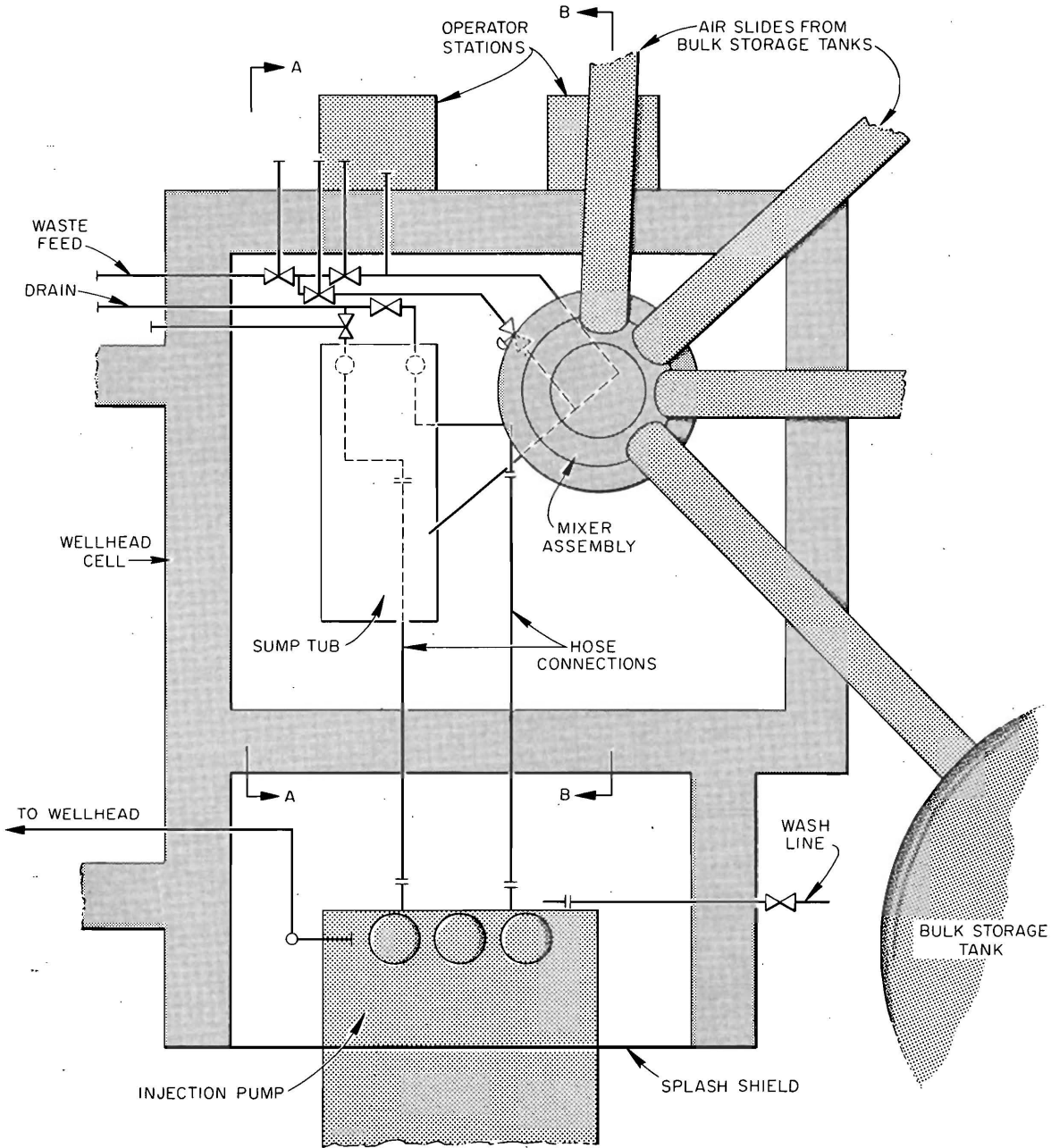
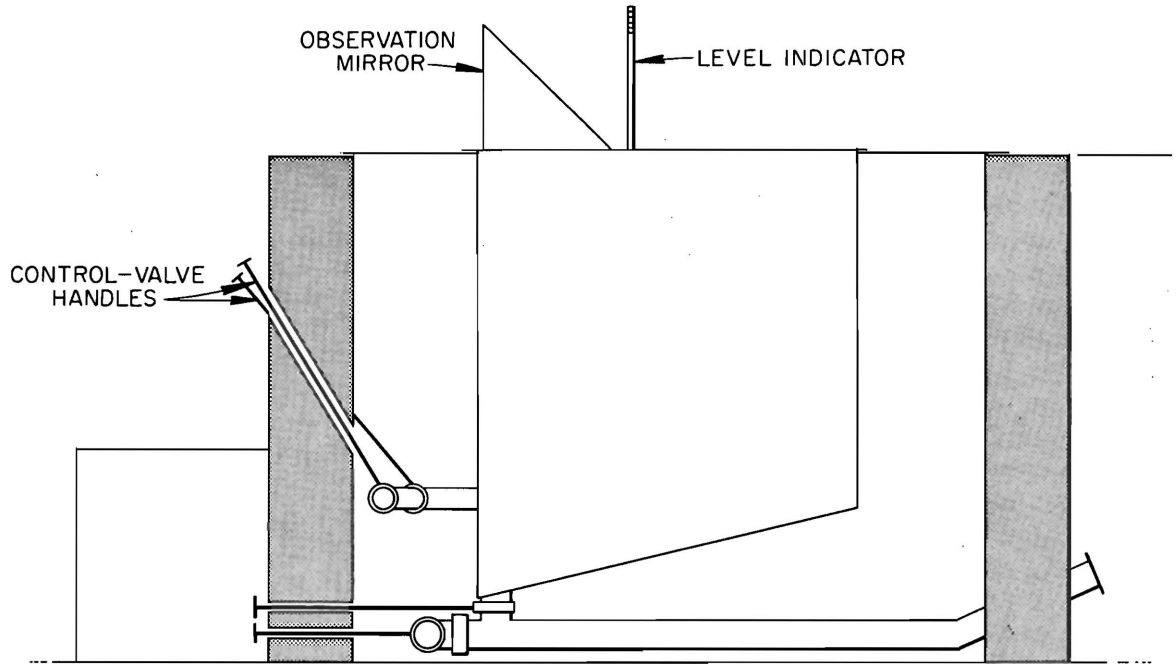
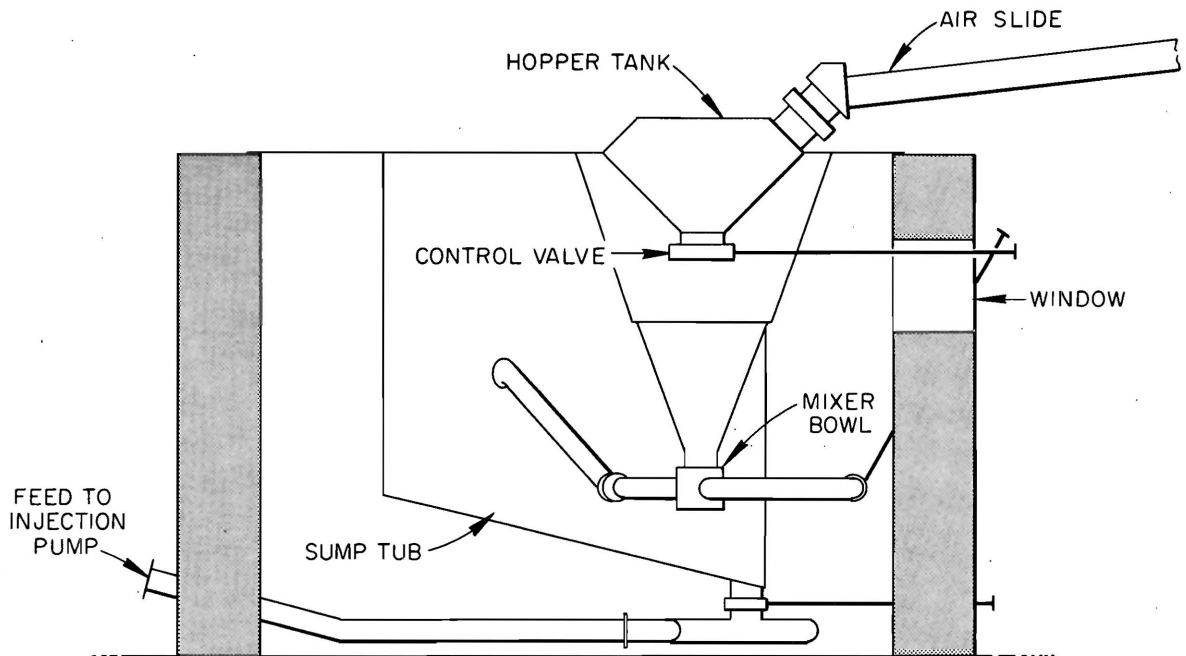


Fig. 5.8. Plan View of Mixing Cell.



SECTION A-A



SECTION B-B

Fig. 5.9. Sectional Views of Mixing Cell.

APPENDIX A

RESULTS OF MICROSCOPIC EXAMINATION

- 89 Mostly extremely fine calcite - less than 10 μ , few particles to 40 μ .
Quartz to 40 μ . Clay minerals too small to be seen individually -
in aggregate particles with fine calcite.
- 95 Calcite extremely fine: mostly less than 10 μ , few particles to 40 μ .
Quartz to 40 μ . Clay minerals too small to be seen individually -
in aggregates many of which show aggregate orientation and high bire-
fringence of micas. Aggregates have only a little calcite as though
clay minerals and calcite not very intimately mixed.
- 205 Calcite mostly 10 to 50 μ . Quartz to 40 μ . Glauconite to 80 μ is
common. Clay minerals in random oriented aggregates - particles too
small to be seen individually - little mixing with calcite.
- 530 Calcite to 40 μ . Quartz to 40 μ - mainly very fine - less than 20 μ .
Clay mineral flakes to 80 μ - many flakes to 40 μ . Some oriented
aggregates. Many green chloritic flakes. Few glauconites to 80 μ .
Dirty appearance probably due to organics.
- 719 Calcite trace to 40 μ . Quartz to 80 μ . Rare grains of glauconite
to 80 μ . Clay minerals in flakes to 20 μ - many flakes to 10 μ .
Aggregates often showing aggregate orientation. Green flakes of
chlorite are quite abundant. Dirty appearance due to organic
material.

- 811 Calcite trace to 40 μ . Quartz to 100 μ . Glauconite common to 80 μ . Clay minerals to about 20 μ - mostly very fine, in dirty-appearing (due to ferric iron) aggregates.
- 942 Quartz to 100 μ . Mica to 40 μ - mostly less than 10 μ . Few clay mineral aggregates - mostly dispersed flakes. Few grains of glauconite. Few green flakes of chlorite. Dirty appearance perhaps due to organics.
- 1010 Quartz to 100 μ unsorted. Trace calcite to 40 μ . Feldspar to 80 μ . Clay minerals in colorless individual flakes to 20 μ .
- 1114 Quartz to 100 μ - unsorted. Feldspar to 100 μ . Clay mineral colorless flakes to 30 μ - no aggregates. Rare glauconite to 40 μ .
- 1244 Calcite, trace to 30 μ . Quartz to 150 μ . Feldspar to 150 μ . Clay minerals many particles to 20 μ - some larger flakes to 40 μ . Green glauconite-looking particles to 80 μ - some few oriented aggregates with dirty appearance probably due to organics.
- 1358 Calcite to 50 μ . Quartz to 50 μ . Clay minerals to 30 μ but mostly too small to be seen individually - in aggregates with little preferred orientation, dirty appearance probably due to ferric iron. Clay mineral has fairly high birefringence.
- 1381 Calcite to 20 μ but mostly very fine, less than a few microns. Quartz exceedingly rare and fine - less than 20 μ . Clay mineral in particles too small to be seen individually and mixed with calcite. No clay mineral aggregates.

- 1552 Calcite substantially all less than 10 μ . No other components definitely determinable.
- 1648 Calcite to 40 μ - mostly less than 10 μ . Quartz less than 20 μ . Clay minerals in individual colorless flakes to 20 μ - mostly less than 10 μ . No glauconite and no clay mineral aggregates.
- 1784 Calcite to 40 μ - mostly less than 10 μ . No other components definitely visible. Any quartz extremely fine. Any clay minerals in individual flakes less than about 10 μ .
- 1867 Calcite to 40 μ , but mostly less than 10 μ . No quartz or clay mineral can be identified definitely.
- 2086 Calcite to 30 μ , but mostly less than 10 μ . Quartz to 30 μ . Clay minerals less than 10 μ , mostly too small to be seen individually. Many dirty appearing (probably due to ferric oxide) aggregates of calcite and clay minerals without aggregate orientation.
- 2286 Calcite to 40 μ , mostly less than 10 μ . No other components definitely determinable. Any clay minerals or quartz extremely small (less than 20 μ). No clay mineral aggregates.
- 2648 Calcite to 50 μ , but mostly less than 10 μ . Quartz to 40 μ . Clay minerals in individual flakes to 20 μ , but mostly less than 10 μ in individual flakes and aggregates with calcite. Aggregates have little preferred orientation. Clay mineral has high birefringence.

- 2701 Calcite to 40 μ . Quartz to 40 μ . Clay mineral to 30 μ in individual flakes and random aggregates - all red ferric iron stained.
- 2705 Calcite to 80 μ unsorted. Quartz to 80 μ . Clay mineral, few flakes to 80 μ - some green chlorite. Most of clay mineral is colorless and less than 10 μ in individual flakes and in random aggregates with the calcite.
- 2826 Calcite to 40 μ unsorted. Quartz to 40 μ unsorted. Clay mineral in flakes to 20 μ , but mostly less than 5 μ - in individual flakes and dirty appearing aggregates (probably due to ferric iron) with little preferred orientation. Clay mineral has high birefringence.
- 2852 Calcite to 40 μ - mostly less than 10 μ . Quartz to 40 μ . Clay mineral in individual flakes less than 10 μ and aggregates with the calcite. Clay mineral colorless and highly birefringent.
- 3035 Calcite to 80 μ , but mostly less than 40 μ (unsorted below 40 μ). Quartz to 80 μ . Clay mineral in flakes to 20 μ but mostly less than 10 μ in individual and dirty appearing aggregates with calcite. Little preferred orientation and high birefringence.
- 3139 Carbonate to 100 μ - much very coarse. No other component can be identified definitely.

APPENDIX B

CLAY ANALYSES

Table B.1. Results of X-Ray Diffraction Analysis of Particles 2 μ or Less in Diameter. The quantitative differentiation of kaolinite and chlorite is difficult. In every case, the value for kaolinite is perhaps high, and, for chlorite, it may be low. Particle sizes are those following dispersion in water.

Sample No.	Calcite	Quartz	Illite ^a	Kaolinite	Chlorite	Miscellaneous
89	60% mostly +2 μ 1/3, -2 μ 1/4, -1 μ	10% mostly -2 μ 1/3, -1 μ	15% highly degraded all -2 μ 1/3, -1 μ mixture di- and trioctahedral	5% mostly -1 μ	10% highly degraded mostly -1 μ	
95	20% mostly -2 μ 1/2, -1 μ	15% mostly -2 μ 1/3, -1 μ	35% moderately degraded all -2 μ mostly -1 μ dioctahedral	10% mostly -1 μ	15% highly degraded mostly -1 μ	tr. feldspar ^b tr. dolomite
205	35% mostly -2 μ 1/3, -1 μ	25% 1/2, -2 μ 1/3, -1 μ	20% slightly degraded all -2 μ mostly -1 μ mixture di- and trioctahedral	5% mostly -1 μ	10% highly degraded mostly -1 μ	5% feldspar
530	trace	25% mostly +2 μ 1/3, -2 μ 1/4, -1 μ	40% moderately degraded all -2 μ mostly -1 μ dioctahedral	15% mostly -1 μ	15% highly degraded mostly -1 μ	tr. feldspar mont- morillonite ?
719		25% mostly +1 μ 1/3, -2 μ 1/4, -1 μ	45% moderately degraded all -2 μ mostly -1 μ dioctahedral	15% mostly -1 μ	15% highly degraded mostly -1 μ	tr. feldspar mont- morillonite ?

Table B.1. continued

Sample No.	Calcite	Quartz	Illite ^a	Kaolinite	Chlorite	Miscellaneous
811	trace	20% mostly +1 μ 1/3, -2 μ 1/4, -1 μ	45% moderately degraded all -2 μ mostly -1 μ mixture di- and trioctahedral	15% mostly -1 μ	15% highly degraded mostly -1 μ	tr. feldspar mont- morillonite ?
942		30% mostly +2 μ 1/4, -2 μ tr., -1 μ	40% slightly degraded all -2 μ mostly -1 μ dioctahedral	10% mostly -1 μ	20% moderately degraded mostly -1 μ	tr. feldspar mont- morillonite ?
1010	5% mostly -1 μ	60% mostly +2 μ 1/3, -2 μ 1/4, -1 μ	15% moderately degraded all -2 μ mostly -1 μ	5% mostly -1 μ	5% highly degraded mostly -1 μ	10% feldspar mont- morillonite ?
1114		60% mostly +2 μ 1/3, -2 μ 1/4, -1 μ	20% slightly degraded all -2 μ 1/2, -1 μ dioctahedral	5% mostly -1 μ	5% moderately degraded mostly -1 μ	10% feldspar
1244	trace	35% mostly +2 μ 1/4, -2 μ	35% slightly degraded all -2 μ 1/2, -1 μ dioctahedral	10% mostly -1 μ	15% moderately degraded mostly -1 μ	5% feldspar
1358	10% mostly +2 μ	20% mostly +2 μ 1/3, -2 μ 1/4, -1 μ	45% moderately degraded all -2 μ 1/2, -1 μ dioctahedral	trace	10% highly degraded mostly -1 μ	5% feldspar 10% mixed-layer

Table B.1. continued

Sample No.	Calcite	Quartz	Illite ^a	Kaolinite	Chlorite	Miscellaneous
1381	50% mostly +2 μ 1/3, -2 μ 1/4, -1 μ	10% mostly +2 μ 1/3, -2 μ 1/4, -1 μ	25% moderately degraded all -2 μ mostly -1 μ mixture di- and trioctahedral	5% mostly -1 μ	10% well degraded mostly -1 μ	
1552	80% mostly +2 μ 1/4, -2 μ	5% mostly +2 μ	10% highly degraded all -2 μ mostly -1 μ mixture di- and trioctahedral	trace	5% well degraded mostly -1 μ	mont- morillonite ?
1648	40% mostly -2 μ 1/3, -1 μ	15% mostly -2 μ 1/3, -1 μ	25% slightly degraded all -2 μ mostly -1 μ mixture of di- and trioctahedral	10% mostly -1 μ	10% moderately degraded mostly -1 μ	mont- morillonite ?
1784	85% mostly +2 μ 1/3, -2 μ	5% only trace -2 μ	5% well degraded all -2 μ	trace mostly -1 μ	5% well degraded mostly -1 μ	5% mixed-layer
1867	80% mostly +2 μ 1/3, -2 μ	5% only trace -2 μ	10% entirely a random mixed-layer assemblage of three-layer clay minerals			10% dolomite
2086	35% mostly -2 μ	15% about 1/2 -2 μ about 1/4 -1 μ	30% slightly degraded all -2 μ mostly -1 μ dioctahedral	5% mostly -1 μ	10% slightly degraded mostly -1 μ	5% dolomite

Table B.1. continued

Sample No.	Calcite	Quartz	Illite ^a	Kaolinite	Chlorite	Miscellaneous
2286	70% mostly +2 μ 1/3, -1 μ	5% mostly +2 μ 1/3, -1 μ	15% moderately degraded all -2 μ mostly -1 μ mixture di- and trioctahedral	5% mostly -1 μ	5% well degraded well degraded mostly -1 μ	tr. dolomite
2648	55% mostly -2 μ 1/2, -1 μ	10% mostly +2 μ 1/3, -1 μ	20% moderately degraded all -2 μ mostly -1 μ mixture di- and trioctahedral	5% mostly -1 μ	10% well degraded well degraded mostly -1 μ	10% dolomite
2701	20% mostly -2 μ 1/2, -1 μ	15% about 1/2, -2 μ 1/4, -1 μ	40% slightly degraded all -2 μ mostly -1 μ mixture di- and trioctahedral	5% mostly -1 μ	10% well degraded mostly -1 μ	10% dolomite mont- morillonite ?
2705	60% mostly +2 μ 1/3, -1 μ	15% mostly +2 μ 1/3, -1 μ	10% well degraded all -2 μ 1/3, -1 μ mixture of di- and trioctahedral	tr. mostly -1 μ	5% well degraded mostly -1 μ	10% dolomite
2826	30% mostly -2 μ 1/3, -1 μ	20% about 1/2, -2 μ 1/3, -1 μ	25% slightly degraded all -2 μ mostly -1 μ mixture di- and trioctahedral	5% mostly -1 μ	10% well degraded mostly -1 μ	10% dolomite

Table B.1. continued

Sample No.	Calcite	Quartz	Illite ^a	Kaolinite	Chlorite	Miscellaneous
2852	30% mostly -2 μ 1/3, -1 μ	15% about 1/2, -2 μ 1/3, -1 μ	30% slightly degraded all -2 μ mostly -1 μ mostly dioctahedral some trioctahedral	5% mostly -1 μ	10% slightly degraded mostly -1 μ	10% dolomite
3035	30% mostly -2 μ 1/3, -1 μ	15% mostly -2 μ 1/2, -1 μ	25% slightly degraded all -2 μ mostly -1 μ mixture of di- and trioctahedral	5% mostly -1 μ	10% slightly degraded mostly -1 μ	15% dolomite
3139	80% mostly +2 μ	5% mostly +2 μ	15% entirely a random mixed-layer assemblage of three-layer clay minerals			35% dolomite mostly +2 μ 1/4, -2 μ

^aUnless so indicated, it is impossible to determine polymorphic form of illite, i.e., whether dioctahedral (muscovite) or trioctahedral (biotite) and form of dioctahedral types.

^btr. = trace; less than 5%.

6. DISPOSAL IN NATURAL SALT FORMATIONS

6.1 High Temperature Experiments

R. L. Bradshaw F. M. Empson W. J. Boegly, Jr.

6.1.1 Array Experiment - Heater Failure

The six peripheral heaters of the array experiment failed shortly after startup. The primary cause of failure was parting of the nickel connecting wire. Analyses of the original nickel hookup wire showed the sulfur content to be 0.0035%, compared with 0.0089% for a fractured sample. Both of these analyses are within the 0.01% sulfur allowed by ASTM specification B160-61 for nickel rod and bar. However, metallography²⁵ of the wire showed the presence of nickel sulfide in the grain boundaries at the fractures, while no sulfide was visible in the original wire. Failure of the nickel leads is believed to be due to localized high concentrations of nickel sulfide, coupled with vibrations produced by the magnetostrictive effect.²⁶

6.1.2 Corrosion of Heater and Thermocouple Sheaths

A number of thermocouple failures occurred during the high temperature heat experiments as a result of scaling and corrosion of the type 304 SS sheath. When the large heaters were removed from the structure, they were also heavily scaled, with the greatest attack on the heaters exposed to the highest temperature.

Thermocouples attached to the wall heater were found by metallography²⁷ to have lost as much as 0.007 in. of the original 0.018 in. thickness by scaling. Heavy intergranular attack also completely penetrated the sheath. This resulted from exposure to approximately 600°C for 33 days. Thermocouples in the salt at 6 in. out from the heater showed much less scaling, but complete penetration due to stress corrosion cracking was observed. At 12 in. out from the heater, there was a small amount of scaling on the thermocouples. The temperature reached approximately 225°C at 6 in. and 190°C at 12 in. out from the heater.

The wall heater that operated at temperatures up to 690°C for 33 days was very heavily scaled, and intergranular attack to 0.045 in. was observed. Significantly, carbide precipitation was also observed at grain boundaries throughout the heater wall, serving to accelerate the intergranular attack. The floor heater that reached a maximum of 590°C in 33 days was less heavily scaled, and intergranular attack penetrated only 0.002 in. Precipitated carbides were present at the grain boundaries. The array heater in the floor had still less scale on the surface after 28 days of operation at a maximum temperature of 435°C, and intergranular attack penetrated only to 0.0015 in. No carbide precipitation was observed in the array heater sheath. Table 29 presents these data. Since carbides may be expected to precipitate in type 304L stainless steel

Table 29. Corrosion of Type 304L Stainless Steel Heater Cans

Location	Maximum Temperature (°C)	Duration (days)	Scaling	Intergranular Penetration	Carbide Precipitation
Wall	690	33	Severe	0.045	Yes
Floor	590	33	Moderate	0.002	Yes
Array	435	28	Slight	0.0015	No

in the range of 800 to 1600°F (426 to 870°C), the long period of operation of the wall and floor heaters within this temperature range provided ideal conditions for carbide precipitation. The array heater operated at the very lower limit of carbide precipitation, and no precipitation was observed. This indicates that calcination operations and storage of calcined waste containers should be carefully controlled to minimize the time containers are in the temperature range of carbide precipitation.

6.1.3 Removal of Wall Heater Hole

In order to inspect in detail the condition of the hole used in the high-temperature test in the wall, the hole was removed as part of a block, 4 x 4 x 8 ft. The block was cut from the wall by means of a short-wall undercutter. It was cut to 9 ft 6 in. from the face, but it broke, as shown in Figs. 6.1 and 6.2. Only that part of the block above the shale parting at 6 ft from the floor broke off at 9 ft 6 in. That portion below the parting broke at 8 ft, even with the zone of maximum temperature. Figure 6.3 shows the last 2 ft of the heater hole remaining in the wall. The fractured surface of the hole may be seen together with radial cracks out into the structure. The original diameter of the hole was 10 in. Dimensions of the present cavity are 7-1/4 in. at the horizontal center line and about 9-1/4 in. at the vertical center line. At the rear of the hole the horizontal dimension is 9 in. and the vertical, 8-13/16 in.

6.1.4 Analysis of Salt Shattering

Determination of Shattering Temperature and Zone.-- In the wall test, salt shattered and fell away from the top surface of the hole in a zone extending from 6 ft 5-1/2 in. from the mouth of the hole to within 2-1/2 in. of the back of the hole. Thus the length of the shattering zone was 41 in., which corresponds to the 4-ft heater length zone. At the ends of this zone the final diameter of the hole was 8.9 in. A 41-in.-long shattering zone in a hole of this diameter indicates that the salt shattered out to the theoretical 290°C temperature profile. This compares well with the 280°C extrapolated temperature at the original hole radius when the first explosion took place.

The diameter at the center of the heater to the 290°C contour is 14.8 in. The diameter of the shattered zone could not be determined exactly, due to the fact that the shattered and expanded salt recomacted around the heater; and it was not possible to determine with certainty the point at which it joins the undisturbed salt. At the top of the hole, after the removal of all salt that readily chipped off, the radius from the center of the original hole was 6 in., indicating that the maximum diameter of the shattered zone was at least 12 in. This 6-in. radius reached to the bottom of a dark band (which may be seen in Fig. 6.3), probably indicating high anhydrite content that may have prevented further shattering. At a point about 45° from vertical, the

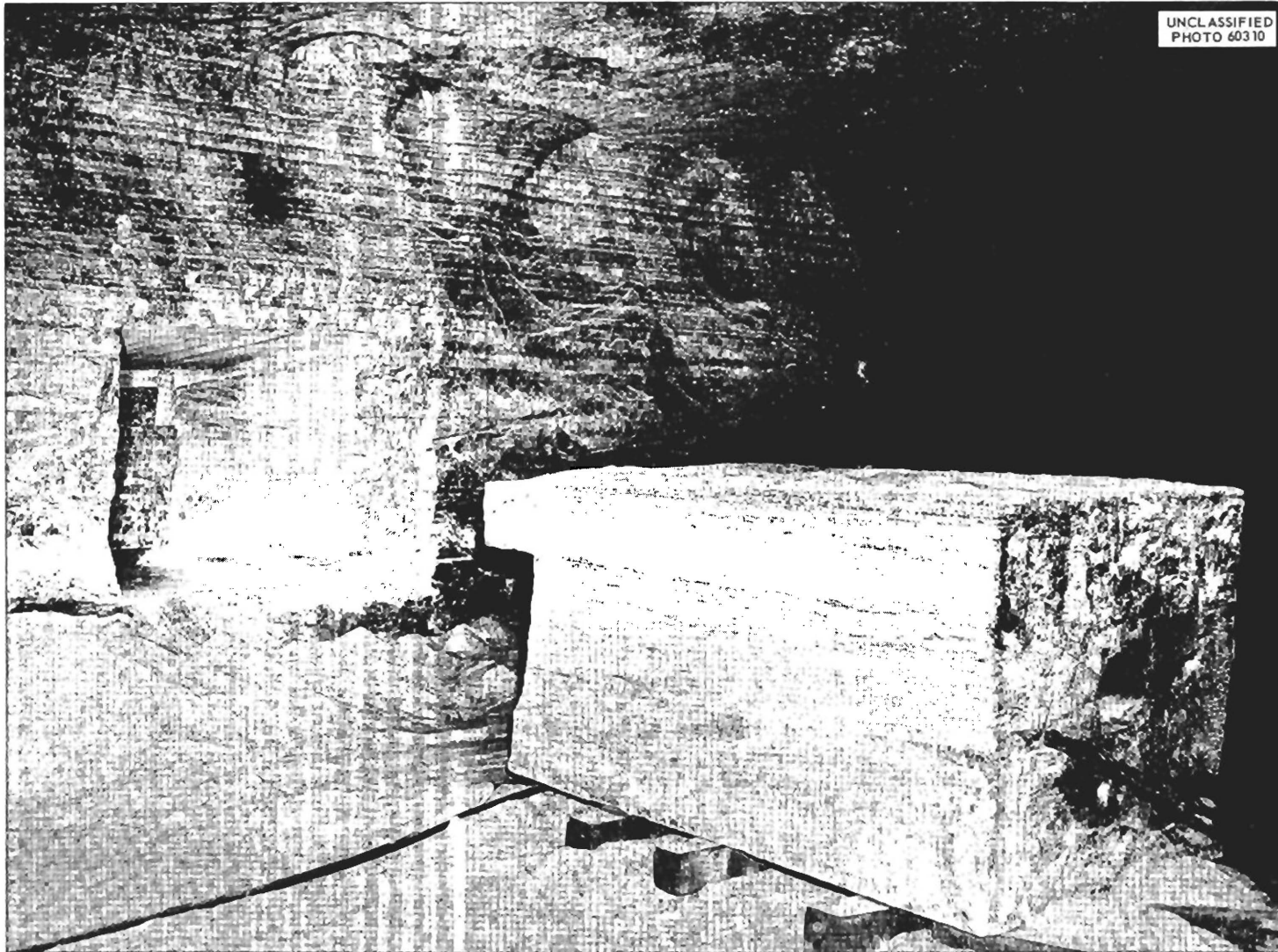


Fig. 6.1. Block of Salt Containing Heat Experiment, After Removal from Wall.

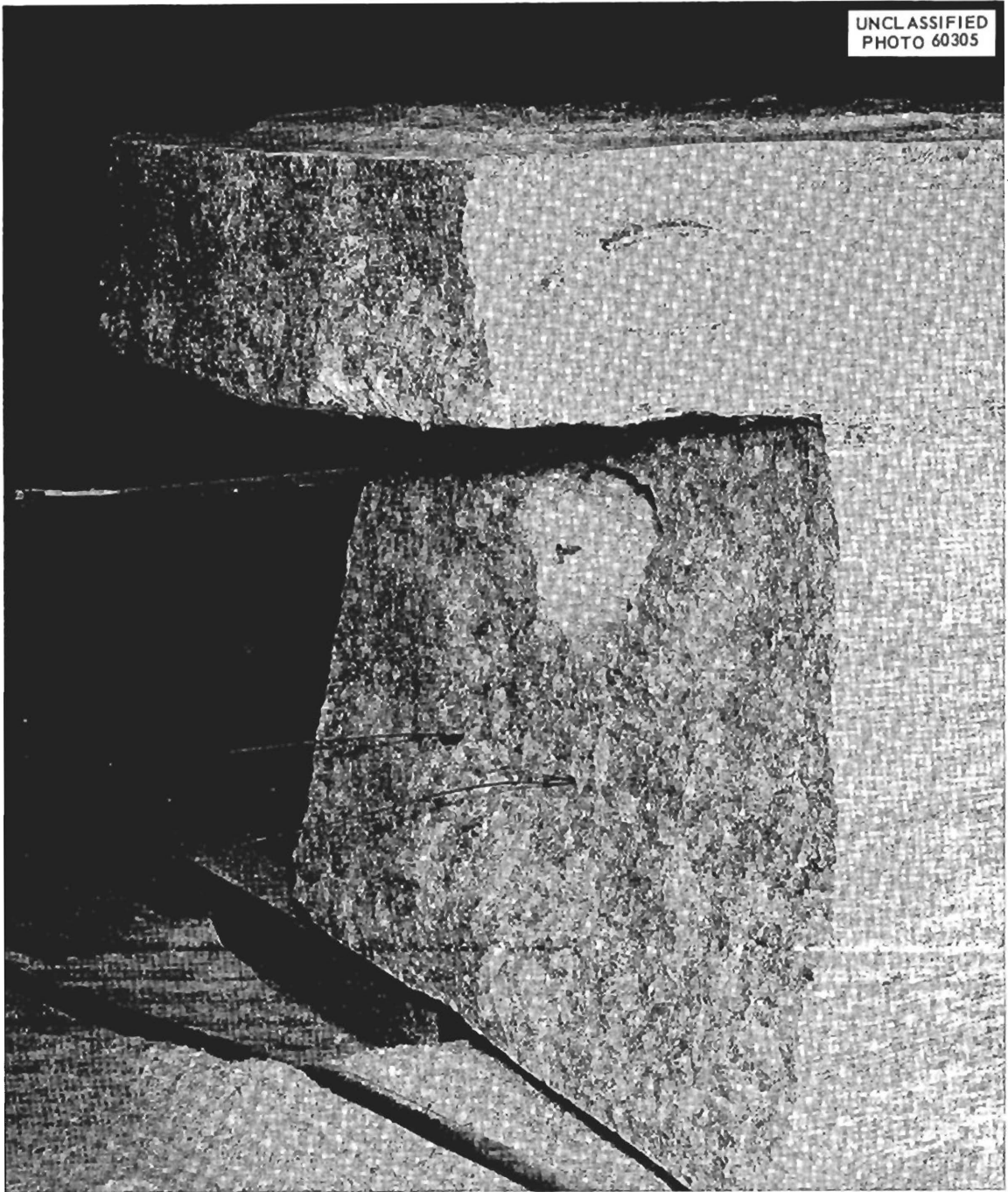


Fig. 6.2. Heated Hole at Rear of Block (Wall-Heat Experiment).



Fig. 6.3. Closer View of Rear of Block, Showing Fracturing in the Hole.

final maximum radius relative to the original center of the hole was about 7 in.

These measurements then tend to confirm 290°C as the approximate maximum temperature below which shattering does not occur in Hutchinson salt. Additional confirmation is gained from the array test in which the maximum salt temperature was about 265°C and in which no shattering was observed.

Water Content of Salt.-- The volume of salt contained in the zone out to the 290°C contour, including that expanded into the hole, is 1.8 ft^3 . The moisture released from samples of Hutchinson salt when exploded in the laboratory averaged about 0.19% by volume. This water content in 1.8 ft^3 amounts to only 97 ml. The actual water collected in the wall test after shattering began was 189 ml. If the sweep air had been saturated at all times, an additional 1550 ml would have been removed from the hole (Inlet air was at 22°C and 65% relative humidity.). If the sweep air had left the condensate trap with the same relative humidity as it had when it entered the hole, then the 189 ml would be the total released from the salt. In any event, 189 ml in 1.8 ft^3 is 0.37 vol% water, and quite likely the total released was considerably greater than this.

There are at least three possible explanations for this apparent water-volume discrepancy. One is that the extra water came from the radial cracks extending away from the hole. A second possibility is that the shattered zone is larger than estimated. The third is that more moisture was released under the test conditions than is released when the explosions take place in the laboratory. That all the moisture is not released in the laboratory tests was confirmed by microscopic examination of several small pieces of a sample that had exploded violently in a laboratory test. Numerous brine-filled negative crystals (cavities), containing small vapor bubbles, were observed.

Effects of Salt Shattering.-- As noted previously²⁸ the shattering of the salt around the heaters in the wall and floor tests did not appear to have any significant effect on temperature rises 6 in. away from the hole (the closest thermocouple) and beyond; however, this was not true for temperatures on the heater pipe itself. Immediately after the first major salt explosion (after 69 hr of operation), the center temperature of the pipe in the wall test rose about 50°C . Immediately after the second major blast (at about 93 hr of operation), the temperature rose an additional 150°C to a peak of about 690°C . At this time the center of the pipe was completely surrounded by shattered salt.

In the floor test the peak temperature of the pipe ranged from about 560 to 580°C from 200 hr on to the end of the test (792 hr). Although there were salt explosions in the floor, the salt never filled in around the center of the heater and, thus, no effect was noted there.

In the wall, as the salt compressed and recrystallized due to thermal closure of the hole, there was some indication that the heat transfer

improved. This was evidenced by the fact that from about 110 hr out to about 640 hr, the center temperature readings dropped slowly from 690°C to 560°C . After this time the readings became erratic, apparently due to corrosion of the thermocouple.

A possibly more serious effect is the moisture released when the salt shatters. This would tend to accelerate container corrosion and would possibly cause the eventual migration of waste to the surface of the floor. (In the floor and array tests, moisture came up through the sand in the thermocouple holes nearest the heater; however, much more moisture was involved in these tests due to the presence of shale bands.)

6.1.5 Hole Closure

Wall Test.-- After 45 hr of operation of the wall test at a power input of 3.5 kw, the change in the diameter of the hole with depth was as shown in Fig. 6.4. The maximum closure of 0.45 in. (representing a 4.5% decrease in diameter) occurred at the center of the heater (depth, 8 ft 1 in.), and the peak salt temperature at this point was about 210°C .

The test was restarted with a power input of 5 kw and continued for a total elapsed time of 792 hr from initial startup. The hole closure at the end of the test is also shown in Fig. 6.4. Just as the shattering radius could not be determined exactly because of thermal expansion into the hole, the thermal expansion cannot be determined directly in the zone where shattering occurred.

When the hole closure that was measured after 45 hr of operation is plotted against the theoretical temperature rise at the points of closure-measurement, a straight line results. It was found that the measured closures after 792 hr of operation also plot a straight line, although of greater slope than the 45-hr line. An estimate of the closure that would have occurred in the shattered zone had shattering not taken place was obtained by extrapolating this line to the peak salt temperature rise (330°C) at the center of the heater. On this basis the maximum permanent hole closure would have been 1.55 in. (a 15% decrease in diameter) at the center of the heater where the peak salt temperature at the original hole radius was about 350°C .

Floor Test.-- Hole closures in the floor test were essentially the same as in the wall test for depths up to 6-1/2 ft. At greater depths the presence of shale and anhydrite bands altered the closure pattern, and closures were generally lower than in the wall.

Array Test.-- In the array test the same shale and anhydrite was present in the bottom part of the hole so that closure measurements in the region of maximum temperature rise are not meaningful.

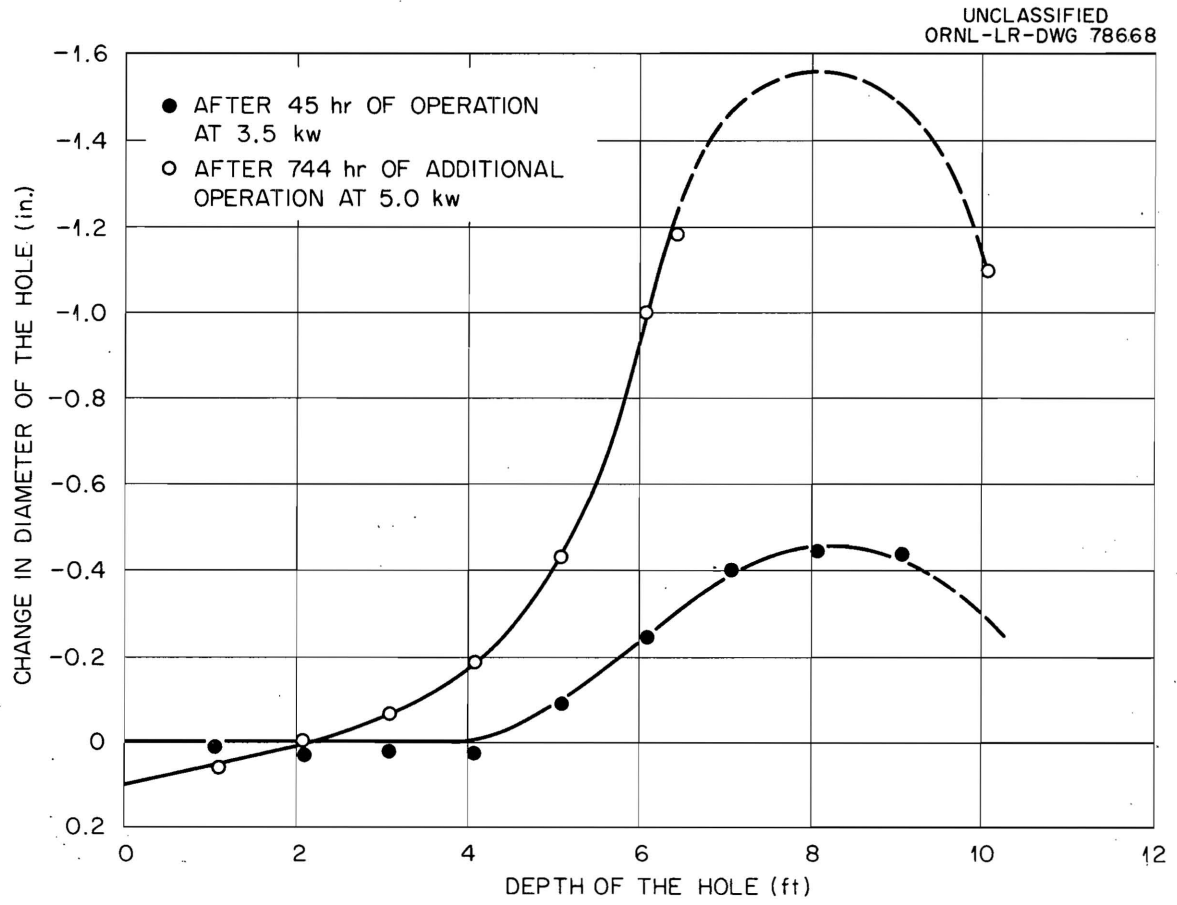


Fig. 6.4. Data Reflecting the Shrinking Diameter of the Hole.

6.2 Thermal Stability of Salt

H. Kubota

The thermal stability of salt masses from various mines are shown below:

<u>Mine</u>	<u>Number of Samples Tested</u>	<u>Fracturing Temperature (°C)</u>	<u>Salt Type</u>
Hutchinson, Kansas	25	260 - 320	Bedded
Lyons, Kansas	8	285 - 320	Bedded
Fairport Harbor, Ohio	2	380	Bedded
Retsof, New York	2	---	Bedded
Winnfield, Louisiana	2	---	Dome
Grand Saline, Texas	2	---	Dome
Weeks Island, Louisiana	2	---	Dome

The dashes indicate that the salt did not fracture up to 400°C.

The possible release of chlorine from salt during irradiation is being studied both with chemically pure salt and mine salt. At present, only chlorine gas actually released from the salt is being investigated. At 30 to 55°C, no chlorine has been detected from samples that had received up to 10^9 rads of Co^{60} radiation. No measurements have been made, as yet, on the production of oxidizers that are formed and then retained within the crystal bodies.

6.3 Permanent Expansion of Negative-Crystal Cavities

R. L. Bradshaw

In the high-temperature cylinder, as well as in the previous large-scale liquid tests, the holes expanded inward, and the surfaces of the wall and floor expanded into the room. Only about 10% of the wall and floor expansion was recovered when the temperatures returned to ambient. This apparent net increase in salt volume could have come from several sources, among which are flow in from other parts of the formation, separation of crystals (thereby producing voids), and expansion of negative crystals (cavities) within the salt crystals. A preliminary study was made of the last possibility.

Mine-run salt from the Hutchinson mine was broken up into small pieces and examined with a low-power microscope. In almost all samples

that were clear enough to see through, numerous negative crystals (cavities), ranging in size from about $1/16$ in. down to the limit of the 15-power microscope, were observed. Most of the cavities were completely filled with brine, but a few contained vapor bubbles.

A sample about $5/8$ in. square by $3/8$ in. thick was tested. Eleven negative crystals, ranging in size from about 0.009 to 0.04 in. cubes, were measured, and then the sample was heated in a furnace at 180°C for 41 hr. After the sample had cooled to ambient temperature, the vapor bubbles that formed in the cavities were measured. Based on the volumes of the vapor bubbles, the volumes of the cavities had increased an average of 4.8%. The sample was then heated for an additional 42 hr at 180°C . After this heating there was no measurable additional increase in volume. The sample was returned to the oven for 18 hr heating at 227°C , and the total net volume increase of the cavities then averaged 7.6%.

Four small samples, ranging in thickness from about $3/32$ in. up to $3/8$ in., with the other dimensions ranging from about $1/4$ up to 1 in., were selected, and nine cavities were measured after heating at 137°C for 1 hr. The net volume increase averaged 3.5%.

These volume increases are shown in Fig. 6.5 as a function of temperature. Also shown (curve 1) is the volumetric expansion of a 20.6% NaCl solution. (A saturated solution is 26.4% at 20°C , increasing to 41.8% at 350°C and 100 atmospheres.) Curve 2 is the theoretical volume increase of the cavity, assuming that the volumetric expansion coefficient is the same as that for the salt. Curve 3 shows the volume increase of the cavity due to the increased solubility of salt at elevated temperatures. Curve 4 is curve 1 minus the sum of curve 2 and 3. It may be noted that the measured cavity expansions amount to about 75% of curve 4. The difference may be due to partial recovery of that part of the cavity expansion produced by the pressure of the solution, or it may be due to curves 1, 2, or 3 not being exact for the actual test conditions.

In order for this cavity expansion effect to completely account for the permanent expansion of the wall and floor, the cavities would have to amount to something like 10% of the volume of the salt; a more likely figure is about 1%. The tests described here were of short duration and are essentially measures of the initial cavity deformation. It is quite possible that creep taking place over a period of several weeks could cause much larger increases in cavity volume.

The total volume expansion into the floor and wall holes was about a tenth of the floor- and wall-surface expansions, and, thus negative crystal cavity expansion could possibly account for the major portion of the hole closure.

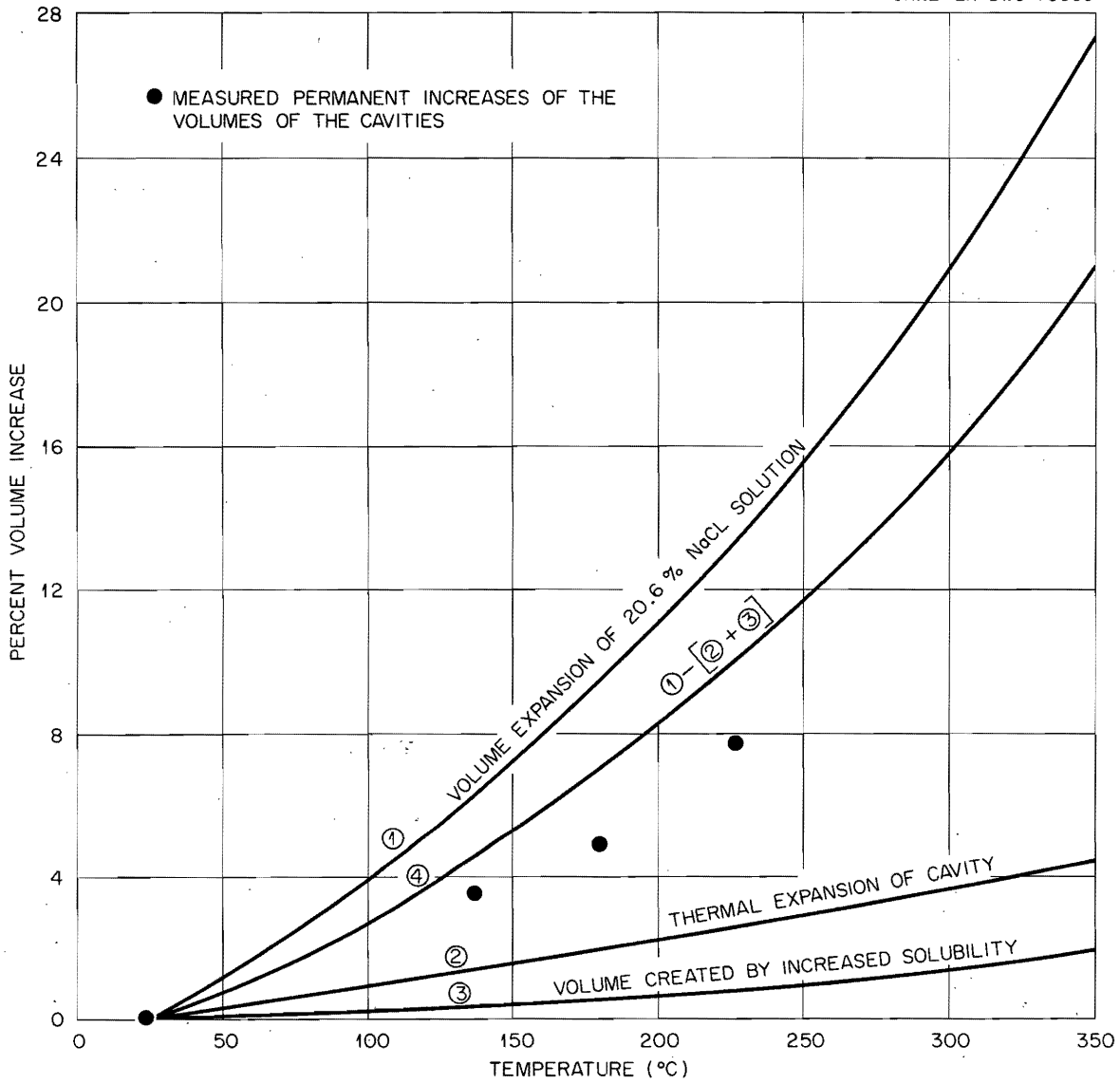


Fig. 6.5. Expansion of Negative-Crystal Cavities.

7. CLINCH RIVER STUDY

7.1 Bottom Sediments

R. J. Pickering*

P. H. Carrigan, Jr.*

7.1.1 Gross Gamma Scanning of Bottom Sediment Cores

Calibration of the "core scanner," a device for determining the vertical variations in gamma activity in intact undisturbed cores of Clinch River bottom sediments (See previous quarterly report.), has been completed, and scanning of cores for gross-gamma activity is in progress. The vertical increment of core scanned through a 2-in.-long collimator with 2- x 2-in. and 1- x 2-in. openings has been determined by using a 3-in.-diam plane source of radioactivity. The source, which consisted of a disc of blotter paper which was impregnated with Cs¹³⁷ and sealed between thin plastic sheets, was placed horizontally at mid-height in a plastic core tube filled with "uncontaminated" bottom sediments from Norris Reservoir. The gross gamma count rate produced by this source was determined at various distances below the center line of the collimators. The results of the determination, shown in Fig. 7.1, indicate that because the collimator will admit direct radiation from the rear edge of the source when the source is at a distance of 4-1/2 in. below the center line of the collimator slit, the core scanner "sees" a segment of core longer than 2 in.

An uncorrected gross-gamma scan of a core from Clinch River Mile (CRM) 1.3 is shown in Fig. 7.2. The results of the scan demonstrate the vertical variations in gross radioactivity within the core and indicate that the segment sampled includes the entire thickness of the zone of radioactivity.

After gross-gamma scanning of the cores has been completed, the vertical distribution of specific radionuclides in selected cores will be determined by routing the output of the core scanner through a 512-channel analyzer. The cores will then be dissected, and the radionuclide content of composites of the cores in each cross section will be determined. In addition, various physical and chemical tests will be performed on the composite samples and on selected cores or core segments in order to gain a better understanding of the processes by which the radionuclides become incorporated in the bottom sediments.

*On loan from Water Resources Division, U. S. Geological Survey.

UNCLASSIFIED
ORNL-LR-DWG 78670

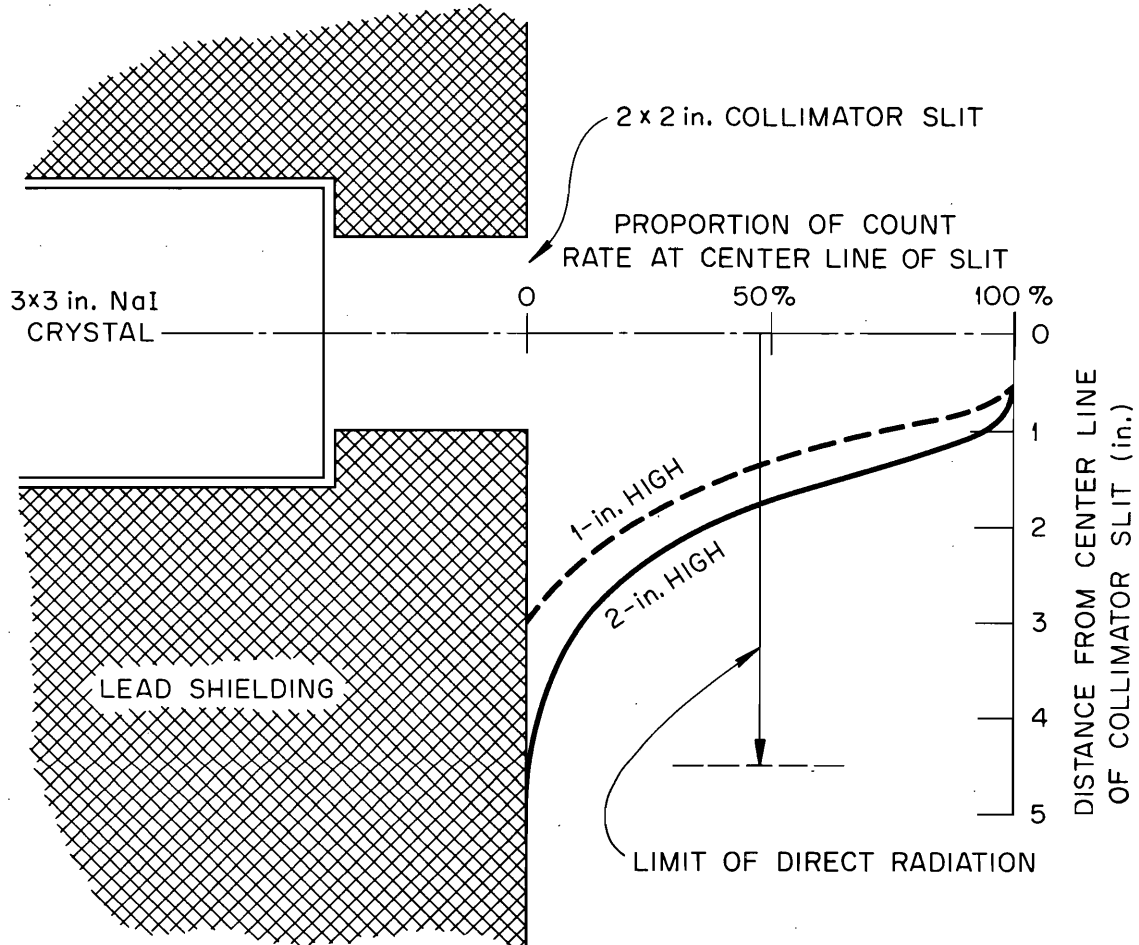


Fig. 7.1. Effective Slit Width of Collimator for 3-in.-diam Plane Source of Cs^{137} Normal to the Face of the NaI Crystal.

UNCLASSIFIED
ORNL-LR-DWG 78671

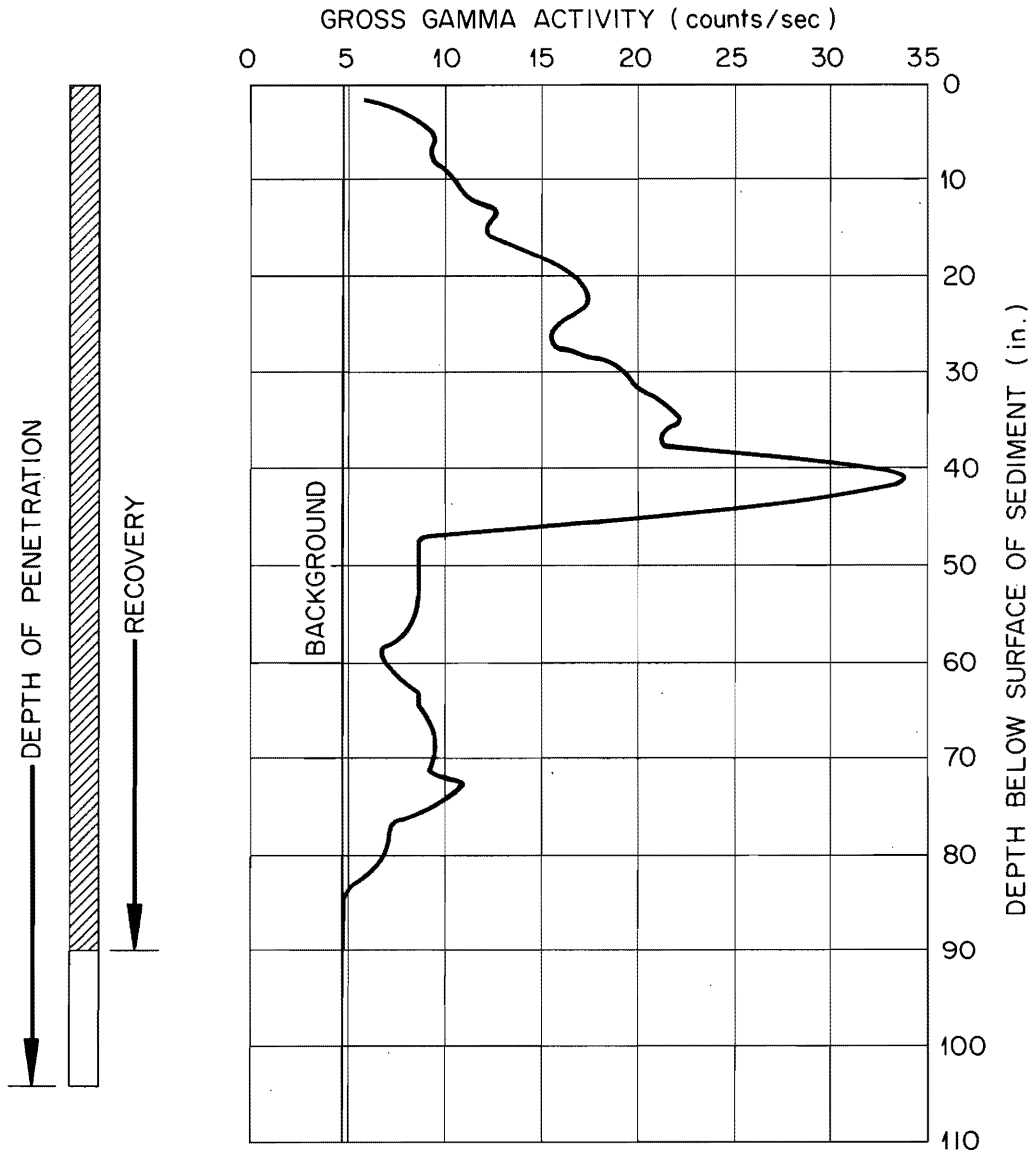


Fig. 7.2. Distribution of Radioactivity in Core 5, in Section at Clinch River Mile 1.3.

7.1.2 Variations of Radionuclide Concentrations in Bottom Sediments with Time

Determinations of the radionuclide content of samples collected annually from the upper portion of the bottom sediment in the Clinch and Tennessee rivers by the Applied Health Physics Section reveal that the content of each of the most abundant radionuclides bears a direct relationship to the total amount of that radionuclide released from White Oak Lake during the preceding 12-month period. This relationship appears to exist whether or not there has been a net gain in sediment at the particular cross section sampled. Possible explanations are: (1) that the radioactivity in the two rivers upstream from the sampling points was primarily associated with suspended solids in the water and that the sediment sampled during the annual sediment surveys, which were always conducted during the summer, had been deposited during the previous year, regardless of whether there had been a net loss or a net gain of sediment during the entire year or (2) that radionuclides in the river water more or less continuously maintain equilibrium with the bottom sediments which thus reflect the most recent radionuclide concentrations in the water. The observed relationship extends at least as far downstream in the Tennessee River as Gunter'sville Reservoir.

The direct relationship between radionuclide release and radioactivity in the upper portion of bottom sediments in the Clinch and Tennessee rivers might possibly be used to predict both the radionuclide content of the bottom sediments and the exposure hazard resulting from their radioactivity on the basis of information on radionuclide release alone. This possibility will be given further attention in subsequent investigations of bottom sediment radioactivity.

7.1.3 Precipitation of Calcite on Current Meter at Clinch River Mile 19.1

Recovery of a current meter that had been submerged for 14 months in the Clinch River at Mile 19.1 revealed that a dark-brown coating of calcite, 0.004 to 0.005 in. thick, had formed on all exposed surfaces of the meter. A radiochemical analysis of the coating showed that each gram (dry weight) contained 123.9 μc of $\text{Ru}^{103-106}$ and 10.1 μc of Sr^{89-90} . A trace of Cs^{137} was detected, and the count on total rare earths was enough above that attributable to Y^{90} to suggest the presence of other rare earths, probably primarily Ce^{144} .

As shown in Table 30, the concentrations of radioactive ruthenium and strontium in the calcite lie between concentrations of those nuclides in Clinch River bottom sediments and concentrations in suspended sediments. Thus, if bottom sediments contained an appreciable amount of precipitated calcite, the calcite would add materially to the Ru^{106} and Sr^{90} content of the sediment. Ashing of the dry calcite at 500°C resulted in a loss in weight of 5.5%.

The presence of fine-grained calcium carbonate in Clinch River bottom sediments has been inferred from the results of determinations of

Table 30. Bottom Sediment

Place Where Analyzed	Sampling Date	Clinch River Mile	Ru ¹⁰⁶ (μuc/g)	Sr ⁹⁰ (μuc/g)	Remarks
ORNL	1960	18.1	21.2	2.30	
ORNL	1960	19.5	27.9	1.08	
USPHS	1960	14.6	3980	5	
USPHS	1960	20.8 (-150 ft)	100	8.6	
USPHS	1960(?)	11	200.8	2.8	Evidence shown in ORNL-3202, Table 6, p. 20, that clams concentrate ruthenium and strontium
ORNL	1961	11.9	18.3	2.6	
ORNL	1961	15.3	16.7	4.0	
ORNL	1961	19.2	7.4	4.0	
Calcite Precipitate on Current Meter					
ORNL	1962	19.1	123.9	10.1	Trace Cs ¹³⁷ , evidence of Ce ¹⁴⁴
Suspended Sediment					
ORNL	Nov. 1960 to June 1961	14.5	764 - 6696	10.8 - 851	General range of more than 30 analyses

the exchangeable cation content of five samples of bottom sediment. The amount of "exchangeable" calcium in all five samples was greater than the total cation exchange capacities of the sediment samples. These anomalous results, together with high pH values reported for the same sediment samples, appear to indicate that calcium carbonate in the sediment was dissolved during the removal of the "exchangeable" cations from the sediment and produced the unreasonably high values for "exchangeable" calcium in the sediment.

In order to determine when, or whether, calcite would precipitate from the river water onto a metal object with no electrical connections, three sets of aluminum plates have been anchored in the Clinch River at Miles 5.5, 15.0, and 19.1. Each set consists of three plates, spaced so one plate will remain near the river bottom, one will remain a short distance below the surface, and the third will remain approximately midway between the water surface and the river bottom. The plates will be observed periodically to see whether calcite has formed on their surfaces.

8. FUNDAMENTAL STUDIES OF MINERALS

T. Tamura

8.1 Column Study of Several Sorbents for Strontium

In studies with columns of sorbents for removing strontium from solution, gibbsite showed a high selectivity for strontium in alkaline NaNO_3 solution. This gibbsite (aluminum hydroxide) had been heated to 400°C . After investigating the properties of unheated and heat-treated gibbsite, it was concluded that the heat treatment had converted the gibbsite into a product similar to that sold as activated alumina by the Aluminum Company of America. A sample of activated alumina, labeled F-20, was obtained from Alcoa, and slurry tests showed that F-20 was also selective for strontium. This development made it highly desirable to compare several materials in column systems in order to ascertain the potential usefulness of this material for waste treatment. The four materials included in the tests were Dowex 50-X12, clinoptilolite, vermiculite, and F-20 alumina. The Dowex 50 and vermiculite were pretreated with NaCl to convert them into the sodium forms. The clinoptilolite was treated with 1 M HCl to decompose the calcite impurity in the sample. Following pretreatment, each sample was washed until tests with AgNO_3 for chloride were negative. No treatment was given to F-20 alumina prior to use in the first column test.

The tests were run with $1/2$ -in. glass tubing, containing 10 g of sorbent (weight based on the air-dry sample). The simulated waste solution was 0.5 M NaNO_3 adjusted to pH 10 with NaOH and containing $10^{-5}\text{ M Sr}(\text{NO}_3)_2$. The flow rate was maintained at $3\text{ ml min}^{-1}\text{ cm}^{-2}$.

The volume throughput and effluent activity measured in the four test runs are shown in Fig. 8.1. It appears that the flow rate was too high for both vermiculite and clinoptilolite to be efficient. The first 50-cc volume showed activity breaking through in both of these columns; the clinoptilolite did show improvement with time. The latter behavior may be due to the change-over of clinoptilolite from the hydrogen to the sodium form. The effluent from Dowex 50 showed very little activity in the first 2 liters, and, with F-20 alumina, very little activity was measured in the effluent up to 5800 cc. Unfortunately, effluent samples from the alumina column were lost in the collection procedure, and the next reliable sample showed 54% activity. The behavior of the alumina is unusual in that the continued flow of solution presumably after the alumina is saturated resulted in an effluent that contained more strontium than the influent solution. This behavior suggests that the surface-layer alumina may be dissolving or "flaking off" with continued flow (The high pH of the influent solution would facilitate this dissolution of the alumina.). After the end of the run the column was monitored along the outside wall with a G-M survey meter, and the activity distribution showed that the influent zone had a lower concentration of strontium than the effluent zone. It is also significant to note that the F-20 alumina does show sorption capacity for strontium to an extent that is competitive with other sorbents.

Since it was thought that the high effluent activity of the F-20 alumina column was caused by the high pH of the influent waste solution, another column was run to test this idea. Prior to passing the simulated waste through the column, it was decided to run 0.5 M NaNO_3 adjusted to pH 10 (without strontium) through until the effluent pH equaled the influent pH of 10. After this treatment the pH of system would be favorable for dissolution or "flaking," and strontium breakthrough was expected to occur after a few column volumes of waste had passed through. However after passage of 1700 cc of solution, the pH was 7.65; and this value had been reached after the first 20-cc increment had a pH of 9.4, and subsequent samples showed gradual reduction in pH. It was, therefore, decided to start the simulated waste through the column with close attention to the pH in addition to the activity of the effluent.

The results of the second F-20 alumina run are plotted in Fig. 8.2. The results of the earlier alumina run are also plotted. The pretreated alumina showed less than 1% breakthrough up to 13,000 cc, compared with 5800 cc for the first run. The effluent activity showed a gradual increase, and, after 35,000 cc, the activity was about 85% of that of the influent. The pH of the effluent, which was measured periodically, showed that it did not reach the influent pH of 10 during the entire test run. The maximum observed pH of the effluent was 9.0 in the 50-cc increment collected after passage of 23,700 cc. The minimum pH was 7.50 in the 50-cc increment collected after 15,500 cc. The pH varied continuously over the reported range during the entire run. Although the results of this column run showed improved performance over the first test run, it should be pointed out that the cause of the improvement is not known.

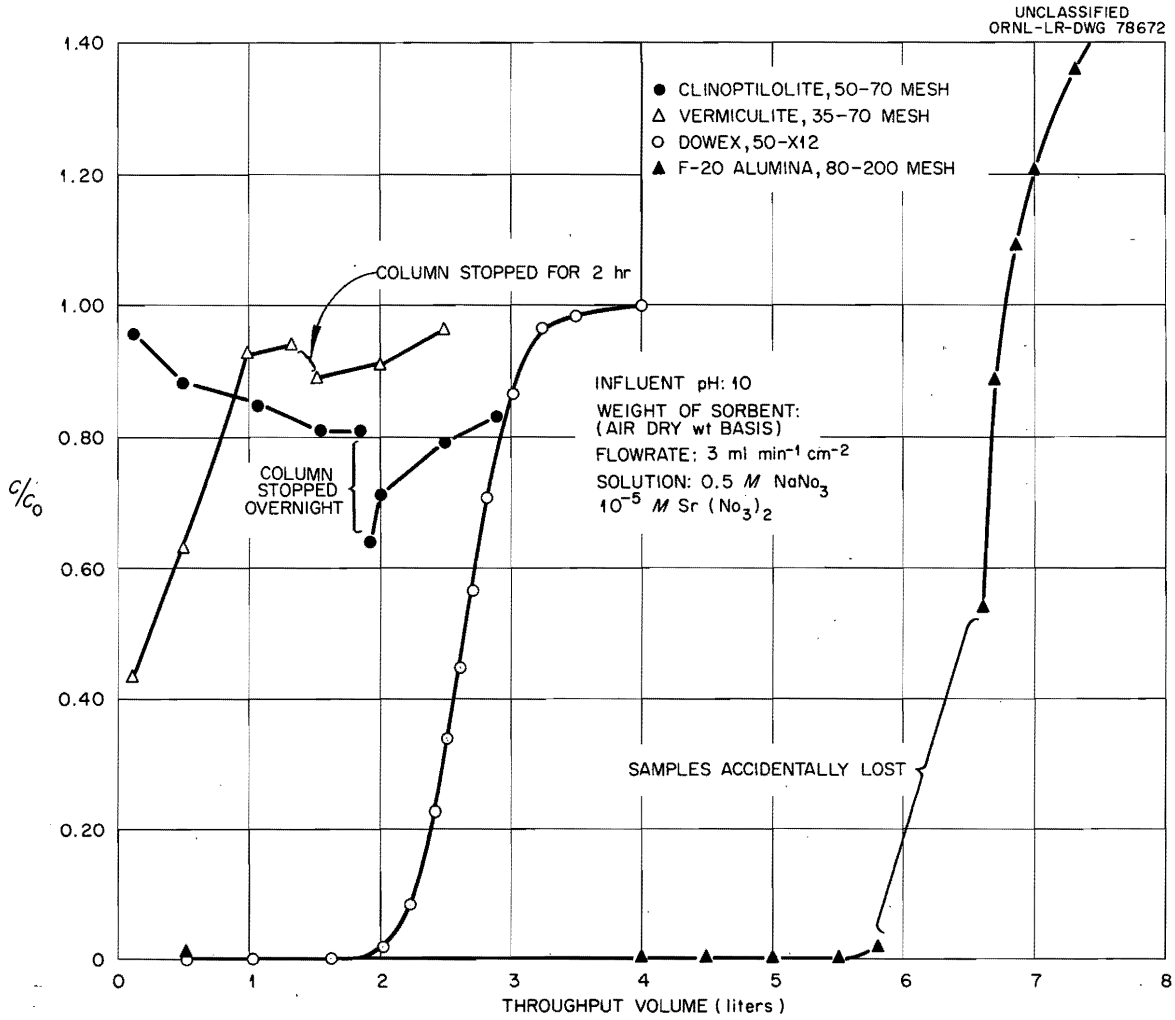


Fig. 8.1. Strontium Removal by Several Sorbents: Effluent Activity of Simulated Waste.

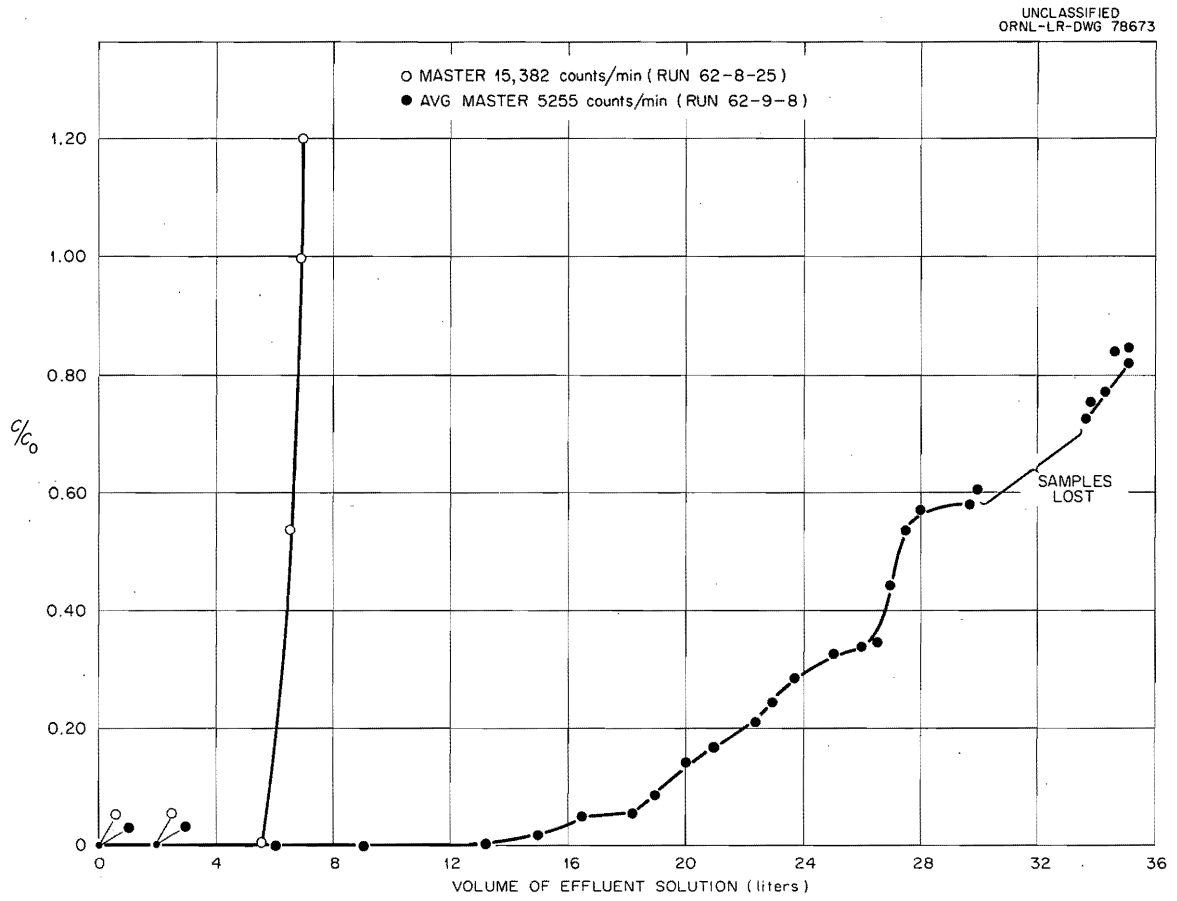


Fig. 8.2. Strontium Removal by F-20 Alumina: Effluent Activity of Simulated Waste.

These tests were run in 0.5 M NaNO_3 solutions; in different Na/Sr ratios or at different pH's the other sorbents could be more effective. Under acid conditions alumina is ineffective, whereas Dowex 50 would still function. With lower Na/Sr ratios the loading on the ion exchangers would favor strontium, whereas the loading on the alumina may be unaffected. The latter possibility appears plausible, since the removal of strontium occurs in a system that expends hydroxide ions, which suggests that ion exchange may not be the mechanism for removing strontium. Work is in progress to elucidate the nature of the alumina reaction, with particular attention being given to comparisons of reactions with known ion exchangers, such as Dowex 50.

9. WHITE OAK CREEK BASIN STUDY*

9.1 Distribution and Transport of Radionuclides in the Bed of Former White Oak Lake

T. F. Lomenick

During the period 1943-1955, White Oak Lake served as a final settling basin for low-level radioactive wastes discharged from the Laboratory. The temporary holdup provided by the impoundment afforded some dilution and a period for the decay of short-lived radionuclides before release to the Clinch River. It also allowed the deposition and accumulation of contaminated sediments. In 1955 the lake was drained, leaving behind about 1,000,000 ft³ of contaminated lacustrine deposits.²⁹

In order to determine the quantity, type, and distribution of radionuclides present in the lake bed and to aid in defining the migration of these products, a series of 250 core samples were taken in the area. A map of White Oak Lake bed showing the sample locations is presented in Fig. 9.1. The lake bed was laid out in a 50-ft-square grid, with sample locations being chosen by use of a table of random numbers. Note the increase in sample points per unit area for zones of progressively higher activity concentrations. The method of allocation of these points is optimum with respect to the area of sections of similar radioactivity (as determined by data collected previously) and with respect to the variability of the previously collected data. Due to the high cost of strontium and total rare earths, compared with gamma identification, only a limited number of the cores and their segmented sections are being analyzed for these nuclides.

*This project, entitled, "Environmental Radiation Studies: Evaluation of Fission Product Distribution and Movement in White Oak Creek Drainage Basin" (AEC Activity 060501000), is supported by the U. S. Atomic Energy Commission's Division of Biology and Medicine. All other projects covered in this report are supported by the Division of Reactor Development (AEC Activity 04640011).

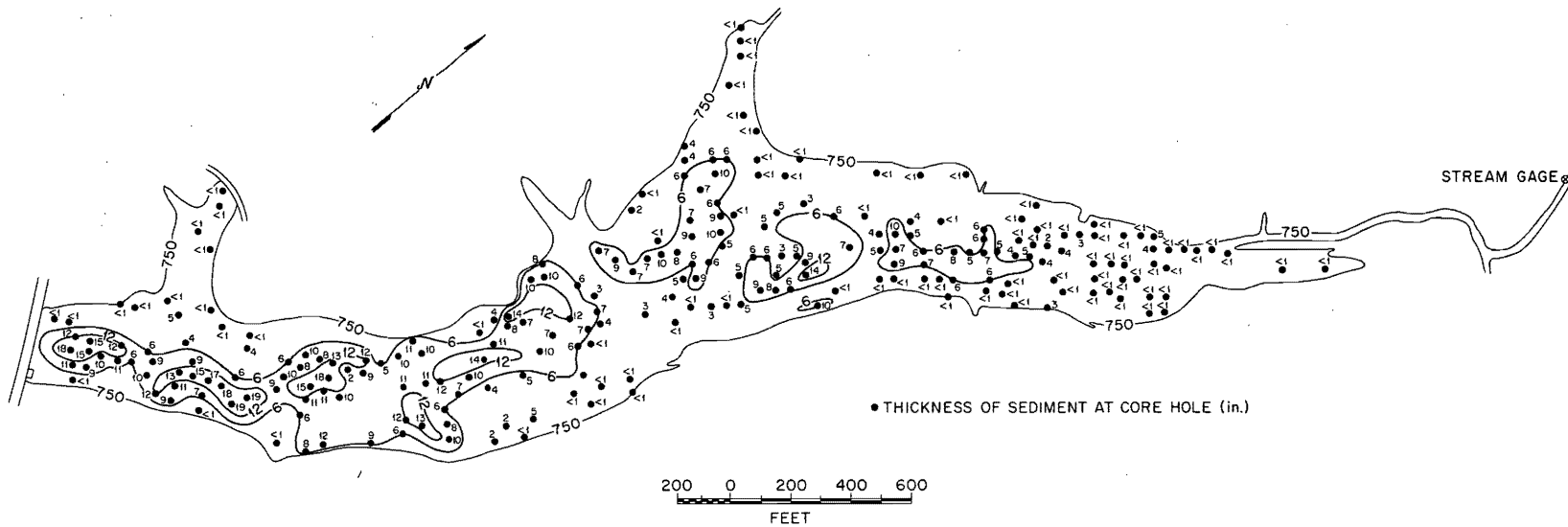


Fig. 9.1. Locations at Which 2-ft Core Samples Were Taken from the Bed of Former White Oak Lake.

A 2-in.-diam thin-wall tube, known as the Shelby Tube Sampler, was used to obtain core samples in the lake bed. The instrument was driven into the earth and recovered manually. As previous work indicated that practically all the contamination was associated with the upper few feet of soil,³⁰ all cores were taken to a depth of 2 ft. The samples were sliced and segmented into increments of 0 to 6 in., 6 to 12 in., 12 to 18 in., and 18 to 24 in. About 10 g from each increment was oven-dried, weighed, and scanned, using a Packard automatic gamma counting system, which consists of a spectrometer with well-type scintillation detector, automatic sample changer and control unit, digital printer, and tape punch. Concentrations of Ru¹⁰⁶, Cs¹³⁷, and Co⁶⁰ are being determined by use of an IBM 7090 computer program for stripping the gamma spectrum. Standard radiochemical procedures are being used for strontium and total rare earth analyses.

By visual inspection of the recovered cores, a generalized depth of lacustrine sediment in the bed was determined (See Fig. 9.2.). It is seen that the sediment is as much as 19 in. thick in the lower part of the lake bed near the dam; however, there is a gradual thinning of the layer upstream and, in general, toward the shore line of the lake.

9.2 Oak Ridge Area Hydrology

R. J. Pickering*

W. M. McMaster*

R. M. Richardson*

On November 1 and 2, 1962, a 26-hr continuous sampling program was undertaken at selected stations on Bear Creek. The primary purpose of the program was to determine the significance of the effect of biologic activity on the concentration of nitrogen compounds in the water and variations in the effect with time and place.

The bulk of nitrogen occurring in Bear Creek originates in the acid waste pits west of the Y-12 Plant. Most of this material enters Bear Creek as nitrate by way of a small spring located more than 1 mile southwest of the pits; a second spring at the Roane-Anderson County line, about 2 miles southwest of the pits, discharges smaller quantities of nitrate into Bear Creek.

Sampling stations were set up at the upper spring, the spring at the county line, Bear Creek at the county line, Bear Creek at Highway 95, and Bear Creek at the U.S.G.S. gaging station near the Oak Ridge Gaseous Diffusion Plant. Flow at the gaging station remained constant through the period at 1.3 ft³/sec.

A diurnal fluctuation was expected in the content of the various nitrogen compounds of the stream water because of biologic activity, whereas a fairly steady concentration was expected in the spring water.

*On loan from Water Resources Division, U. S. Geological Survey.

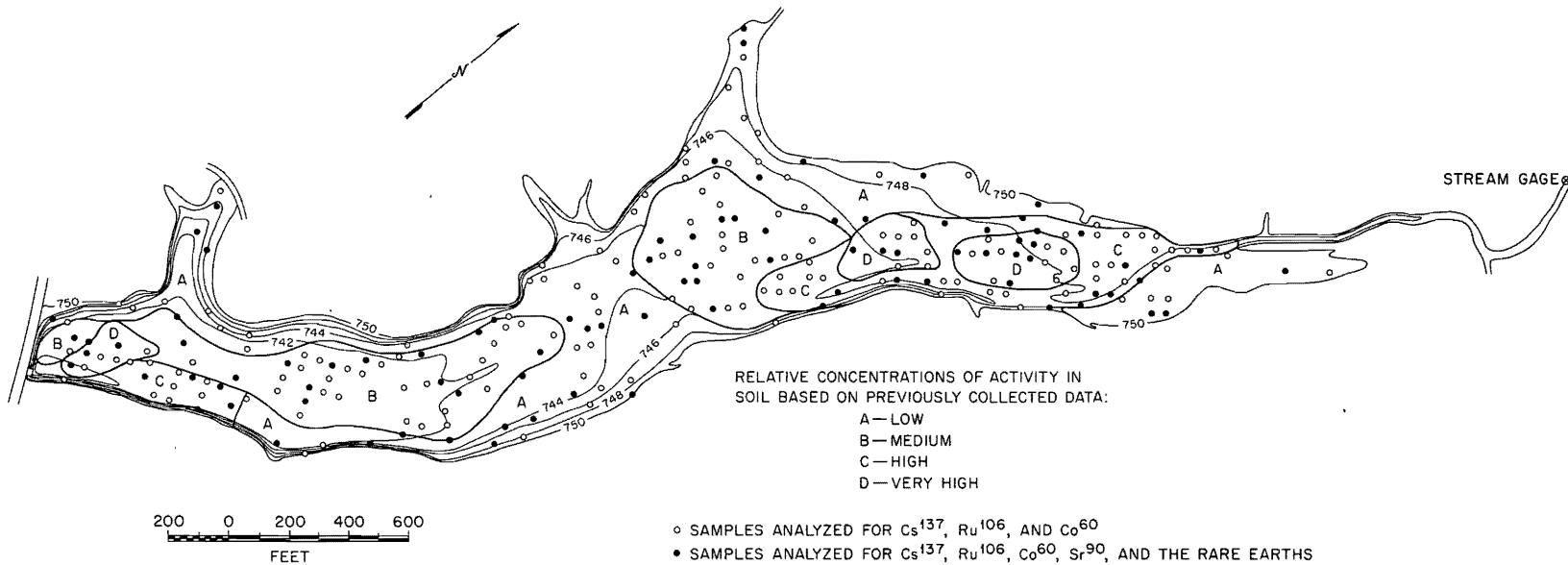


Fig. 9.2. Map of Former White Oak Lake Bed, Showing Thickness of Contaminated Sediment.

Seventy-one samples collected at the stations were analyzed for nitrate, nitrite, organic nitrogen, ammonia, calcium, magnesium, chloride, and fluoride, and measurements were made for dissolved and suspended solids and for specific conductance. From previous samples at various points on Bear Creek, it was known that nitrate concentration decreases markedly with distance from the upper spring. Dilution of the concentration with distance and additional inflow accounts for a large part of the decrease, and it is believed that biologic uptake might also account for much of the decrease. Contrary to expectations, however, the variations with time at each station were apparently random rather than diurnal, and the samples taken from the springs showed greater variation in nitrogen-compound content than the samples from Bear Creek, even though flow conditions were stable.

The most highly contaminated water was obtained at the upper spring, where the nitrate content ranged from 355 to 475 ppm. Downstream stations showed decreasing contamination with distance, and at the U.S.G.S. gaging station the nitrate content was nearly constant at 55 ppm through the sampling period. Organic nitrogen, ammonia, and nitrite concentrations varied somewhat at each station, generally remaining below 0.2 ppm, although the ammonia content at the upper spring reached 0.4 ppm at times. No diurnal cycle was apparent in any of the results.

10. FOAM SEPARATION

Foam separation is being studied as a new method for treating low-level wastes. Development work has proceeded over the past few years both at ORNL and at Radiation Applications, Incorporated, under a contract from ORNL. In one method of operation a sludge column is operated prior to the foam column in order to remove calcium and other hardness ions and thus prevent saturation of the foam-complexing agent with hardness ions. In a second method, the hardness would be precipitated in a small flash mixer, and both the precipitate and the ionic contaminants would be removed in the foam column. Both methods are scheduled to be tested in the ORNL 10-gal/min pilot plant for decontaminating low-level waste.

10.1 Laboratory Development

W. Davis, Jr.

E. Schonfeld*

A. H. Kibbey

Pretreatment of ORNL Low-Activity Process Waste Water.-- Since removal of strontium from water by foam separation is much more efficient if the calcium concentration is in the 5 ppm range (calculated as calcium

*On subcontract 2024 with Radiation Applications, Incorporated.

carbonate) rather than the 65 ppm range (as it is in ORNL tap water or low-activity waste), a head-end calcium precipitation step was tested.³¹ Analyses of samples taken during studies with ORNL low-activity process waste water as feed are continuing. Precipitation was performed in a 9-in.-diam column in which the water flowed upward through a sludge bed of calcium carbonate-magnesium hydroxide formed as a result of making the water 0.005 M each in Na_2CO_3 and NaOH and by using 2 ppm of Fe^{3+} (calculated as its concentration before precipitation as hydrous ferric oxide) as a coagulant.³¹

In addition to reducing the dissolved hardness to values of 2 to 5 ppm, strontium decontamination factors in the range 10 to 15 were achieved (Table 31). Thus, dissolved hardness and turbidity were decreased about 10 times lower than that achieved in the ORNL lime-soda treatment plant during the same period of operation (September 17 to September 28 and October 17 to October 30, 1962) while strontium decontamination factors were 3 to 4 times higher (Table 31). Average decontamination factors for the radioactive contaminants Co^{60} , Cs^{137} , Ru^{106} , and Ce^{144} were, respectively, 30, 1.1, 2.0, and 40. The Cs^{137} decontamination factor was low, but the effluent was below the maximum permissible concentration for 168-hr occupational exposure. Removal of Cs^{137} can be increased by the addition of illite or grundite clay to the sludge bed.

Phosphate Concentration in Low-Activity Waste.-- Since phosphates at concentrations as low as 1 ppm (as PO_4^{3-}) were shown to inhibit the precipitation of calcium from 0.005 M NaOH in beaker tests,² concentrations of phosphate in ORNL process waste during the above described head-end precipitation studies were determined. The primary sources of phosphate are commercial cleaning agents, of which "Fab" is used at ORNL, and Turco 4324, which is used at irregular periods for equipment decontamination. From "Fab" and process water usage during 1962, the average "Fab" concentration in the water was about 5 ppm. One analysis of "Fab" showed it to contain 28.7% phosphate (calculated as PO_4^{3-}). Thus, this material contributed an average of about 1.5 ppm phosphate. With one exception, phosphate concentrations in "grab" and composite low-activity waste water during the head-end precipitation studies were in the range 1 to 2 ppm (Figs. 10.1 and 10.2). The one exception, on September 26, 1962, showed 5.4 ppm of PO_4^{3-} .

10.1.1 Alkylbenzene Sulfonate Concentration in Low-Activity Waste

Although sodium dodecylbenzene sulfonate, which is similar to or identical with the surfactants of household cleaning formulations such as "Fab", was shown not to inhibit the precipitation of calcium in beaker tests,³³ alkylbenzene sulfonate (ABS) concentration is of importance in the water treatment industry because it is not rapidly destroyed by bacteria. Thus, among other things, it produces foam in river water and sewage disposal plants.

Table 31. Head-End Precipitation of Calcium and Magnesium from ORNL Process Waste Water: Sludge Column vs Lime-Soda Treatment

9-in. diam. Stirred Sludge Column ^a						ORNL Present Lime-Soda Treatment					
Feed Flow Rate (gal ft ⁻² hr ⁻¹)	Effluent Total Hardness (ppm, as CaCO ₃)	Effluent Turbidity (ppm)	Decontamination Factor					Feed Flow Rate (gal ft ⁻² hr ⁻¹)	Effluent Total Hardness (ppm, as CaCO ₃)	Effluent Turbidity (ppm)	Sr ⁹⁰ Decont. Factor
			Ce ¹⁴⁴	Cs ¹³⁷	Co ⁶⁰	Ru ¹⁰⁶	Sr ⁹⁰				
10	2.0 - 3.5	1 - 1.5	40		30	1.7	11 - 15	21	~ 35		3.7
15	2.0 - 4.0	0 - 1.5			20		10	21	~ 35		
20	2.0 - 4.0	0 - 3.5	40	1.1	10	2.2	11 - 15	21	40 - 60	30 - 40	
26	2.0 - 2.5	0 - 1.5			15		11 - 13	21	40 - 60		~ 3.0
40	2.0 - 4.0	1.0 - 2.0	30		30		11 - 14	21	40 - 60		
60	2.5 - 4.5	1.0 - 5.0			50		10	21	40 - 60		

^aWater was made 0.005 M in NaOH, 0.005 M in Na₂CO₃, and 2 ppm in ferric iron.

Nearly all the ABS in ORNL process waste water originates from "Fab", the ABS concentration of which was 33 to 35%. Thus, the ABS concentration in ORNL process waste water should also be about 1.7 ppm. Analyses for ABS in water used in the calcium-magnesium head-end precipitation studies ranged from 0.03 to 2.2 ppm, the average being about 0.75 ppm. This is less than half the expected average value.

10.1.2 Determination of Alkylbenzene Sulfonate by the Methylene Blue Method⁵⁴

Optical density-vs-concentration calibration curves for the methylene-blue-ABS salt formed upon addition of the indicator to aqueous ABS-NaH₂PO₄ solutions were made with a Bausch and Lomb spectrophotometer. The determinations were made for light paths of 18 and 23 mm. The methylene-blue-ABS end-product is selectively extracted in three chloroform passes, and the optical density of this organic phase is measured at its characteristic absorption peak at 652 mμ. The light adsorption, obeying Beer's Law, gives a straight line function as ABS concentration varies. The aqueous phases, prior to extraction, contained 0.0 to 1.6 ppm ABS and 1.88×10^{-5} M methylene blue at pH 2.2, adjusted with dilute sulfuric acid. The mole ratios, methylene blue/ABS, ranged from 3.86 to 76.33.

Two modified procedures in the absence of NaH₂PO₄ were tested by using single chloroform extractions of aqueous phases containing 0.0 to 9.1 ppm ABS and 5.68×10^{-4} or 5.68×10^{-5} M methylene blue, which is at least a 100% excess of the dye. The pH range for these solutions was 2.3 to 2.5, adjusted with dilute hydrochloric acid. At both these methylene blue concentrations, sensitivity to changing ABS concentrations was very much less than for the corresponding standard curve. Since hydrochloric acid is known to interfere in the methylene blue - ABS extraction, sulfuric acid was used for pH adjustment in later development work. This modified method for ABS determination was used to analyze ORNL low-activity waste water (Figs. 10.1 and 10.2) in the head-end precipitation studies described above.

10.1.3 Rate of Calcium Phosphate Precipitation

Beaker tests were performed to obtain preliminary data on the residual hardness after precipitating calcium and magnesium compounds from alkaline phosphate solution. Oak Ridge National Laboratory tap water used in these tests had the following composition: Ca(HCO₃)₂, 65 ppm as CaCO₃; Mg(HCO₃)₂, 35 ppm as CaCO₃.

This water was made 60 ppm in PO₄³⁻ (as Na₃PO₄) and 0.005 M in NaOH. The data show that after 3 or 15 min of agitation, calcium and magnesium concentrations are reduced to 8 and 5 ppm (as CaCO₃), respectively.

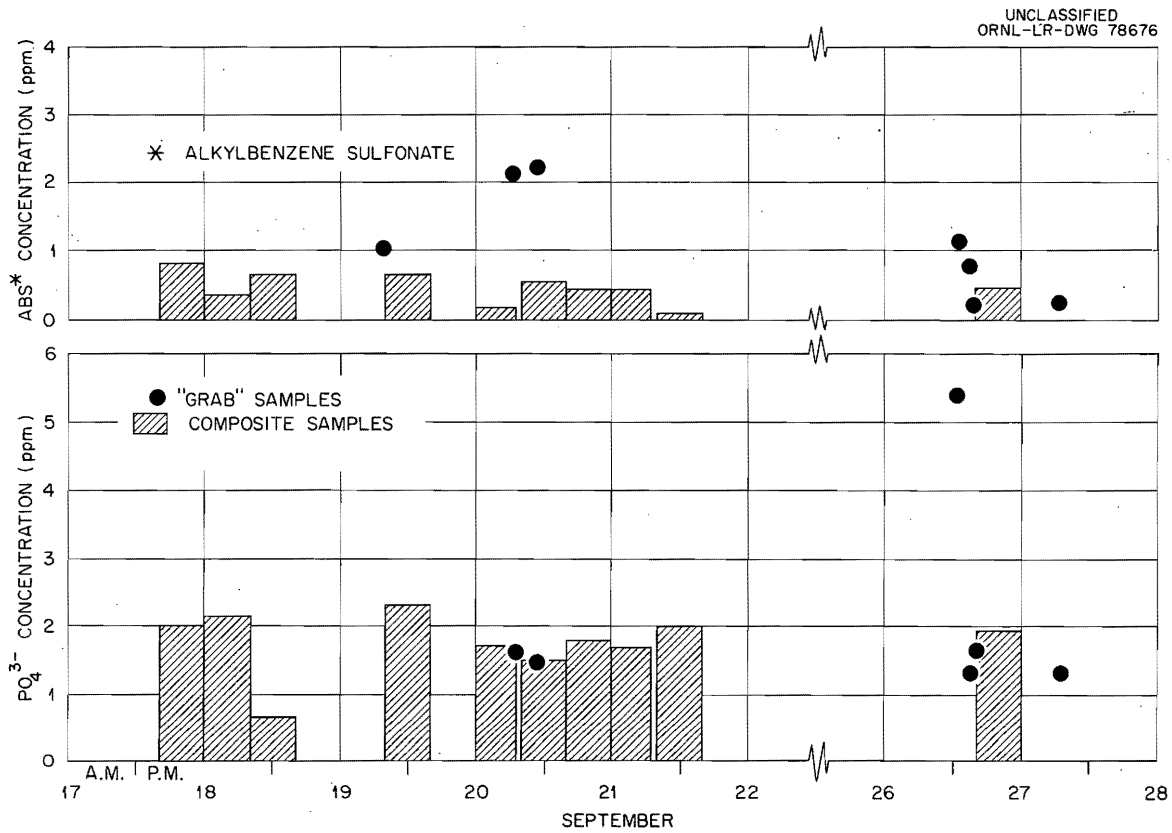


Fig. 10.1. Alkylbenzene Sulfonate and Phosphate Ion Composition of ORNL Low-Level Waste Water During a Ten-Day Feed-Clarification Run (Run 1).

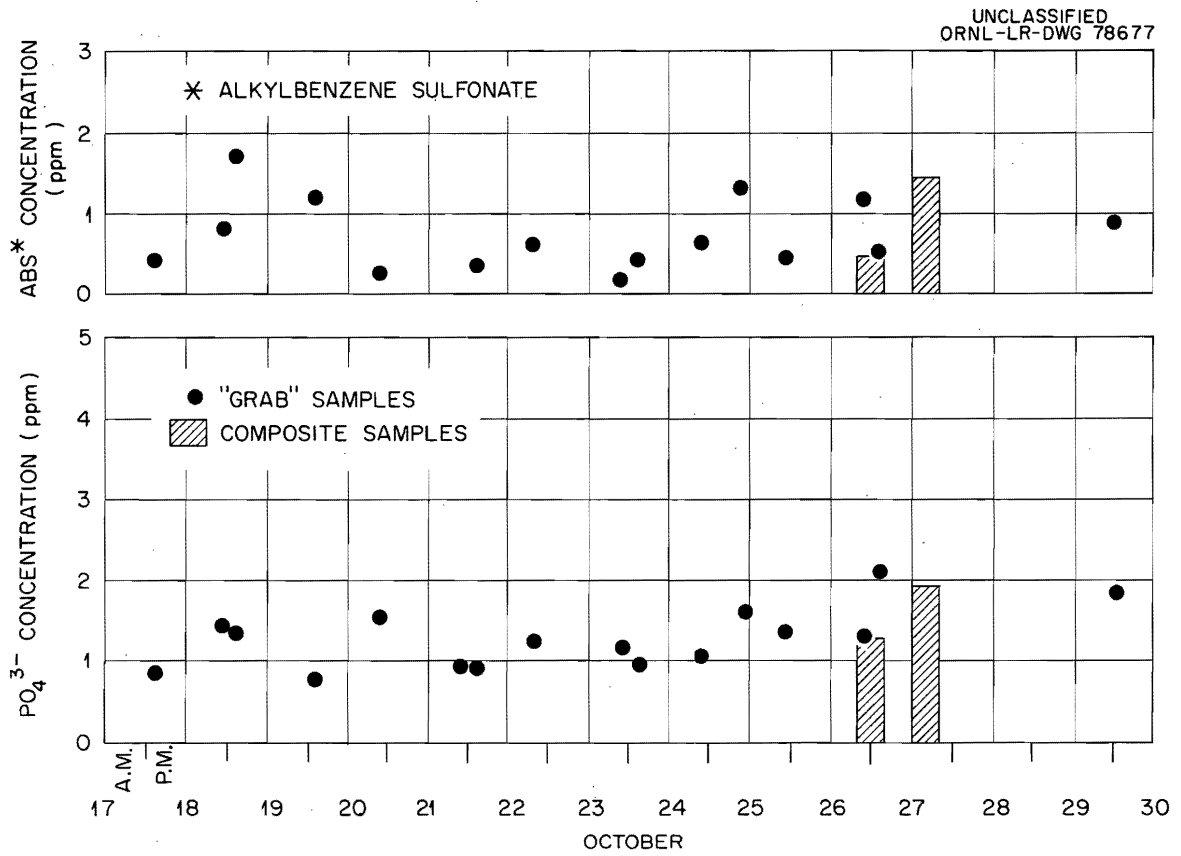


Fig. 10.2. Alkylbenzene Sulfonate and Phosphate Ion Composition of ORNL Low-Level Waste Water During a Ten-Day Feed-Clarification Run (Run 2).

10.1.4 Fixation of Decanted Sludge with Cement

Sludge, composed of calcium carbonate and magnesium hydroxide, obtained from precipitating these materials from water made 0.005 M in NaOH, 0.005 M in Na_2CO_3 , and 2 ppm in Fe^{3+} , was decanted to a slurry containing 10 to 12% solids. Three samples of this were then mixed with cement as follow:

- Sample A - 16.7 g cement per 100 g (sludge + cement)
- Sample B - 28.5 g cement per 100 g (sludge + cement)
- Sample C - 37.5 g cement per 100 g (sludge + cement)

After 24 hr all samples had lost their fluidity; hardness had increased from sample A to sample C. The volume of sample C was 15% greater than the volume of sludge it contained. This case corresponds to 5 lb of cement per gallon of sludge, or a cement cost of \$0.06 per gallon of sludge. Since the sludge represents a calcium and magnesium (and strontium, in the case of low-activity waste) volume reduction of about 1200, this cement waste corresponds to about \$0.05 per 1000 gallons of water treated.

10.1.5 Precipitation-Foam Separation Decontamination of ORNL Low-Activity Waste

Laboratory equipment was set up, calibrated, "cold-tested," and revised prior to making tracer runs on the complete feed clarification-foam separation cycle.

10.2 Engineering Development

P. A. Haas

Engineering problems were studied for design and application of foam separation columns. The performance of a centrifugal foam breaker was studied. Decontamination factors for strontium were determined for effluent from the laboratory clarifier and for slurry feed formed by the addition of reagents to precipitate calcium and magnesium. Installation and preliminary operation of a 24-in.-diam column to mock up a pilot plant were completed.

10.2.1 Centrifuge Foam Breaker

A screen-lined centrifuge bowl, found convenient for laboratory condensation of foam, was tried in an engineering study. Two bowls were made of perforated metal sheet to permit changing the screen liners. Either of these bowls was coupled directly to a commercial electric motor. The speed was controlled by a variable voltage transformer in the motor power supply and was measured by use of a stroboscopic light. Foam from a

6-in.-ID column with about 1 ft of 6-in.-diam drainage section was introduced 1 to 3 in. below the top edge of the bowl. The rate of accumulation of uncondensed foam was measured with centrifuge speed, foam rate, mesh size of the screen, and solution concentrations as the variables (Table 32). If the foam overflowed the top of the centrifuge, the flow rate was considered to be in excess of the capacity at those conditions.

The most significant conclusions were:

1. The efficiency with which foam is condensed is higher for a low rate of dry foam, than for a higher rate of wetter foam.
2. Screen sizes of 100 or 120 mesh per inch are more efficient in condensing foam than are 200- or 40-mesh-per-inch screens.
3. The capacity increases as the speed of the centrifuge is increased.
4. Foam condensation is more efficient at lower speeds if the capacity of the bowl is not exceeded.

The capacities of the centrifugal foam breakers decreased rapidly as the speed decreased below 2000 rpm. Typical values for the 4-in.-diam, 4-in.-high bowl with 120 mesh screen were 3500 cc/min at 1515 rpm, 4000 cc/min at 1670 rpm, and 10,000 cc/min at 2000 rpm. The initial bowl of about 4-5/8 in. ID, 6 in. high, was limited to less than 1600 rpm because of poor balancing and low capacity.

The percentage of uncondensed foam was decreased, and the results were much more reproducible when the edges of the screen were sealed to the perforated bowl wall with paraffin. Although the screens were carefully cut to fit the bowls, apparently small gaps permitted escape of the foam without passing through the screen when the paraffin seals were not used. The tabulated results (Table 32) are from runs using the paraffin seals.

10.2.2 Decontamination of Synthetic Low-Level Waste

Two runs were made with process water plus Sr⁸⁹ to simulate low-level waste in the 6-in.-diam foam column. The slurries precipitated by addition of $4 \cdot 10^{-3}$ N NaOH, 50 ppm PO₄³⁻ as Na₃PO₄ solution, and 10 ppm Fe³⁺ as FeCl₃ solution were fed to the foam column. For the second run, 10 ppm or "Fab" commercial detergent were added prior to the precipitation to simulate impurities in low-level waste.

Decontamination factors for strontium for these runs were 19 to 52, without any consistent variation from the addition of 10 ppm of "Fab" (Table 33). When the same precipitation conditions were used in beakers and when samples were taken through fine filter paper, the strontium decontamination factors were about 7 in 10 min and about 10 in 2 or 68 hr.

Several undesirable effects of the precipitated solid on foam column operation were noted. Visible areas of foam downflow at the wall were

Table 32. Results of Test of Centrifuge Foam Breaker

Bowl: 4 in. I.D., 4 in. high of perforated sheet, 1/8 in.-diam. holes on 3/16-in. triangular spacing.

Foam: "EC" fritted-glass gas sparger, 6 in. diam., 12 in. high drainage section.

Foam Rate (cc/min)	Screen Mesh (per in.)	Breaker (rpm)	For 250 ppm of Trepolate F-95 and 0.01 N NaOH		For 500 ppm of Trepolate F-95 and 0.01 N NaOH	
			Uncondensed Foam (cc/min)	(%)	Uncondensed Foam (cc/min)	(%)
2,000	120	2,000	4	0.2		
		2,500	6	0.3		
		3,000	12	0.6		
		3,500	12	0.6		
3,500	120	2,000	13	0.4	110	3.1
		2,500	25	0.7	160	4.6
		3,000	19	0.6	240	6.9
		3,500	46	1.3	380	11.0
	200	2,000	10	0.3		
		3,500	123	3.5		
6,000	120	2,000	72	1.2		
		2,500	100	1.7		
		3,000	310	5.2		
		3,500	290	4.8		
10,000	120	2,000	140	1.4	540	5.4
		2,500	490	4.9	710	7.1
		3,000	470	4.7	710	7.1
		3,500	760	7.6	800	8.0
	200	2,000	650	6.5		
		3,500	990	9.9		

Table 33. Decontamination of Synthetic Low-Level Waste in a 6-in.-diam Foam Column

Surfactant: Dodecylbenzenesulfonate added as Trepolate F-95 to the liquid pot for the column
 Feed: Process water for run 51; process water plus 10 ppm "Fab" for run 52 plus chemicals as listed
 Column conditions: 85-cm countercurrent length; "F" liquid distributor; 10.5-in.-diam drainage section; EC fritted-glass gas spargers
 Zero time: Start of feed at conditions listed

Quantity	Symbol	Units	Run Numbers					
			51A	51B	51C	52A	52B	52C
Time of addition of $4 \cdot 10^{-3}$ M NaOH and 50 ppm PO_4	--	minutes	-20	-120	-200	-15	-115	-195
Time of addition of 10 ppm Fe^{+3} as $FeCl_3$ solution	--	minutes	-15	-115	-195	-10	-110	-190
Liquid rate in	$L + E_p$	cc/min	600	1,100	600	600	1,100	600
Condensed foam rate	E_p	cc/min	18	40 ^a	21 ^a	20	33	10
Net liquid rate	L	cc/min	580	1,060	580	580	1,070	590
Surfactant concentration out	-	ppm	220	310	220	230	360	230
Gas rate	V/a	cc/min	4,100	4,100	4,100	4,100	4,100	4,100
Surface rate	V	10^5 sq cm/min	4.8	4.8	4.8	4.8	4.8	4.8
Surface/liquid ratio	V/L	sq cm/cc	830	450	830	830	450	810
Gross β in liquid feed	x_2	cpm/cc	8,200	8,200	8,200 ^b	9,300	9,300	9,300 ^b
Gross β in liquid out	x_B (also x_1^*)	cpm/cc	410	300 ^a	290 ^a	400	500	180
Gross β in condensed foam	$y_2 V + x_2^* E_p$	10^3 cpm/min	2,700	5,800 ^a	1,600 ^{a,b}	4,600	5,500	1,200 ^b
Gross β material balance	-	%	60	68 ^a	37 ^{a,b}	87	59	23 ^b
Decontamination factor	DF	dimensionless	20	27	28	23	19	52
Volume reduction	VR	dimensionless	33	28	29	29	31	59

123

^aAn accumulation of nonmoving foam and solids started in the foam breaker during run 51B and increased until the end of run 51. This partially explains the lower volume reductions and material balances.

^bThe liquid level in the feed tank dropped below the agitator level during 51C and 52C. This results in a short period of high concentration of solids in the feed to the column, followed by a relatively low slurry concentration.

slightly more numerous, were much more persistent, and extended over greater lengths of column. The volumes of condensed foam (overhead after drainage) for these slurry feed runs were 2 to 3 times the volumes for solid-free runs at similar conditions.

During run 51B, an accumulation of stationary foam and solids started in half of the 10.5-in.-ID drainage section. This accumulation increased until only half the drainage section showed visible flow of foam by the end of run 51C. When the foam collapsed after the column was shut down, gram quantities of solids as agglomerates up to 1/4 in. across fell to the bottom of the column. The volume reductions practical when the calcium and magnesium precipitates are fed to the foam column are probably only about a tenth of the maximum volume reductions practical if nearly all the precipitates are removed as a pretreatment.

Two periods of high concentrations of solids probably account for the poor material balances of runs 51 and 52 (Table 33). The analyses are for steady-state operation after an initial transient period to allow the column to come to steady state. The feed tank is a conical-bottom drum with an agitator near the conical-cylindrical intersection. The feed leaves through the bottom of the cone. Some solids settle in spite of the gentle agitation, and these result in a high solids concentration during the steady-state part of runs 51A or 52A. When the liquid level drops below the agitator level, the remaining solids tend to settle out and give a short period of high concentrations of solids during the nonsteady-state parts of runs 51C or 52C. Thus, the liquid feed has a below-average concentration of precipitated solids during the steady-state parts of 51A, 51B, 52A, and 52B, and a low concentration of precipitated solids during the steady-state parts of 51C and 52C.

10.2.3 Large Column

Installation was completed of a foam column using a 24-in.-ID, 48-in.-long transparent plastic cylinder as the column body (Fig. 10.3). This column will serve as a mockup for a 24-in.-diam foam separation column proposed as a pilot plant for decontaminating low-level waste. Conical end sections were used with 19 tubes on a 5-in. triangular spacing as the liquid-feed distributors. A new sonic foam breaker and extra coarse porosity fritted glass gas spargers were used for preliminary tests. The capacity of the sonic foam breaker was determined for the 48-in. length of the 24-in.-diam columns as the drainage section. The capacity was about 24 liters/min for 250 ppm of Trepolate F-95 surfactant in 0.01 N NaOH, and 20 liters/min for 500 ppm of surfactant. Channeling was noticeable immediately below the feed distributor tubes, but persisted only for 1 to 2 ft of column length.

10.2.4 Decontamination of Clarifier Effluent

Several runs were made to determine strontium decontamination factors in the 6-in.-diam foam column for low-level waste that had been passed through the 9-in.-diam clarifier to precipitate calcium and magnesium (see

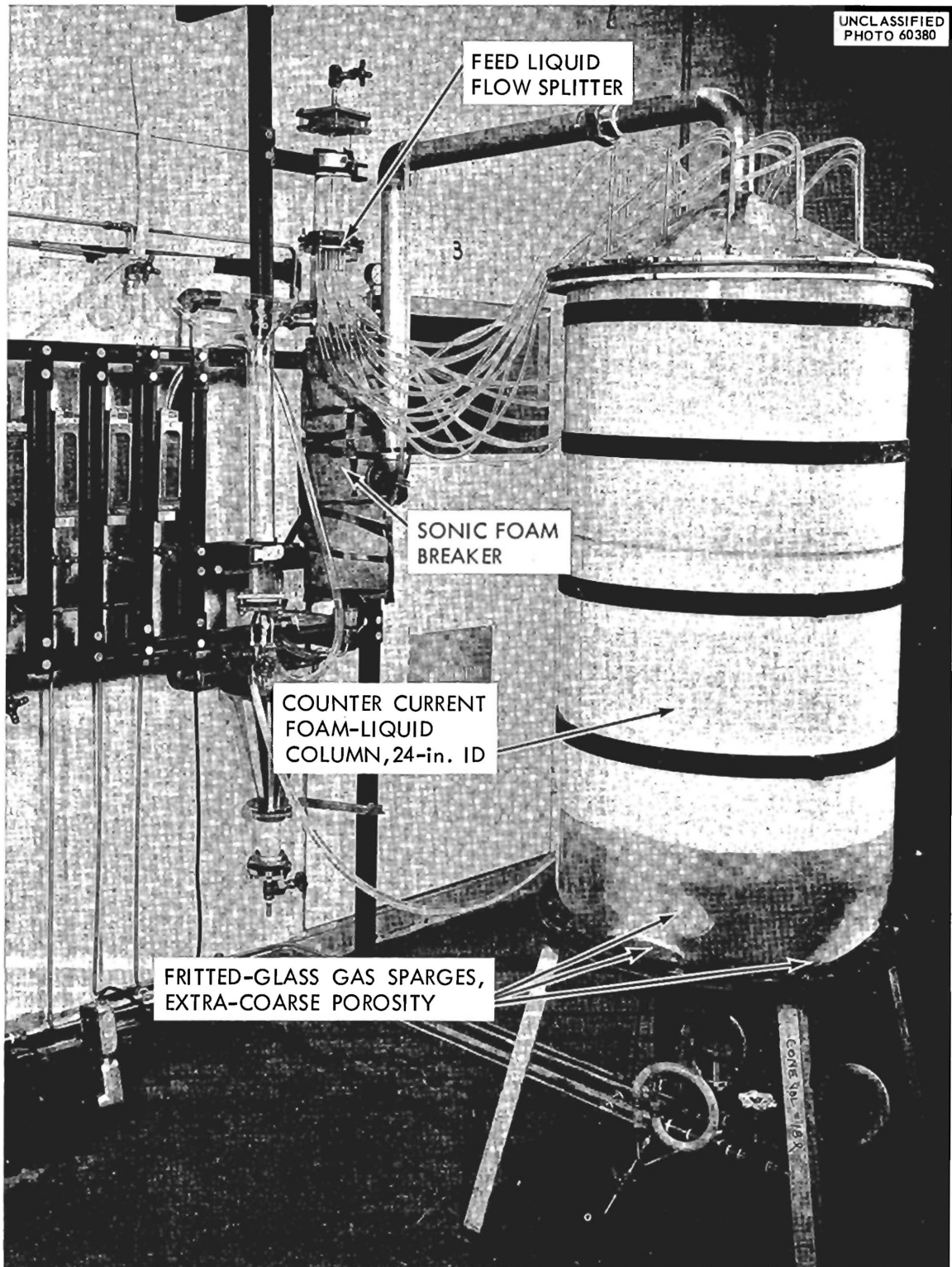


Fig. 10.3. Twenty-Four-Inch-Diameter Column and Associated Apparatus for Foam Separation Studies.

above). This clarifier reduced the hardness from about 100 to 2 to 4 ppm, as CaCO_3 .³⁵ While 100 ppm of hardness would require an excessive amount of surfactant and surface per volume of liquid, good decontamination for strontium, calcium, and magnesium should be practical for 2 to 4 ppm of hardness.

Effluent from the 9-in.-diam clarifier as operated on low-level waste in Building 2528 (ref 35) was used for foam column feed after the addition of Sr^{89} and dodecylbenzene sulfonate. The clarifier effluent was collected during the 24-hr periods of operation with intermittent attention and appeared to be free of either suspended or settled solids. The foam-column conditions and procedures were similar to those previously used to obtain low HTU_x values, except that the surface/liquid volume ratio was increased to favor high decontamination.

Decontamination factors for strontium were 24 or greater for one countercurrent run (Table 34) and two batch runs to determine (r/c) for strontium (Table 35). The same lot of clarifier effluent was used for batch-run 56 and the continuous countercurrent runs 56A and 56B. The variable effluent concentrations of 56B might be explained by the effects of small flow variations since $(r/c)_{\text{Sr}}V \approx L$. The conditions of 56A should have given more than 10 transfer units and a strontium decontamination factor greater than 300.

The strontium decontamination factors for the other continuous countercurrent runs were low values of 2 to 4 (Table 36). Since previous results showed that a large number of transfer units (more than 10) are obtained for this column, these low decontamination factors must be the result of pinching of the operating and equilibrium lines at the feed point. The surface and liquid must be close to equilibrium at this point, and the distribution coefficient for strontium, $(/c)_{\text{Sr}}$, can be calculated from material balances:

$$(r/c)_{\text{Sr}} = \left(1 - \frac{x_B}{x_2}\right) \frac{L}{V} \quad \text{or} \quad (r/c)_{\text{Sr}} = \frac{V y_p + E_p x_2^*}{V x_2} - \frac{E_p}{V},$$

where

x_2 is the feed liquid concentration,

x_B is the effluent liquid concentration,

L is the net liquid flow down the column,

V is the surface flow up the column,

E_p is the volume flow rate of condensed foam, and

$V y_p + E_p x_2^*$ is the solute (i.e., Sr^{89}) effluent rate as condensed foam.

Distribution coefficients estimated by this procedure vary from (0.6 to 1.8) $\times 10^{-3}$ cm (Table 36). This variation is probably due to a variation in the calcium and magnesium concentration in the clarifier effluent.

Table 34. Experimental Data and Calculations for Continuous-Countercurrent Stripping of Strontium From LLW Clarifier Effluent

Liquid Feed Distributor F
 Gas Sparger: EC-porosity fritted glass
 Sr Distribution Coefficient: $1.7 \cdot 10^{-3}$ cm

Quantity	Symbol	Units	Run Number	
			57A	57B
Countercurrent length	Z	cm	85	85
Liquid feed rate	$L + E_p$	cc/min	400	800
Condensed foam rate	E_p	g/min	9	12
Net liquid rate	L^p	cc/min	390	790
Gas rate	V/a	cc/min	4,000	4,000
Surface area rate	V	10^5 sq cm/min	4.8	4.8
Surfactant concentration in effluent liquid	-	ppm	190	190
Phase flow ratio	$(\alpha V + E)/(L + E)$	dimensionless	2.06	1.03
Gross β in liquid feed	x_2	cpm/cc	3,400	3,400
Gross β in effluent liquid	x_B (also x_1^*)	cpm/cc	140	240-1100
Gross β in condensed foam	$y_2 V + x_2^* E_p$	10^3 cpm/min	1,310	2,100
Gross β in material balance	--	%	101	90-120
Decontamination factor	$DF = x_2/x_B$	dimensionless	24	3-15
Volume reduction	$VR = (L + E)/E_p$	dimensionless	45	65

Table 35. Determination of Γ/c for Strontium by Batch Runs on LLW Clarifier Effluent

Gas Sparger: "A" Spinnerette with 50 μ holes
 Sr Concentration: 5 mc of Sr-89 tracer only
 Liquid Gross β Half Lives: From Figure 2.

Quantity	Units	Run Number		
		49	56A	56B
Trepolate F-95 concentration	ppm	330	330	~ 220
Gas rate, V/a	cc/min	2,100	2,100	4,800
Surface area rate, V	10^5 cm ² /min	1.8	1.8	2.5
Liquid volume in column	cc	14,800	9,900	9,200
Gross β half life in liquid, $t-1/2$	min	37	22	16
$\Gamma/c = \left(\frac{0.693}{t-1/2}\right) \left(\frac{\text{volume}}{V}\right)$	10^{-3} min	1.5	1.7	1.6
Gross β half life of cond. foam rate, $t-1/2$	min	42	-	-
$\Gamma/c = \left(\frac{0.693}{t-1/2}\right) \left(\frac{\text{volume}}{V}\right)$	10^{-3} min	1.4	-	-
Maximum gross β DF	dimensionless	27	42 for whole run	

Table 36. Determination of (Γ/c) for Strontium by Continuous Countercurrent Runs with Pinching at the Feed Point

Quantity	Symbol	Units	Run Numbers					
			45A	45B	45C	46	53A	53B
Feed solution (before reagent additions)	--	--	LLW Clarifier Effluent (as collected in Bldg. 2528)					
Sr concentration	--	10^{-6} M	tracer	tracer	tracer	tracer	tracer	tracer
NaOH concentration added	--	M	.001	.001	.001	none	none	none
Effluent Trepolate F-95 concentration	--	ppm	260	260	260	260	380	220
Gas sparger used	--	--	A Spin.	A Spin.	A Spin.	EC glass	EC glass	EC glass
Countercurrent column length	z	cm	85	85	85	85	85	85
Estimated number of transfer units ^a	N_x	dimensionless	20	20	20	8	8	8
Liquid feed rate	$L + E_p$	cc/min	900	900	1200	600	600	600
Condensed foam rate	E_p	cc/min	7	3	10	19	16	8
Net liquid rate	L	cc/min	890	900	1190	580	585	590
Gas rate	V/a	cc/min	4700	2900	5700	4000	4000	4000
Surface area rate	V	10^5 sq. cm/min	2.5	2.0	2.8	4.8	4.8	4.8
Gross β in liquid feed	x_2	cpm/cc	9400	9400	9400	11500	11500	11500
Gross β in effluent liquid	x_B	cpm/cc	5400	5950	5600	2800	3350	5100
Gross β in condensed foam	$y_2V + x_2^*E_p$	10^3 cpm/min	5200	3450	6500	5300	3600	3300
Gross β material balance	--	%	118	104	117	100	81	87
Γ/c for Sr from x_2 and x_B	(Γ/c) Sr	10^{-3} cm	1.5	1.7	1.7	0.9	0.9	0.7
Γ/c for Sr from x_2 and $y_2V + x_2^*E_p$	(Γ/c) Sr	10^{-3} cm	2.2	1.8	2.4	0.9	0.6	0.6
Decontamination factor	$DF = x_2/x_B$	dimensionless	1.7	1.6	1.7	4.1	3.5	2.3

^aNumber of transfer units for similar conditions with demineralized water.

Analyses of calcium, magnesium, and total hardness at these concentrations in the presence of 0.01 N Na^+ and variable low-level-waste impurity concentrations is difficult. Except for the effluent used for run 49, the clarifier effluents were partly collected during periods of unattended operation, and short periods of poor operation could have occurred without detection.

The strontium distribution coefficients of $(1.4 \text{ to } 1.7) \times 10^{-3}$ cm determined by batch tests with clarifier effluent (Fig. 10.4, Table 35) agreed with that from continuous countercurrent runs (Table 36). Batch charges were foamed, and the distribution coefficient calculated from the slope of the concentration vs time curve by assuming one theoretical stage. These values agreed with those reported for about 5 ppm Ca^{2+} in laboratory studies.

These results indicate strontium distribution coefficients of $(1.4 \text{ to } 2) \times 10^{-3}$ cm for the effluent of the clarifier as usually operated on low-level waste. This coefficient did not vary as the strontium was removed during two batch foamings. The decontamination of strontium was much less for a continuous countercurrent run than would be expected for the $(\%/c)_{\text{Sr}}$ and the conditions used. This result could be explained by the existence of a strontium complex of low surface activity, which is slowly converted to the dodecylbenzene sulfonate complex of strontium or by a high saturation of the surface and a slow exchange due to the high sodium concentrations in solution. Either of these causes would explain the lower strontium distribution coefficients for clarifier effluent, compared with that expected from the effluent calcium concentrations.

11. REFERENCES

1. R. E. Blanco and F. L. Parker, Waste Treatment and Disposal Quarterly Progress Report, August-October 1962, ORNL-TM-482 (Mar. 25, 1963).
2. R. E. Blanco and E. G. Struxness, Waste Treatment and Disposal Progress Report for April-May 1962, ORNL-TM-376 (Nov. 5, 1962).
3. R. E. Blanco and E. G. Struxness, Waste Treatment and Disposal Progress Report for October and November 1961, ORNL-TM-133 (Mar. 13, 1962).
4. J. T. Roberts and R. R. Holcomb, A Phenolic Resin Ion Exchange Process for Decontaminating Low-Radioactivity-Level Process Water Wastes (Mar. 17, 1961).
5. R. R. Holcomb and J. T. Roberts, Low-Level Waste Treatment by Ion-Exchange, II. Use of a Weak Acid, Carboxylic-Phenolic Ion-Exchange Resin, ORNL-TM-5 (Sept. 25, 1961).
6. R. R. Holcomb, Low-Level Waste Treatment. Part I. Decontamination of Low-Radioactivity-Level Process Water Wastes by a Scavenging-Precipitation Ion-Exchange Process, ORNL-3322.

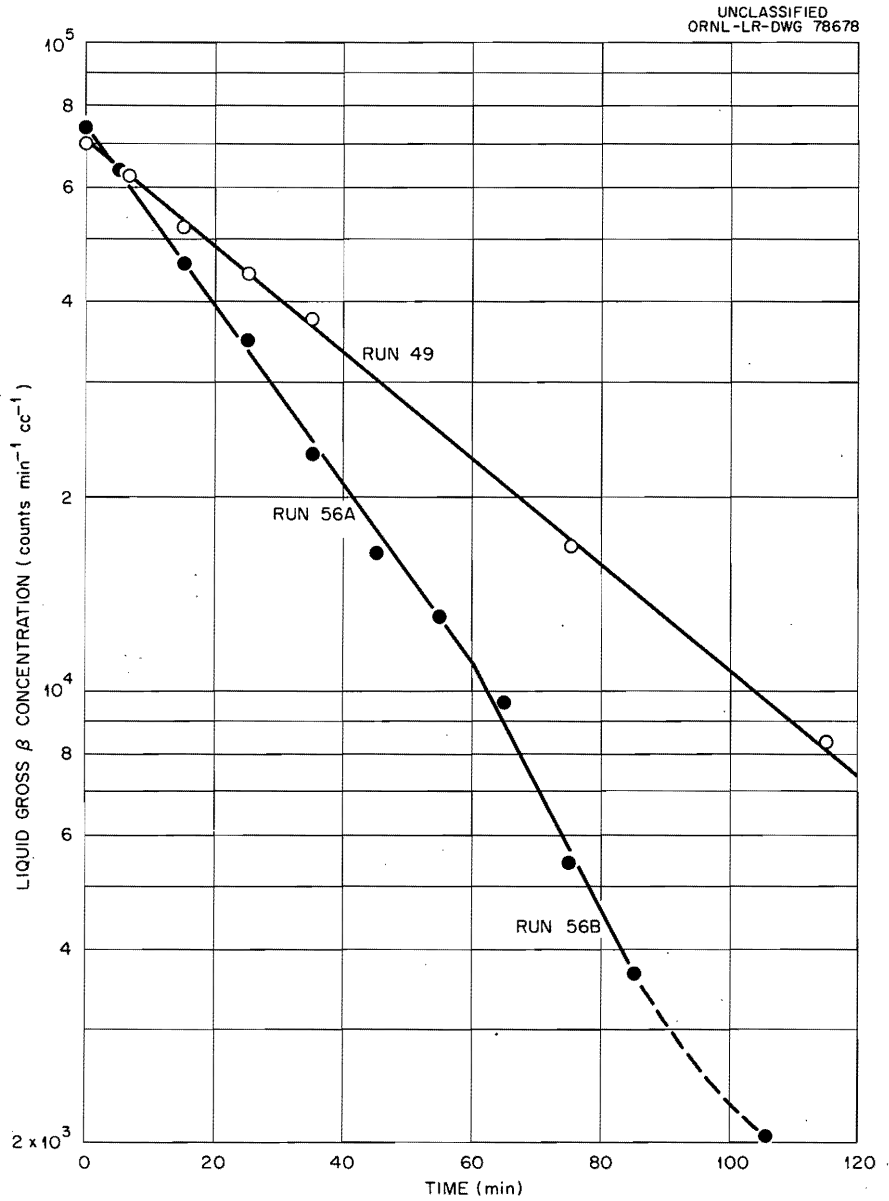
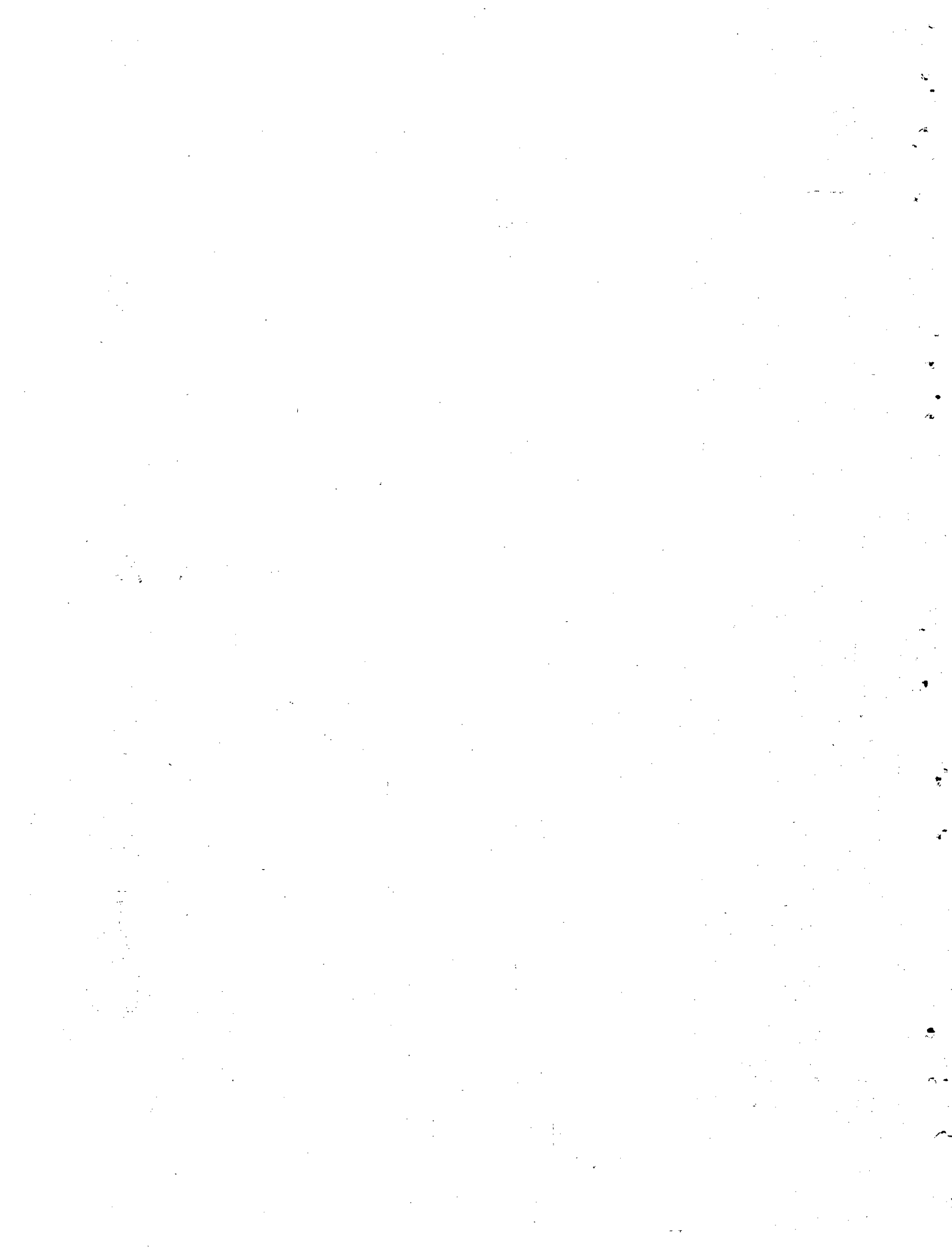


Fig. 10.4. Results of Batch Determinations of Strontium Distribution Coefficients for Effluent from the Clarifier for Low-Level Waste.

7. R. E. Brooksbank et al., Low-Radioactivity-Level Waste Treatment. Part II. Pilot Plant Demonstration of the Removal of Activity from Low-Level Process Waste by a Scavenging-Precipitation Ion-Exchange Process, ORNL-3349.
8. P. Hamer, J. Jackson, and E. F. Thurston, Industrial Water Treatment Practice, pp 22-37, Butterworths-Imperial Chemical Industries Limited, London, 1961.
9. W. Davis and E. Schonfeld, personal communication, May 1962.
10. Calgon in Industry, Hagan Chemical and Control, Incorporated, Pittsburgh, Pennsylvania.
11. R. E. Blanco, Chemical Technology Division, Chem. Dev. Sec. B., Quarterly Progress Report, July-September 1962, ORNL-TM-403:
12. Letter, I. R. Higgins to R. E. Blanco, January 1963.
13. R. E. Blanco and E. G. Struxness, Waste Treatment and Disposal Progress Report for June and July 1962, ORNL-TM-396 (Dec. 19, 1962).
14. J. O. Blomeke et al., Evaluation of Ultimate Disposal Methods for Liquid and Solid Radioactive Wastes. Part III, ORNL 3355 (in press).
15. R. E. Blanco and F. L. Parker, Waste Treatment and Disposal Quarterly Progress Report, August-October 1962, ORNL-TM-482 (Mar. 25, 1963).
16. W. D. Cottrell, Radioactivity in Silt of the Clinch and Tennessee Rivers, ORNL-2847 (Nov. 18, 1959).
17. R. J. Morton (ed.), Status Report No. 1 on Clinch River Study, ORNL-3119 (July 27, 1961), pp 28-42.
18. R. E. Blanco and F. L. Parker, Waste Treatment and Disposal Quarterly Progress Report, August-October 1962, ORNL-TM-482 (Mar. 25, 1963).
19. K. Z. Morgan et al., Health Physics Division Annual Progress Report for Period Ending July 31, 1959, ORNL-2806 (Oct. 23, 1959).
20. R. L. Bradshaw et al., Evaluation of Ultimate Disposal Methods for Liquid and Solid Radioactive Wastes. Part I. Interim Liquid Storage, ORNL-3128 (Aug. 7, 1961).
21. A Meteorological Survey of the Oak Ridge Area, ORO-99.
22. F. A. Gifford, Nuclear Safety 2, 56-59 (1960).
23. R. E. Blanco and E. G. Struxness, Waste Treatment and Disposal Progress Report for December 1961 and January 1962, ORNL-TM-169 (June 15, 1962).

24. R. E. Blanco and E. G. Struxness, Waste Treatment and Disposal Progress Report for June and July 1962, ORNL-TM-396 (Dec. 19, 1962).
25. T. M. Kegley, Jr., Fracture of Nickel Lead Wire, Metallography Report No. 438 (Sept. 14, 1962).
26. American Institute of Physics Handbook, sec 5, p 225, McGraw Hill, 1957.
27. R. S. Crouse, Metallographic Examination of Heaters and Thermocouples from Carey Salt Mine Experiments, Metallography Report No. 449 (Jan. 7, 1963).
28. R. E. Blanco and E. G. Struxness, Waste Treatment and Disposal Progress Report for June and July 1962, ORNL-TM-396 (Dec. 19, 1962).
29. A. S. Fry, ORNL, memorandum to M. A. Churchill, Sediment Investigations, White Oak Lake (June 30, 1953).
30. R. E. Blanco and E. G. Struxness, Waste Treatment and Disposal Progress Report for June and July 1961, ORNL-TM-15 (Oct. 24, 1961).
31. R. E. Blanco and F. L. Parker, Waste Treatment and Disposal Quarterly Progress Report, August-October 1962, ORNL-TM-482 (Mar. 25, 1962).
32. E. Schonfeld and W. Davis, Jr., Head-End Treatment of Low-Level Waste Prior to Foam Separation, ORNL-TM-260 (May 1962)
33. R. E. Blanco and E. G. Struxness, Waste Treatment and Disposal Progress Report for June and July 1962, ORNL-TM-396 (Dec. 19, 1962).
34. Standard Methods for the Examination of Water and Waste Water, 11th ed., 1st printing, September 1960, pp 245-248, American Public Health Association, Incorporated, 1790 Broadway, New York 19, New York.
35. R. E. Blanco and F. L. Parker, Waste Treatment and Disposal Quarterly Progress Report, August-October 1962, ORNL-TM-482 (Mar. 25, 1963).



INTERNAL DISTRIBUTION

- | | | | |
|--------|-------------------------------|--------|-----------------------------|
| 1. | ORNL - Y-12 Technical Library | 36. | J. M. Googin |
| | Document Reference Section | 37. | P. A. Haas |
| 2-4. | Central Research Library | 38. | C. W. Hancher |
| 5-14. | Laboratory Records Department | 39. | C. E. Haynes |
| 15. | Laboratory Records, ORNL-RC | 40. | R. F. Hibbs |
| 16-17. | R. E. Blanco | 41. | R. R. Holcomb |
| 18. | J. O. Blomeke | 42. | J. M. Holmes |
| 19. | W. J. Boegly, Jr. | 43. | D. G. Jacobs |
| 20. | R. L. Bradshaw | 44. | W. H. Jordan |
| 21. | J. C. Bresee | 45. | H. Kubota |
| 22. | R. E. Brooksbank | 46. | T. F. Lomenick |
| 23. | F. N. Browder | 47. | K. Z. Morgan |
| 24. | K. B. Brown | 48. | R. J. Morton |
| 25. | P. H. Carrigan, Jr. | 49. | E. L. Nicholson |
| 26. | W. E. Clark | 50-51. | F. L. Parker |
| 27. | K. E. Cowser | 52. | J. J. Perona |
| 28. | F. L. Culler | 53. | R. M. Richardson |
| 29. | W. Davis, Jr. | 54. | J. T. Roberts, IAEA, Vienna |
| 30. | W. de Laguna | 55-56. | E. G. Struxness |
| 31. | F. M. Empson | 57. | J. C. Suddath |
| 32. | D. E. Ferguson | 58. | J. A. Swartout |
| 33. | E. J. Frederick | 59. | T. Tamura |
| 34. | H. W. Godbee | 60. | J. W. Ullmann |
| 35. | H. E. Goeller | 61. | M. E. Whatley |

EXTERNAL DISTRIBUTION

62. E. L. Anderson, AEC, Washington, D. C.
63. W. G. Belter, AEC, Washington, D. C.
64. H. Bernard, AEC, Washington, D. C.
65. Arnold B. Joseph, AEC, Washington, D. C.
66. J. A. Lieberman, AEC, Washington, D. C.
67. W. H. Regan, AEC, Washington, D. C.
68. Robert F. Reitemeier, AEC, Washington, D. C.
69. Vincent Schultz, AEC, Washington, D. C.
70. John N. Wolfe, AEC, Washington, D. C.
71. H. M. Roth, AEC, ORO
72. C. S. Shoup, AEC, ORO
73. J. R. Horan, AEC, Idaho
74. K. K. Kennedy, AEC, Idaho
75. J. A. Buckham, Phillips Petroleum Company
76. J. A. McBride, Phillips Petroleum Company
77. C. M. Slansky, Phillips Petroleum Company
78. H. J. Carey, Jr., Carey Salt Company, Hutchinson, Kansas
79. C. W. Christenson, Los Alamos Scientific Laboratory
80. J. C. Frye, State Geological Survey, Div., Urbana, Ill.
81. W. B. Heroy, Sr., Geotechnical Corp., Dallas, Texas

82. E. F. Gloyna, University of Texas, Austin
83. W. J. Kaufman, University of California, Berkeley
84. L. Silverman, Harvard Graduate School of Public Health
85. G. M. Fair, Harvard University, Pierce Hall
86. H. A. Thomas, Jr., Harvard University, Pierce Hall
87. John Geyer, Johns Hopkins University
88. C. R. Naeser, George Washington University
89. W. A. Patrick, Johns Hopkins University
90. H. C. Thomas, University of North Carolina
91. L. P. Hatch, Brookhaven National Laboratory
92. H. H. Hess, Princeton University
93. Abel Wolman, Johns Hopkins University
94. O. F. Hill, Hanford
95. C. R. Cooley, Hanford
96. E. R. Irish, Hanford
97. A. M. Platt, Hanford
98. W. H. Reas, Hanford
99. G. Rey, Hanford
100. R. L. Moore, Hanford
101. W. H. Swift, Hanford
102. J. H. Horton, Savannah River
103. R. M. Girdler, Savannah River
104. Harvey Groh, Savannah River
105. C. H. Ice, Savannah River
106. J. W. Morris, du Pont, Savannah River
107. C. M. Patterson, du Pont, Savannah River
108. W. B. Scott, Savannah River
109. E. B. Sheldon, Savannah River
110. D. S. Webster, Savannah River
111. V. R. Thayer, du Pont, Wilmington
112. A. A. Jonke, Argonne National Laboratory
113. S. Lawroski, Argonne National Laboratory
114. W. A. Rodgers, W. R. Grace and Company, Naperville, Ill.
115. J. J. Weinstock, RAI
116. J. F. Honstead, IAEA, Vienna
117. D. W. Pearce, IAEA, Vienna
118. R. L. Nace, USGS, Washington, D. C.
119. P. H. Jones, USGS, Washington, D. C.
120. C. P. Straub, U. S. Public Health Service, Cincinnati, Ohio
121. Dade Moeller, U. S. Public Health Service, Winchester, Mass.
122. W. J. Lacy, Office of Civil Defense, Washington, D. C.
123. J. E. Crawford, U. S. Bureau of Mines, Washington, D. C.
124. J. W. Watkins, U. S. Bureau of Mines, Washington, D. C.
125. L. C. Watson, AECL, Chalk River, Canada
126. John Woolston, AECL, Chalk River, Canada
127. AECL, Chalk River, Canada, Attn: C. A. Mawson, I. L. Ophel
128. AEC, Sidney, Australia, Attn: R. C. Cairns, L. Keher
129. AERE-Harwell, England, Attn: H. J. Dunster
130. AERE-Harwell, England, Attn: R. H. Burns, R.D.B. Johnson
131. CEA, Grenoble, France, Attn: G. Wormser
132. CEA, Saclay, France, Attn: F. Duhamel, A. Menoux, C. Gailledreau

133. Peter A. Krenkel, Vanderbilt University, Nashville, Tennessee
134. Yehuda Feige, Ministry of Defence, Atomic Energy Commission,
Rehovoth, Israel
135. CEA, Fontenay-aux-Roses, Attn: P. Regnaut, P. Faugeras,
M. Bourgeois
136. Centre d'Etude Nucleaire, Mol, Belgium, Attn: L. Baetsle
137. Centre d'Etude Nucleaire, Mol, Belgium, Attn: P. de Jonghe
138. Euratom (ISPRA), Casella Postale No. 1, Attn: M. Lindner
139. Eurochemic, Mol, Belgium, Attn: E. Luscher, H. Moeken,
R. Rometsch
140. Jitender D. Sehgal, Bombay, India
- 141-155. DTIE

